

Mechanistic and structural characterization of the SUMO-specific protease Ulp2

Inaugural-Dissertation
zur
Erlangung des Doktorgrades
der Mathematisch-Naturwissenschaftlichen Fakultät
der Universität zu Köln

vorgelegt von
Julia Eckhoff
aus Buchholz in der Nordheide

Köln, 2016

1. Berichterstatter: Prof. Dr. R. Jürgen Dohmen

2. Berichterstatter: Prof. Dr. Kay Hofmann

Tag der mündlichen Prüfung: 05.07.2016

This is for everyone who loves science, the moment it kisses you after it has just beat you up for month... And then kicks you in the face again. Once you accept that this is the dynamic of your relationship, you'll have a fun ride together.

TABLE OF CONTENTS

Abstract	1
Zusammenfassung	2
1 Introduction	3
1.1 SUMO genes	3
1.2 SUMO protein	4
1.2.1 SUMO isoforms.....	4
1.3 The sumoylation cycle	6
1.4 Polysumoylation	7
1.5 Sumoylation motif	8
1.6 SUMO interacting motif	9
1.7 The ubiquitin-proteasome system	10
1.8 SUMO-targeted ubiquitin ligases	11
1.9 Desumoylating enzymes	12
1.9.1 Structures of SUMO proteases and catalytic mechanism.....	13
1.9.2 Regulation of SUMO proteases.....	14
1.9.3 Misregulated SUMO proteases.....	15
1.9.4 Proteases.....	16
1.9.4.1 In mammals.....	16
1.9.4.2 In budding yeast.....	17
1.9.4.2.1 Ulp1.....	17
1.9.4.2.2 Ulp2.....	18
1.9.4.2.3 Wss1.....	21
1.10 Thesis objectives	21
2 Material and Methods	23
2.1 Material	23
2.1.1 <i>Escherichia coli</i> strains.....	23
2.1.2 <i>Saccharomyces cerevisiae</i> strains.....	23
2.1.3 Plasmids.....	24
2.1.4 Material.....	26
2.1.4.1 Chemicals and consumables.....	26
2.1.4.2 Electrical equipment.....	28
2.1.5 Enzymes.....	29
2.1.6 Antibodies.....	29
2.1.7 Media.....	30
2.1.7.1 Media for <i>E. coli</i>	30
2.1.7.2 Media for <i>S. cerevisiae</i>	30
2.1.7.2.1 Standard yeast media.....	30
2.1.7.2.2 Special yeast media.....	31
2.2 Methods	32
2.2.1 Cell cultivation.....	32
2.2.1.1 Standard conditions.....	32
2.2.1.1.1 <i>Escherichia coli</i>	32
2.2.1.1.2 <i>Saccharomyces cerevisiae</i>	32
2.2.1.2 Special conditions.....	32
2.2.1.2.1 Protein expression in <i>E. coli</i>	32
2.2.1.2.2 Growth assays of <i>S. cerevisiae</i>	33
2.2.2 Biomolecular techniques.....	34
2.2.2.1 DNA isolation.....	34

2.2.2.1.1	Isolation of plasmid DNA from <i>E. coli</i>	34
2.2.2.1.2	Isolation of genomic DNA from <i>E. coli</i>	34
2.2.2.2	PCR amplification	34
2.2.2.2.1	...for cloning purposes	35
2.2.2.2.2	...for screening purposes	37
2.2.2.3	Agarose gel electrophoresis	37
2.2.2.4	DNA restriction digestion	38
2.2.2.5	Vector dephosphorylation	38
2.2.2.6	Ligation of DNA fragments	38
2.2.2.7	Generation of transformation-competent <i>E. coli</i> cells	39
2.2.2.8	Transformation of <i>E. coli</i> cells	39
2.2.2.9	Transformation of <i>S. cerevisiae</i> cells	39
2.2.3	Genetic techniques	40
2.2.3.1	Mating and sporulation of <i>S. cerevisiae</i> strains	40
2.2.4	Biochemical techniques	41
2.2.4.1	SDS polyacrylamide gel electrophoresis (SDS-PAGE)	41
2.2.4.2	Coomassie staining of proteins in SDS polyacrylamide gels	42
2.2.4.3	Detection of proteins by immunoblotting (Western Blot)	42
2.2.4.4	Antibody removal	43
2.2.4.5	Protein purification	44
2.2.4.5.1	Purification of Ulp substrates	44
2.2.4.5.2	Purification of sumoylated Ubc9	45
2.2.4.5.3	Purification of Ubp41	46
2.2.4.5.4	Purification of full-length Ulp2	46
2.2.4.5.5	Purification of the Ulp2 active domain	47
2.2.4.6	<i>In vitro</i> desumoylation assay	48
2.2.4.7	Ulp2 binding assay	49
2.2.4.8	Preparation of crude extracts from <i>S. cerevisiae</i>	50
2.2.5	Crystallization and crystal analysis	50
2.2.5.1	Crystallization and data collection	50
2.2.5.2	Data processing, structure determination and refinement	51
3	Results	52
3.1	Characterizing Ulp2 cleavage mechanism	52
3.1.1	Ulp2 dismantles poly-Smt3 chains in a sequential manner	52
3.1.2	Three linked Smt3 moieties are the minimum Ulp2-target requirement	58
3.1.3	Efficient cleavage by Ulp2 requires free access to N-terminal region or surrounding surfaces of the distal Smt3 moiety	59
3.1.4	Ulp2 needs at least three consecutive Smt3 moieties to capture a target	62
3.1.5	The active domain of Ulp2	63
3.1.5.1	Characteristics of the Ulp2 mechanism are grounded in the active domain ..	63
3.1.5.2	A SIM close to the active domain might be controlled by the NTD	65
3.1.6	Ulp2 hardly recognizes SUMO2	66
3.1.7	Ulp2 recognizes different surface areas of each of its three binding partners in trimeric Smt3	67
3.1.7.1	Exchanging four defined residues in Smt3 creates a version to which Ulp2 exhibit a very high affinity	75
3.2	The crystal structure of the Ulp2 active domain	75
3.2.1	Crystallization of the Ulp2 active domain	75
3.2.2	The structure of the Ulp2 active domain underlines its classification	77
3.2.3	Putative Smt3 binding sites in the Ulp2 active domain	80
3.2.4	Electrostatic surface potential of the Ulp2 active domain	81

3.3	Characterizing the relationship between Ulp2 and the proteasomal degradation system <i>in vivo</i>	83
3.3.1	HMW Smt3 conjugates are the causing agent of a proteolysis defect in <i>ulp2-Δ</i>	83
3.3.2	Ulp2 is the major player in SUMO recycling	84
4	Discussion	86
4.1	Ulp2 <i>in-vitro</i>-characterization setup	86
4.2	Ulp2 mechanism	87
4.2.1	Ulp2 cleaves polymeric SUMO chains from their distal ends	87
4.2.2	Its <i>exo</i> behavior differentiates Ulp2 from its subfamily members	88
4.2.3	Structure of the Ulp2 active domain	89
4.2.3.1	Determinants for the <i>exo</i> mode of Ulp2 are not known	90
4.2.3.2	Ulp2 and SENP7 are well superimposable	90
4.2.4	Ulp2 targets polymeric Smt3 chains.....	90
4.2.4.1	Ulp2 recognizes different regions in the three most distal members of polymeric Smt3	91
4.2.4.2	The active site of the UD has a comparatively low surface charge	92
4.2.4.3	Co-crystallization of Ulp2 and its target was not possible.....	93
4.2.5	SIMs in Ulp2.....	93
4.2.5.1	The SIM close to the active site must be subject to control <i>in vivo</i>	93
4.2.5.2	Possible role of SIMs in the non-catalytic domains of Ulp2	94
4.2.6	Ulp2 maintains short Smt3 chains	94
4.2.7	Ulp2 and STUBLs	95
4.2.8	Poly-ubiquitin does not interfere with target recognition by Ulp2.....	97
4.2.9	A high-affinity Smt3 variant.....	97
4.2.10	Ulp2 location	98
5	Outlook	100
6	References	101
	List of Oligonucleotides	115
	Appendix	118
	Abbreviations	118
	Acknowledgements	121
	Eidesstattliche Erklärung	122

Abstract

Posttranslational attachment of the small ubiquitin-related modifier (SUMO) to a protein, commonly known as sumoylation, is a highly dynamic process of conjugation and deconjugation. This work is concerned with the latter. Via different approaches it characterizes the *S. cerevisiae* SUMO-specific protease Ulp2, giving insight into its mechanism, its structure, as well as its role *in vivo*. It was found that Ulp2 dismantles poly-SUMO sequentially starting from the distal end (*exo* mode) down to two linked SUMO moieties. This differentiates Ulp2 from all other members of the Ulp/SEN7 family of proteases that have been analyzed, so far. Previous studies suggested rather stochastic mechanisms for all of them. Apparently, Ulp2 recognizes a region at the N-terminus or surrounding surfaces of SUMO that are not accessible in moieties of the chain other than the most distal one. Full accessibility to the N-terminus needs to be granted in order to achieve full cleavage efficiency. Additionally, Ulp2 requires at least tri-SUMO to bind and/or to process a target chain. Binding seems to happen in a cooperative manner, meaning that all three binding sites have to be occupied in order to achieve interaction. It was found that in each one of the units of a trimeric SUMO chain a different surface area is involved in SUMO/Ulp2 interactions in the event of cleaving off the most distal unit. The entire mechanism and preferences of Ulp2 are contained in its catalytic domain (UD). In the course of this work, the crystal structure of this domain was solved. The structural insights confirmed Ulp2's family affiliation with Ulp1, and underscored its close relation to SEN7. Nevertheless, concrete unique regions in the structure open up opportunities for discovering the reasons for the distinct mechanistic characteristics Ulp2 exhibits. Also, surface charge and hydrophobicity of the UD is significantly different to Ulp1 as well as SEN7 active domains. *In vivo* studies in the course of this work showed that polymeric SUMO is not subjected to degradation alongside the anchor protein it is attached to, but rather liberated beforehand. Ulp2 was identified as the major, if not only, SUMO-specific protease involved in this SUMO recycling process. However, it is yet to be clarified whether mono- and di-SUMO modifications are subjected to degradation, since Ulp2 would not process that. In the light of the mechanistic findings, the *in vivo* analysis led to a model in which Ulp2 is in an antagonistic relationship with STUbLs: While it prevents SUMO chains from getting long enough for STUbLs to capture them, once a STUbLs has bound polymeric SUMO, it obstructs the chain in such a way that it is not possible for Ulp2 to attack it, thus the substrate inevitably falls into degradation by the proteasome.

Zusammenfassung

Sumoylierung, die posttranslationale Modifikation eines Proteins mit SUMO (small ubiquitin-related modifier), ist ein hoch dynamisches Wechselspiel aus Konjugation und Dekonjugation. Im folgenden Text liegt der Fokus auf letzterem, genauer noch auf der SUMO-spezifische Protease Ulp2. Diese Arbeit charakterisiert Ulp2 sowohl mechanistisch als auch strukturell und erlaubte durch gezielte *In-vivo*-Experimente, den mechanistischen Gegebenheiten eine Funktion im größeren, zellulären Kontext zuzuordnen. Wie sich zeigte, baut Ulp2 poly-SUMO-Ketten von ihrem distalen Ende her ab. Das unterscheidet Ulp2 signifikant von sowohl Ulp1, der einzigen anderen bekannten *S. cerevisiae* SUMO-Protease, als auch seinen humanen Orthologen, SENP6 und SENP7, die Ketten eher ungeordnet, stochastisch prozessieren.

Bei einer Kettenlänge von zwei SUMOs stoppt der Abbau durch Ulp2. Weder mono- noch di-SUMO-Modifikationen werden von Ulp2 als Substrate erkannt, dementsprechend weder dekonjugiert noch gebunden. Die Resultate aus unterschiedlichen experimentellen Ansätzen deuten darauf hin, dass die Oberfläche von Ulp2 drei verschiedene SUMO-Bindestellen aufweist, die simultan besetzt sein müssen, um eine ausreichend starke Interaktion zwischen Enzym und Kette zu erhalten. Sterisch unbeschränkter Zugang zum Aminoterminal des distalen SUMO erwies sich als Grundvoraussetzung für maximale Prozessierungseffizienz. Scheinbar erkennt Ulp2 eine Region am N-Terminus oder umliegende Oberflächen von SUMO, die in anderen Gliedern einer poly-SUMO-Kette weniger zugänglich sind. Es zeigte sich, dass Ulp2 in jedem seiner drei Bindungspartner eine andere Oberfläche erkennt. Sämtliche genannte Eigenschaften sind in der aktiven Domäne angelegt; die nicht-katalytischen Domänen haben mechanistisch keine Relevanz. Im Zuge dieser Arbeit wurde die Kristallstruktur der aktiven Domäne von Ulp2 (UD) gelöst. Sie zeigte klare Ähnlichkeiten, aber auch signifikante Unterschiede zwischen der Tertiärstruktur und der Oberflächenbeschaffenheit (Ladung/Hydrophilie) von Ulp2 und Ulp1. Die Ähnlichkeit zu SENP7 erwies sich als wesentlich größer, doch auch hier gab es prägnante Divergenzen, die Ansätze für weitere mechanistische Aufklärung bieten. *In-vivo*-Experimente in *S. cerevisiae* zeigten, dass polymeres SUMO nicht gemeinsam mit seinem Substrat abgebaut, sondern vorab von Ulp2 dekonjugiert wird. Vor dem Hintergrund der mechanistischen Erkenntnisse dieser Arbeit ergibt sich ein Modell, in dem Ulp2 die Kettenlänge von SUMO-Konjugaten in einem gewissen dynamischen Rahmen hält und damit auch eine antagonistische Rolle zu STUbLs (SUMO-targeted Ubiquitin ligases) einnimmt, die ausschließlich poly-SUMO-Ketten binden können, um das an ihnen haftende Substratprotein seinem Abbau zuzuführen.

1 Introduction

This year (2016) marks 20 years since SUMO was first reported on. It was found as a covalently linked attachment to RanGAP1, a GTPase activating protein in humans (Mahajan *et al.* 1997; Matunis *et al.* 1996). The name SUMO, small ubiquitin-related modifier, was chosen as a tribute to its similarity to ubiquitin. Ubiquitin and its kinsman, collectively termed ubiquitin-like proteins (Ubls), are posttranslational modifiers. Upon conjugation to proteins, they alter the properties of their targets, thereby increasing the variety of the proteome in eukaryotic cells. So far, hundreds of proteins have been found to be sumoylated at some point during the cell cycle (Wohlschlegel *et al.* 2004; Zhou *et al.* 2004; Denison *et al.* 2005; Hannich *et al.* 2005; Panse *et al.* 2004; Wykoff *et al.* 2005; Vertegaal *et al.* 2006; Golebiowski *et al.* 2009; Schou *et al.* 2014; Hendriks *et al.* 2014). This makes SUMO the Ubl modifying the second largest pool of proteins, only outnumbered by ubiquitin itself. SUMO-conjugated proteins are frequently found in the nucleus, pointing towards sumoylation being an important nuclear process (Rodriguez *et al.* 2001).

Many sumoylated proteins are tumor suppressors, transcription factors and nuclear body proteins, a fact that accounts for a fast-growing interest in the understanding of the SUMO system. Since usually only a small fraction, frequently less than 1 %, of a substrate is sumoylated at any given time (Johnson 2004), studying sumoylation is not trivial, and there might be many more SUMO targets yet to be discovered.

1.1 SUMO genes

SUMO has been shown to be essential in most eukaryotes (Johnson *et al.* 1997; Nacerddine *et al.* 2005). *Schizosaccharomyces pombe* represents a known exception from this general view. Its sole SUMO-encoding gene, *pmt3*, is not essential, but a knockout mutant suffers from severe genome maintenance defects and is barely viable (Tanaka *et al.* 1999). Another exception is the filamentous fungus *Aspergillus nidulans* (Wong *et al.* 2008). In *Saccharomyces cerevisiae* (*S. cerevisiae*), SUMO is expressed from a single gene, *SMT3* (suppressor of mif two), which encodes a 101-amino acid molecule (Meluh *et al.* 1995). Like *S. cerevisiae*, *Caenorhabditis elegans* features only a single SUMO gene (Choudhury *et al.* 1997). In contrast, plants have several; e.g. *Arabidopsis thaliana* expresses SUMO from 8 different genes (Kurepa *et al.* 2003; Novatchkova *et al.* 2012). In higher eukaryotes, so far, 4

isoforms have been found: SUMO1-4 (Mahajan *et al.* 1997; Matunis *et al.* 1996; Johnson 2004; Shen *et al.* 1996; Kamitani *et al.* 1998; Mukhopadhyay *et al.* 2007; Bohren *et al.* 2004).

1.2 SUMO protein

SUMO has a molecular weight of ~11 kDa, but on an SDS-PAGE adds a ~20 kDa increment in size to the protein it is linked to. While SUMO shares only ~18 % sequence identity with ubiquitin, the two structures are for the most part superimposable (Fig. 1) (Johnson 2004; Bayer *et al.* 1998). Like all UbIs, SUMO features the ubiquitin superfold, a β -grasp fold in which four β -strands surround an α -helix which diagonally transverses the molecule (Bayer *et al.* 1998; Welchman *et al.* 2005; Vijay-Kumar *et al.* 1987). But unlike ubiquitin, SUMO has an N-terminal extension of ~20 amino acids, which is flexible in solution (Bayer *et al.* 1998). This region is rich in proline, glycine, and charged residues. Notably, this flexible part has been shown to be dispensable, as a corresponding N-terminally truncated SUMO mutant can still serve its essential functions (Bylebyl *et al.* 2003).

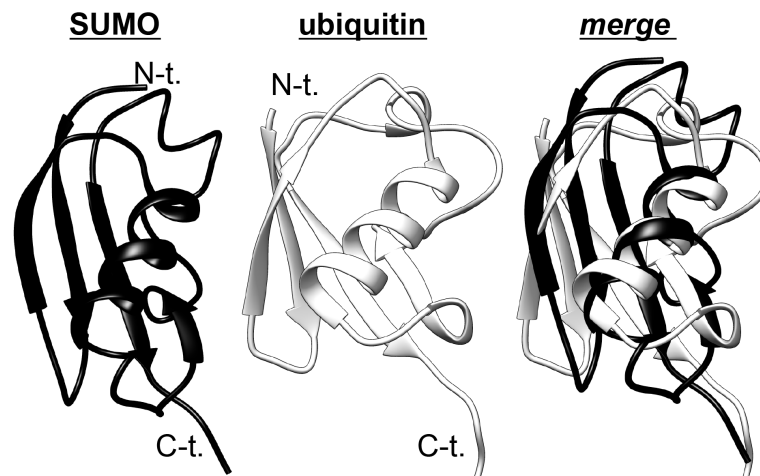


FIGURE 1: Structures of SUMO and ubiquitin. Graphics were prepared with Chimera using PDB 1L2N (Smt3) and PDB 1UBQ (ubiquitin) in *ribbon* representation. N-t. = amino-terminus; C-t. = carboxy-terminus.

1.2.1 SUMO isoforms

The four different SUMO genes in mammalian cells translate to four different SUMO isoforms. The human SUMO1 (also known as sentrin, Ubl1 and Smt3c) was the first one to be discovered in a homology screen to yeast SMT3 (Shen *et al.* 1996). SUMO4, the latest discovered member, is a special case and will be discussed separately below.

SUMO1 shares only ~45 % sequence identity with SUMO2 and SUMO3, which are virtually identical (~95 % similarity), hence frequently referred to as SUMO2/3 (Johnson 2004; Flotho *et al.* 2013). Despite the fact that SUMO1 and SUMO2/3 are activated and conjugated by the same E1 and E2 enzymes, they have significantly different features (Johnson 2004; Mukhopadhyay and Dasso 2007; Flotho and Melchior 2013). To start with, they show unique intracellular abundance: The cell cycle-dependent distribution of SUMO2/3 has been shown to be distinct from SUMO1 location, mobility and dynamics (Ayaydin *et al.* 2004). Additionally, conjugation of SUMO2/3 is strongly induced upon various stresses; SUMO1 modification, in contrast, dominates under non-stress conditions (Seifert *et al.* 2015). Another noticeable difference between SUMO1 and the other two paralogues is its inability to efficiently form chains (Tatham *et al.* 2001). While SUMO2/3 efficiently form polymers on their substrates, the existence of poly-SUMO1 has been debated (Flotho and Melchior 2013; Tatham *et al.* 2001; Saitoh *et al.* 2000). Even though, SUMO1 polymerization has been observed *in vitro* (Pichler *et al.* 2002; Yang *et al.* 2006a; Pedrioli *et al.* 2006), the prevalent role of SUMO1 in *in vivo* poly-SUMO conjugates seems to be terminating SUMO2/3 chain elongation by capping (Matic *et al.* 2008). Yet another difference of the SUMO paralogues lies in the abundance of their free forms. There is a large pool of free, unconjugated SUMO2/3, but SUMO1 exists predominantly in its conjugated form (Saitoh and Hinchey 2000). That does not implicate SUMO1 as being favored by the conjugation machinery, but might find its origin partly in the fact that SUMO2/3 is expressed ten times more than SUMO1 (Saitoh and Hinchey 2000). The difference in abundance is counterbalanced by significantly faster cleavage of SUMO2/3- than SUMO1-conjugates (Flotho and Melchior 2013; Kolli *et al.* 2010). Although targets and downstream effectors of the SUMO paralogues significantly overlap, some proteins are preferentially conjugated to a certain subfamily. So far, two distinct mechanisms that account for this have been reported on. One of them is based on intrinsic preferences of the substrate protein itself (Meulmeester *et al.* 2008; Zhu *et al.* 2008); the other one has been described in the course of RanGAP1 studies. It was found that while being efficiently modified with either of the paralogues, only RanGAP1-SUMO1 was stably incorporated in a Ubc9-RanBP1-RanGAP1 complex, and that this complex formation prevents desumoylation of RanGAP1 (Zhu *et al.* 2009; Werner *et al.* 2012). Other mechanisms –possibly involving E3 ligases– have been subject to speculation, but are yet to be discovered (Flotho and Melchior 2013).

While SUMO1 and SUMO2/3 are ubiquitously distributed in most tissues, SUMO4 apparently is expressed in a tissue- or organ-specific way. So far, it has been detected only in discrete areas like spleen, pancreatic islets, kidney or lymph node (Guo *et al.* 2004; Wang *et al.* 2008). Several important transcription factors involved in immune response have been found to be modified by SUMO4, suggesting a regulatory role in that field (Wang and She 2008). However, its maturation is not yet understood. Despite 86 % identity to SUMO2/3 (Bohren *et al.* 2004), none of the known SUMO-specific proteases recognizes SUMO4 as a target (Mukhopadhyay and Dasso 2007). Interestingly, a single-site mutation modulates pre-SUMO4 amenable to processing by SENP2 (Wang and She 2008; Liu *et al.* 2014). Nevertheless, its biological relevance is still unclear.

1.3 The sumoylation cycle

SUMO proteins are translated as immature precursors that require processing to become conjugation competent. The proteolytic reaction trims off several C-terminal residues to expose a diglycine motif. Attachment of SUMO happens via an ATP-dependent enzymatic cascade strongly reminiscent of ubiquitination (Komander *et al.* 2012). In general, sumoylation involves three different classes of enzymes: A SUMO-activating enzyme (E1), which renders the C-terminal carboxyl group of SUMO active for reaction, and then forms a thioester with it; a SUMO-conjugating enzyme (E2), and a SUMO ligase (E3) (Gareau *et al.* 2010; Hickey *et al.* 2012). Chemically speaking, the result of the sumoylation cascade is the formation of an isopeptide bond between the C-terminal carboxyl group of SUMO and an ϵ -amino group of an acceptor lysine on the surface of a substrate molecule (Johnson 2004; Geiss-Friedlander *et al.* 2007; Kerscher *et al.* 2006; Capili *et al.* 2007). A general overview of the SUMO cycle is given in Fig. 2. In the first step, the SUMO-specific E1 activating heterodimer consisting of SUMO-activating enzyme subunit 1 (SAE1; also known as Aos1) and SUMO-activating enzyme subunit 2 (SAE2; also known as Uba2) activates the C-terminus of SUMO in a two-step reaction: First, it forms a SUMO adenylate with it. Then, after a dramatic remodeling of the E1 active site, a conserved cysteine residue on the E1 attacks the adenylate to result in an SAE2~SUMO thioester bond (Olsen *et al.* 2010; Dye *et al.* 2007; Schulman *et al.* 2009). The E2 conjugating enzyme Ubc9 binds to a ubiquitin fold-domain of SAE2. Upon interaction of the thioester-charged E1 enzyme with Ubc9, SUMO is transferred to the catalytic Cys residue of the E2 enzyme, again forming a thioester bond. At this point, there are two possibilities: Either Ubc9 directly interacts with the SUMO target to

modify an acceptor lysine on its surface, or E3 protein ligases facilitate this process. The latter is usually the case and much more efficient. Basically, there are two mechanisms: Either, the SUMO E3 enzymes recruit the substrate protein into a complex with the Ubc9~SUMO thioester, thereby promoting specificity, or in case of direct E2-substrate interaction, they expedite sumoylation by stimulating the E2 enzyme to transfer SUMO to the target protein. Either way, the result is a SUMO moiety covalently attached to a Lys residue on the surface of an acceptor.

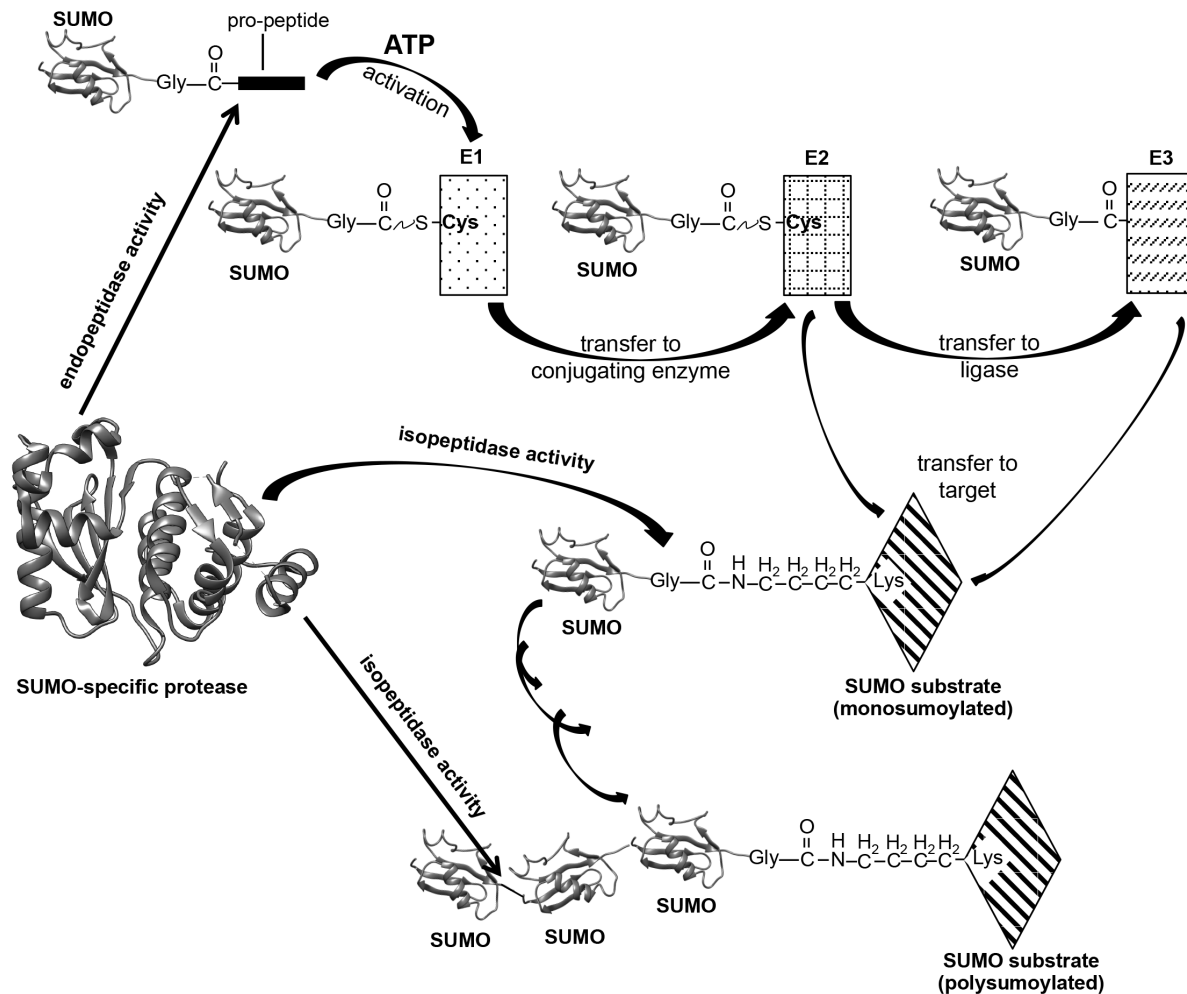


FIGURE 2: Schematic representation of the SUMO cycle. SUMO precursors are processed by specific proteases to expose their C-terminal di-glycine motives. The mature SUMO is activated and conjugated to a target SUMO via an E1-E2(-E3) cascade. In an ATP-dependent step it forms a thioester bond to the active Cys of the E1. This is then transesterified to the Cys of the E2 enzyme. Then, directly or via an E3 ligase, the conjugation-competent SUMO is transferred to an ϵ -amino group of an acceptor lysine on the surface of a SUMO substrate. The SUMO modification itself can then serve as a target, leading to SUMO chain formation. SUMO-specific proteases are able to dismantle the chains again.

1.4 Polysumoylation

Notably, not only mono- and multisumoylation (several SUMO molecules attached to different Lys residues on the same protein), but also polysumoylation, meaning formation of SUMO chains, is possible. The finding of SUMO chains came as a surprise, as *in vivo* most

substrates are decorated with single SUMO moieties –frequently at multiple sites, though (Johnson *et al.* 1999; Mahajan *et al.* 1998). Polymeric SUMO is possible, because the SUMO sequence itself contains lysine residues, which can serve as a docking site for another SUMO moiety. These residues lie in a favoring environment, a so-called sumoylation motif (see section 1.5) (Bylebyl *et al.* 2003; Tatham *et al.* 2001; Johnson *et al.* 2001; Bencsath *et al.* 2002). Generally, they are located in the flexible N-terminal appendix. While SUMO2/3 have only one such lysine, Lys11, Smt3 features three of them: Lys11, Lys15, and Lys19 (Johnson 2004; Tatham *et al.* 2001; Ulrich 2008). They are known as the canonical attachment sites. However, in the last few years it has become obvious that formation of polymeric SUMO chains is by far not restricted to these prominent lysine residues. For instance, rendering them inoperable as linkage sites by replacing them with arginine does not significantly reduce buildup of SUMO chains. Only exchange of all lysine residues present in SUMO inhibits polysumoylation (amongst other reports of this, it was confirmed in this work, though data not shown). Poly-SUMO chains accumulate upon heat shock, osmotic- and replicative stress (Vertegaal 2010). However, the relevance of SUMO chains is still not clear. In yeast, polysumoylation can be eliminated without notable effects on SUMO function or conjugates pattern (Bylebyl *et al.* 2003; Takahashi *et al.* 2003). Many endeavors have been made to unravel this puzzle, and for instance the discovery of SUMO-targeted ubiquitin ligases (see section 1.8) gave the explanation of polymeric SUMO one plausible direction, but the exact function of SUMO chains still awaits elucidation. The fact that they are rapidly turned over, hence scarce *in vivo*, is a major obstacle to investigations in that direction.

1.5 Sumoylation motif

Usually, SUMO is attached to a lysine residue embedded in the consensus motif $\Psi Kx E$ on the surface of a target protein. In this recognition pattern, Ψ stands for a hydrophobic residue, while “x” can be any residue. Of note, the glutamate is the most highly conserved position (Rodriguez *et al.* 2001; Sapetschnig *et al.* 2002). $\Psi Kx E$ is the recognition site for the E2 Ubc9 (Sampson *et al.* 2001), and the interaction between motif and enzyme are key to the conjugation mechanism (Bernier-Villamor *et al.* 2002; Lin *et al.* 2002; Reverter *et al.* 2005). Obviously, this motif is too short and too undefined to confer specificity on the sumoylation process. Indeed, more than one third of all proteins characterized to date contain such a patch, but only a small amount of them are sumoylated (Yang *et al.* 2006b). Consequently, there must be further determinants to account for accurate sumoylation. It has been shown that the

steric environment is another determinant for SUMO attachment signals (Pichler *et al.* 2005), likely, because the target lysine residue must be accessible to the SUMO-conjugating machinery. Apart from secondary structure elements factoring in, extended variants of the core consensus motif were described. Among them were a negatively charged amino acid-dependent sumoylation motif (NDSM) (Yang *et al.* 2006b), and a phosphorylation-dependent sumoylation motif (PDSM). For both of them, clusters of residues downstream of the Ψ KxE core were found to strengthen the interaction between substrate and Ubc9, thereby promoting SUMO conjugation (Yang *et al.* 2006b; Mohideen *et al.* 2009; Hietakangas *et al.* 2006). There are also reports of sumoylation of the inverted motif [(E/D)xK Ψ] (Ivanov *et al.* 2007; Matic *et al.* 2010). In addition to that, several proteins have been found to be modified on sites that do not conform to Ψ KxE (Hendriks *et al.* 2014; Adamson *et al.* 2001; Ishov *et al.* 1999; Lin *et al.* 2003; Chakrabarti *et al.* 2000; Picard *et al.* 2012). Indeed, this seems to be quite frequently the case (Hendriks *et al.* 2014). Taken together, the exact set of determinants for sumoylation remains elusive.

1.6 SUMO interacting motif

At its basis, units of SUMO attached to a target protein create a new interaction platform on the surface of this protein. In order for this role to be fulfilled, there must be patches in the respective interaction partners that recognize SUMO. In 2000, the first conserved SUMO-interacting motifs (SIMs) were reported (Minty *et al.* 2000). SIMs are typically composed of a hydrophobic core with the loose consensus sequence V/L/I-x-V/L/I-V/L/I (x = any amino acid) and several acidic amino acids, frequently juxtaposing the core (Minty *et al.* 2000; Song *et al.* 2004; Hecker *et al.* 2006; Kerscher 2007). Frequently, SIMs are located in unstructured protein regions. Upon binding, the hydrophobic core arranges itself in a β -strand conformation that fits in a pocket of SUMO formed by its α_1 -helix and its β_2 -strand (Hecker *et al.* 2006; Song *et al.* 2005). The core motif binds SUMO in a parallel or anti-parallel orientation, depending on the distribution of the negatively charged residues, that extends the SUMO β -sheet (Gareau and Lima 2010; Reverter and Lima 2005; Song *et al.* 2005). This allows interactions between the aliphatic residues of the SIM and the hydrophobic pocket of SUMO. The negatively charged residues can be decisive for the affinity, polarity, as well as for the paralogue-specificity of the SUMO/SIM interaction, probably by salt bridging and hydrogen bonding with conserved basic residues on the SUMO surface (Meulmeester *et al.* 2008; Hecker *et al.* 2006; Chang *et al.* 2011). So far, three different types of SIMs are known:

SIMa ($\Psi\Psi_x\Psi A_{c_n}$), SIMb ($\Psi\Psi DLT$) and SIMr, ($A_{c_n}\Psi_x\Psi\Psi$) (Praefcke *et al.* 2012; Sriramachandran *et al.* 2014). In the bracketed description, Ψ is a hydrophobic residue (V, I or L), n is a number between two and five, and Ac stands for Asp, Glu or Ser. Even though it is not an acidic amino acid, Ser is frequently found in SIMs, probably due to it being a target for phosphorylation (Sriramachandran and Dohmen 2014). Compared to the 16 known ubiquitin-binding domains (Grabbe *et al.* 2009), the diversity of SIMs as it is to date is small. This might indicate that there are additional types of SIMs, still awaiting their discovery.

1.7 The ubiquitin-proteasome system

A eukaryotic cell has two main systems for protein degradation: The lysosomal pathway and the ubiquitin-proteasome system (UPS) (Haas *et al.* 2008; Laney *et al.* 2001). While the former is autophagy-based, degrading extracellular proteins that have been imported into the cell by pinocytosis or endocytosis, the UPS operates the degradation of intracellular proteins (Hochstrasser 1995; Goldberg 1995). It degrades approximately 80-90 % of the intracellular proteins involved in every cellular function and process (Chen *et al.* 2010). Compared to the autophagy-lysosome system, this degradation pathway is highly selective.

The UPS consists of many different molecules, with the main players being ubiquitin, ubiquitinating enzymes, deubiquitinating enzymes (DUBs), and proteasomes (Zhong *et al.* 2016). The 26S proteasome is a 673-kDa multi-catalytic proteinase complex, which is found in the nucleus as well as in the cytosol (Chen and Dou 2010; Lowe *et al.* 1995). It is composed of several subunits: The 20S core particle consists of 28 subunits, 14 α -subunits, each weighting 25.8 kDa, and 14 β -subunits (22.3 kDa each), which form a barrel-shaped structure of four stacked rings arranged in a $\alpha_7\beta_7\beta_7\alpha_7$ -manner (Lowe *et al.* 1995). This is the proteolytic heart of the proteasome. The core is capped at one or both ends by the 19S regulatory particle. The 19S regulatory particle can be further subdivided into the lid- and the base subcomplexes. The former consists of ~ 10 subunits; the latter features 6 AAA-type ATPases plus 2 non-ATPase subunits (Sauer *et al.* 2011). A simplified overview of the UPS is given in Figure 3.

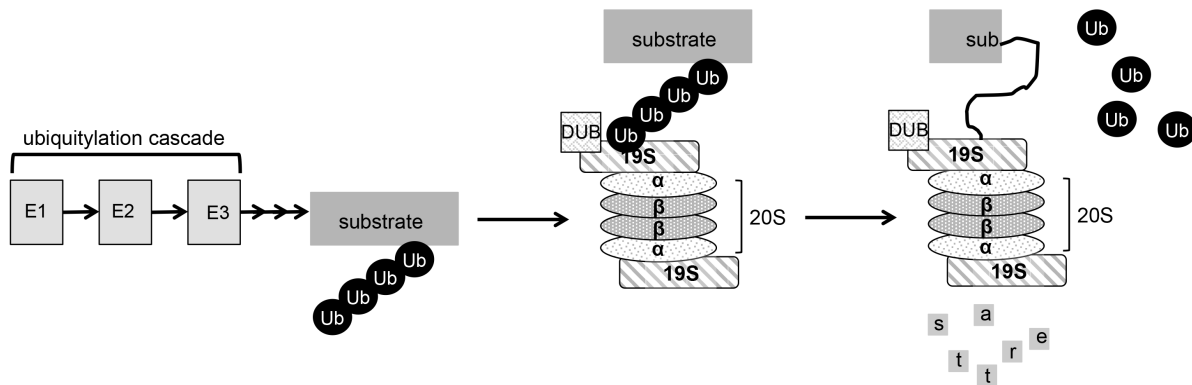


FIGURE 3: Schematic representation of the UPS pathway of degradation. Sizes of the individual components are not proportionate. A substrate is polyubiquitinated via an enzymatic cascade analogous to the sumoylation cascade presented in Fig. 2. Thereby, it is targeted to the 26S proteasome, a barrel-shaped protease consisting of multiple subunits. Before fed into the proteolytic core (20S), deubiquitinating enzymes dismantle the ubiquitin chain and the 19S regulatory particle unfolds the substrate protein.

The degradation signal is ubiquitin, a highly conserved 76-amino acid protein (Goldknopf *et al.* 1977). Ubiquitinated proteins are recognized by receptors in the 19S particle. Proteasome-attached DUBs remove ubiquitin from the target protein, before it is unfolded by ATPases in the 19S base. From there, the polypeptide is translocated into the 20S core for destruction. Three different proteolytic activities act there: Chymotryptic-, tryptic- and caspase-like activities attack the target, and typically cleave it into peptides of 4-25 amino acids (Voges *et al.* 1999; Geng *et al.* 2012; Groll *et al.* 2000; Köhler *et al.* 2001a; Köhler *et al.* 2001b). The ubiquitin molecules liberated before the destruction process add to the pool of free ubiquitin competent to be used in another round of target protein ubiquitination.

1.8 SUMO-targeted ubiquitin ligases

The SUMO- and the ubiquitin pathways maintain a certain level of crosstalk. For long, it has been thought that this was of purely antagonistic nature (Ulrich 2005). Therefore, it came as a surprise when it was found that the two also work hand in hand. SUMO-targeted ubiquitin ligases (STUbLs) [also known as ubiquitin ligases for sumoylated proteins (ULS)] recognize poly-SUMO chains and decorate them with ubiquitin (Uzunova *et al.* 2007; Perry *et al.* 2008; Lallemand-Breitenbach *et al.* 2008). This files the target protein in the UPS pathway of degradation (Praefcke *et al.* 2012; Sriramachandran and Dohmen 2014; Uzunova *et al.* 2007; Perry *et al.* 2008; Heideker *et al.* 2009; Geoffroy *et al.* 2009; Hunter *et al.* 2009). In the last decade, several STUbLs have been identified by the presence of SIMs, their interaction with SUMO, or via homology studies (Weisshaar Stefan R. 2008; Sun *et al.* 2007; Prudden *et al.* 2007; Xie *et al.* 2007; Köhler *et al.* 2015; Westerbeck *et al.* 2014). The proteins distinguish

themselves by combining two features in their structures: A RING-finger domain (variants of zinc-fingers that coordinate two zinc atoms in a cross-brace structure; mediates protein-protein interaction (Borden *et al.* 1995; Saurin *et al.* 1996)) that allows for interaction with a ubiquitin-conjugating enzyme, and several SIMs. The former characterizes them as ubiquitin ligases, the latter as SUMO-binding proteins (Sriramachandran and Dohmen 2014; Uzunova *et al.* 2007; Perry *et al.* 2008). The existence of more than one SIM in STUbLs enables them to selectively ubiquitinate target proteins that carry poly-SUMO chains (Hannich *et al.* 2005; Uzunova *et al.* 2007; Lallemand-Breitenbach *et al.* 2008; Sun *et al.* 2007; Prudden *et al.* 2007; Xie *et al.* 2007; Weisshaar *et al.* 2008; Tatham *et al.* 2008). In *S. cerevisiae*, to date two STUbLs have been identified, named Uls1 and Uls2. Uls1 (also known as Ris1, Dis1 and Tid4) is a 1612-amino acid protein accommodating a RING finger motif, a Swi2/Snf2-like translocase domain, and four predicted SIMs (Hannich *et al.* 2005; Sriramachandran and Dohmen 2014; Uzunova *et al.* 2007). Uls2, in contrast, is a heterodimer consisting of Slx5 and Slx8. Slx5 (synthetic lethal of unknown function 5; also known as Hex3) contains two SIMs and a RING finger domain (Uzunova *et al.* 2007; Xie *et al.* 2007; Ii *et al.* 2007; Wang *et al.* 2006). Aberrant levels of the human STUbL Rnf4 have been implicated in a number of diseases including cancer (Perry *et al.* 2008; Pero *et al.* 2001). This highlights the importance of STUbLs for cellular homeostasis.

In summary, linking ubiquitin and SUMO pathways, STUbLs represent another regulatory mechanism for levels of sumoylated forms of a substrate.

1.9 Desumoylating enzymes

Posttranslational modification in general offers the opportunity to provoke much faster responses than regulation via transcription alteration. Sumoylation is not an exception: It provokes an immediate cellular response to various intracellular signals and extracellular stimuli. Obviously, for this regulatory mechanism detachment of the modification is as important as conjugation. Deconjugation is carried out by specific enzymes broadly referred to as SUMO proteases. They cleave between the terminal Gly of SUMO and the Lys residue on the substrate it is attached to. Some SUMO proteases are also capable of processing SUMO precursors, thereby making it competent for conjugation in the first place.

SUMO proteases are not only responsible for maturation of nascent SUMO, and deconjugation of the modifier from its target, but by doing so they also regulate the pool of conjugation-competent SUMO in the cell (Xu *et al.* 2009). All known SUMO-specific proteases are cysteine proteases featuring a papain-like proteinase fold (Hickey *et al.* 2012).

Although they share some catalytic features, the different superfamilies distinguish themselves by the specific fold of their catalytic domains (Hickey *et al.* 2012). All SUMO-specific peptidases of the Ulp/SEN1 superfamily known to date belong to the C48 family of thiol proteases (Hickey *et al.* 2012; Shin *et al.* 2012; Schulz *et al.* 2012).

The first SUMO-specific protease to be described was the budding yeast enzyme ubiquitin-like protein-specific protease 1 (Ulp1) (Li *et al.* 1999). Shortly thereafter, sequence comparison of its catalytic domain to databases uncovered the existence of a second protease of that kind in *S. cerevisiae*, Ulp2 (Li *et al.* 2000a), as well as the first mammalian SUMO protease SENP1 (Gong *et al.* 2000), and many others in various organisms (Mukhopadhyay and Dasso 2007).

1.9.1 Structures of SUMO proteases and catalytic mechanism

In 2001, the first structure of a SUMO-specific protease was solved. It was the catalytic domain of Ulp1 in complex with Smt3 trapped in a transition-state-like conformation (Mossessova *et al.* 2001). The high-resolution insight into its active site confirmed Ulp1 to belong to the cysteine proteases, as its sequence similarity to the adenovirus processing protease (AVP) had previously suggested (Li and Hochstrasser 1999). The structure revealed that Ulp1 makes contact with Smt3 via an extensive surface area, and that unique hydrophilic interactions and a high number of salt bridges account for its specificity for SUMO. Notably, Ulp/SEN1 proteases bind SUMO via surfaces distinct from SIMs (Hickey *et al.* 2012; Mossessova and Lima 2001). The active-site pocket harbors the catalytic triad (His-Asp-Cys) and an additional fixed Gln residue in close proximity, which stabilizes the transition state during catalysis (Mossessova and Lima 2001; Reverter *et al.* 2004, 2006). The SUMO C-terminal diglycine motif is positioned in a shallow tunnel formed by the side chains of two Trp residues. This tunnel is so narrow that insertion of any residue other than glycine is sterically hindered (Mossessova and Lima 2001). Structures of SENP1 and SENP2 in complex with SUMO or sumoylated substrates showed many similarities, including the Trp tunnel and SUMO-enzyme interfaces (Reverter and Lima 2004, 2006; Shen *et al.* 2006a; Shen *et al.* 2006b). The structures of SENP1 and -2 bound to real substrates revealed that the scissile bond (= bond that is subject to cleavage) is oriented in a *cis* configuration with respect to the amide nitrogens for cleavage. It is kinked in a right angle to the C-terminus of SUMO (Reverter and Lima 2006; Shen *et al.* 2006a). If in *trans*, the nitrogen atoms would cause a clash between the residue C-terminal to the scissile peptide bond and the active site

loop of the protease. A *cis* arrangement positions the carbonyl group of the scissile bond in an optimal position for catalysis (Hay 2007).

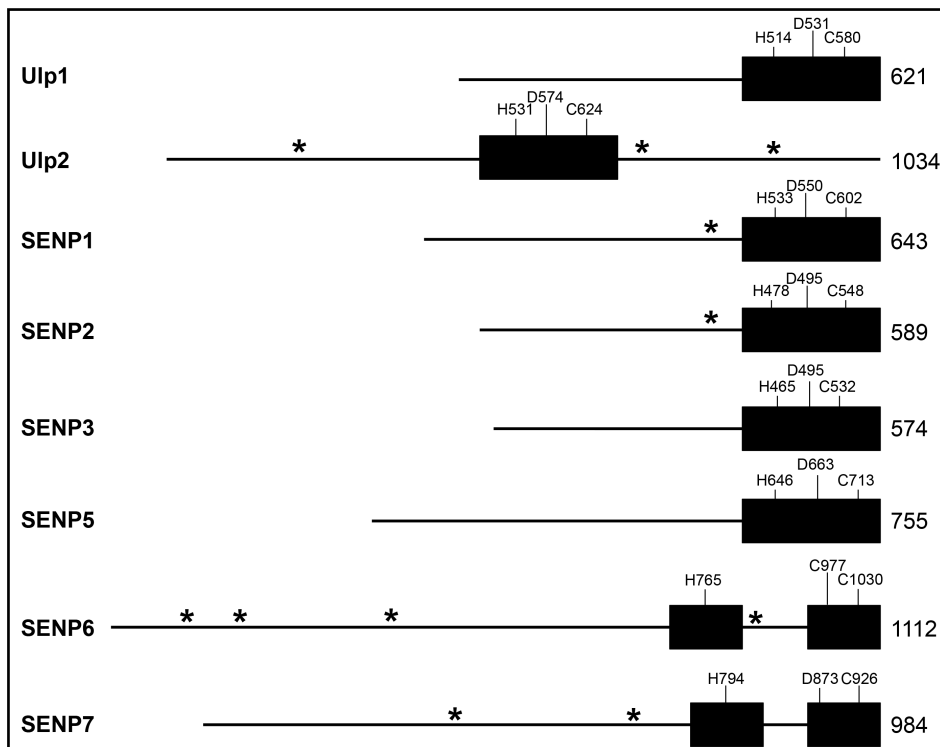


FIGURE 4: Domain architecture of Ulp/SENp family members. Black boxes = catalytic domains; line = non-catalytic domain; residues of catalytic triad are marked in one-letter code; total length of protease (in amino acids) is given on the far right of every schematic. Putative SIMs are indicated by asterisk (*).

Unlike other members of the Ulp/SENp family, Ulp2, SENP6 and SENP7 carry large loop insertions within their catalytic domains (Hickey *et al.* 2012) (Fig.4). SENP6 and SENP7 both have four of these. Resolution of the structure of the active domain of SENP7 showed that its loop1, which is not conserved in Ulp2, projects towards the putative SUMO binding interface, and mutant analysis indicated that it is decisive for SUMO paralogue specificity (Lima *et al.* 2008). So far, no structure information is available for SENP6.

1.9.2 Regulation of SUMO proteases

SUMO proteases are regulated in a number of different ways. Firstly, localization limits their activity radius (Kolli *et al.* 2010). Secondly, transcriptional regulation controls the abundance of e.g. specific SENPs. For instance, the promoter region of SENP1 contains androgen response elements as well as a hypoxia response element, thus is stimulated under such conditions. Additionally, it has been proposed that SENP1 itself triggers its own transcription via a positive feedback loop (Bawa-Khalife *et al.* 2007; Xu *et al.* 2010; Cheng *et al.* 2007).

SEN2, in contrast, participates in a negative feedback loop (Lee *et al.* 2011). Thirdly, SUMO proteases are frequently subject to post-translational modification, influencing their activity and/or stability. For example, under normal conditions, SENP3 is ubiquitinated and turned over via the UPS. Upon oxidative stress, its ubiquitination is attenuated (Kuo *et al.* 2008; Yan *et al.* 2010). Ulp2, in turn, is subject to cell cycle-dependent phosphorylation (Baldwin *et al.* 2009). Fourthly, protease activity can be directly affected by specific cellular stresses. To name just one, heat shock was found to render several SENPs irreversibly inactive (Pinto *et al.* 2012). Another very interesting activity-regulation mechanism has been suggested: SENP1 has been found to dimerize via an intersubunit disulphide bond in response to oxidative stress (Xu *et al.* 2008). Since the active-site cysteine was involved, the authors of that study proposed that the transient disulphide bond might protect the enzyme from irreversible oxidation of the catalytic cysteine residue.

Last but not least, shielding may play a role for the rate of desumoylation of a given substrate. Still not completely understood, substrate binding by other, competing cellular proteins can hinder SUMO proteases to process a target (Hickey *et al.* 2012; Xu *et al.* 2005).

1.9.3 Misregulated SUMO proteases

In the last decade, the SUMO cycle has attracted a considerable degree of attention since its deregulation has been associated with various pathological conditions including pathogen proliferation, neurological disorders or cancer (reviewed in e.g. (Droescher *et al.* 2013; Wimmer *et al.* 2012; Sarge *et al.* 2009)). At any given time during the cell cycle, a distinctive pattern of SUMO conjugates is observed (Kolli *et al.* 2010). Disturbance of the crosstalk between sumoylation and other post-translational modifications (e.g. ubiquitin) can easily tip over the finely tuned levels of sumoylated proteins and thereby severely impair homeostasis (shown for specific proteins by e.g. (Song *et al.* 2015; Dou *et al.* 2010; Román González-Prieto 2015; Liu *et al.* 2013; Mukhopadhyay *et al.* 2010a)). Unsurprisingly, SUMO-specific proteases have been found to be implicated in the development of several important conditions (Chun-Jie Huang 2015). In the last few years, misregulation of the two mammalian SUMO proteases SENP6 and SENP7 have been identified as a factor in development of certain types of cancer and other disorders. For example, recently, elevated SENP6 activity was reported to promote gastric cancer by liberating SUMO1 from the transcription factor FoxM1 (Song *et al.* 2015). SENP6 also plays a role in toll-like receptor (TLR) inflammatory signaling. SENP7, in turn, was found to modulate the stability of c-Myc,

an oncogene, by balancing out the STUbL pathway of degradation (Román González-Prieto 2015).

1.9.4 Proteases

1.9.4.1 In mammals

SUMO is also known as sentrin. This explains the naming of the first-discovered family of SUMO deconjugation enzymes in mammals, sentrin-specific proteases (SENPs). So far, six different, highly specific SUMO proteases have been identified: SENP1-3 and SENP 5-7 (Mukhopadhyay and Dasso 2007). They are tightly controlled, and are equipped with distinct features and biological significance in cells; accordingly, they are not redundant (Chun-Jie Huang 2015). On a side note: For some time, another protease identified in human cells was counted among them, and accordingly termed SENP8. However, SENP8 represents a special case: It is non-specific for SUMO, but, in fact, it is specific for neddylation. Neural-precursor-cell-expressed developmentally downregulated protein-8 (NEDD8) is a Ubl and conjugated to substrates in a process called neddylation (Shin *et al.* 2011; Kamitani *et al.* 1997). Appropriately, SENP8 is often referred to as human deneddylase 1 (DEN1) or NEDD8-specific protease (NEDP1) (Gan-Erdene *et al.* 2003; Wu *et al.* 2003; Mendoza *et al.* 2003). *In vitro*, desumoylation of specific substrates by individual SENPs is generally not strongly paralogue specific, even though the activity levels have been found to be different for some SENPs depending on the SUMO isoform they are confronted with. However, some of the SENPs have clear preferences for certain isoforms *in vivo* (Hickey *et al.* 2012). Due to their early connection to Ulp, SENPs have been grouped into two branches: the Ulp1 branch and the Ulp2 branch. The classification is made according to the architecture of their active domains. Those SENPs featuring unconventional elements, specifically big loop insertions, fall into the Ulp2 branch, all others are assigned to the Ulp1 branch (Mukhopadhyay and Dasso 2007; Hickey *et al.* 2012; Hay 2007; Nayak *et al.* 2014). Most SENPs localize in the nucleus or colocalize in distinguishable subnuclear compartments (Kolli *et al.* 2010). Since many cytoplasmic proteins, e.g. FAK, NEMO and I κ B α , have been found to be sumoylated at some point (Shin *et al.* 2012; Kadaré *et al.* 2003; Mabb *et al.* 2006; Takahashi *et al.* 2008), it has long been speculated on how their respective SUMO modifications would be removed. Recently, a new class of desumoylation enzymes was discovered in mammalian cells and characterized to some degree: Desumoylating isopeptidases (DeSI), of which currently two members (DeSI-1 and DeSI-2) are known (Shin

et al. 2012). They belong to the C97 family of proteases. DeSIs recognize substrates distinct from SENP targets, suggesting that they are highly selective for specific substrates. As just one example, DeSI-1 specifically desumoylates the transcription repressor BZEL (Shin *et al.* 2012). Interestingly, DeSI-1 and DeSI-2 have been suggested to feature only a catalytic dyad (Suh *et al.* 2012). However, this hypothesis requires structural analysis of a DeSI in complex with SUMO, which is not available yet. Shortly after the identification of DeSIs, a third type of SUMO proteases was found. Ubiquitin-specific protease-like 1 (USPL1), a low-abundance protein, localizes exclusively in cajal bodies, where it plays an essential role (Schulz *et al.* 2012). Of note, this role is separate from its catalytic activity. USPL1 belongs to the C98 family of proteases and is neither related to the Ulp/SENP-, nor to the DeSI family. However, its catalytic domain shows some homology to the C19 family of ubiquitin-specific proteases (Schulz *et al.* 2012). Taken together, to date there are three distinct classes of SUMO proteases in humans. This is reminiscent of the diversification seen for deubiquitinating enzymes (DUBs), which are each filed into one of five structural classes (Komander *et al.* 2009). However, the paralogue diversity within the DUB superfamily exceeds by far the number of SUMO-specific enzymes, with ~100 predicted DUBs, none of these resembling Ulps or SENPs. Though, as its name indicates, USPL1 shows remote similarity to the USP class of DUBs (Schulz *et al.* 2012). Considering the plethora of sumoylated proteins which has already been found in mammals (Li *et al.* 2004; Zhao *et al.* 2004b; Yang *et al.* 2015), it is likely that there are even more SUMO protease families, yet to be identified.

1.9.4.2 In budding yeast

To date, in *S. cerevisiae* two SUMO-specific proteases are known, Ulp1 and Ulp2. Genetic studies with yeast strains carrying mutations in either of the two revealed distinct phenotypic defects in the absence of each protease, as well as unique sumoylation patterns in the different strains, indicating distinct substrate specificity (Li *et al.* 2000b). Localization in the cell strongly influences this selectivity.

1.9.4.2.1 Ulp1

As mentioned above, the 621-amino acid enzyme Ulp1 was the first SUMO-specific protease to be discovered. It is essential, and the temperature sensitive mutants, with whom it has been studied *in vivo*, exhibit a severely sick phenotype even at permissive temperature (Li and Hochstrasser 1999; Li *et al.* 2003; Soustelle *et al.* 2004). Despite their common classification, Ulp1 distinguishes itself from Ulp2 by its ability to process SUMO precursors in addition to

general SUMO deconjugation (Li and Hochstrasser 1999, 2003). Unlike Ulp2, Ulp1 lends itself very well to recombinant expression in *E. coli* and *in vitro* analysis (Li and Hochstrasser 1999; Mossessova and Lima 2001). Even high-definition structural information is available for Ulp1 –alone and in complex with Smt3 (Mossessova and Lima 2001; Xu *et al.* 2008). This, however, only allows limited insight into what might be true for Ulp2, since the catalytic domains of the two Ulp1s are only ~27 % identical, and there is no obvious similarity at all between their non-catalytic domains (Li and Hochstrasser 2000a; Schwienhorst 2000). Despite all this information that has been collected about Ulp1, its substrate selectivity, like for Ulp2, is still poorly understood. However, as correct localization of Ulp1 seems to be highly important for cell homeostasis, its spatial sequestration might be a crucial part of that. Ulp1 localizes at the nuclear periphery, primarily to the inner surface of the nuclear pore complex (NPC) (Li and Hochstrasser 2003; Panse *et al.* 2003; Palancade *et al.* 2007; Lewis *et al.* 2007; Zhao *et al.* 2004a). Precisely, it interacts with Pse1, Kap95 and Kap60 via its NPC-targeting domain, that comprises the first 340 residues of the enzyme (Panse *et al.* 2003). A Ulp1 mutant, in which this domain is deleted, localizes throughout the cell (Li and Hochstrasser 2003), and causes accumulation of Rad52 foci, which indicate endogenous DNA damage and repair (Palancade *et al.* 2007). Notably, when this truncated version of Ulp1 is expressed in a Ulp2-deficient strain, it partially suppresses several growth defects coming along with a *ULP2* knockout, and reduces the levels of sumoylated Ulp2 substrates (Li and Hochstrasser 2003). This, as well, highlights the importance of a tight restriction of Ulp1 localization in order to control its *in vivo* activity. Even more so, high levels of Ulp1 activity mislocalized to the nucleoplasm have been found to be lethal (Li and Hochstrasser 2003; Panse *et al.* 2003). Interestingly, transiently during M-phase a fraction of Ulp1 is exported to the cytoplasm, where it desumoylates septin proteins (Takahashi *et al.* 2000; Elmore *et al.* 2011; Makhnevych *et al.* 2007). Septins are heavily sumoylated in a cell-cycle dependent manner and arrange into filaments at the bud neck of dividing cells (Takahashi *et al.* 2008). The details of this temporary Ulp1 delocalization still await their discovery.

1.9.4.2.2 Ulp2

The second known SUMO-specific protease in *S. cerevisiae*, Ulp2, is far less studied than Ulp1. At least in parts, this is because this 1034-amino acid protein is not easy to recombinantly express and has exhibited very weak enzymatic activity *in vitro* in previous

studies (Li and Hochstrasser 2000b). This is just one of many features it shares with its mammalian orthologs SENP6 and SENP7 (Lima and Reverter 2008; Drag *et al.* 2008). *In vivo*, Ulp2 has been studied to a much larger extent.

1.9.4.2.2.1 *Ulp2 regulation and localization*

Ulp2 is a low-abundance, cell cycle-regulated phospho-protein (Baldwin *et al.* 2009; Strunnikov *et al.* 2001). It is phosphorylated during mitosis at at least two sites in the C-terminal non-catalytic domain (CTD), and this transient modification is dependent on Cdc5 and cyclin-dependent kinase 1 (Cdk1) (Baldwin *et al.* 2009). Indeed, Cdc5 revealed itself as a negative regulator of Ulp2 when it was found that two known Ulp2 targets, Top5 and Pds5, fail to accumulate in a sumoylated state in the absence of Cdc5 (Baldwin *et al.* 2009). Apart from this, Ulp2 is spatially controlled. Ulp2 localizes throughout the nucleus and occasionally the nucleolus (Kroetz *et al.* 2009; Srikumar *et al.* 2013). Its nuclear localization is critical for most, if not all, functions of the protease (Kroetz *et al.* 2009). A strain in which Kap95, a nuclear import receptor, is mutated, is defective in nuclear import of Ulp2, which results in aberrant accumulation of poly-SUMO structures (Kroetz *et al.* 2009). Ulp2 binds chromatin and has been suggested to desumoylate chromatin-associated proteins such as histones and topoisomerase II (Hannich *et al.* 2005; Strunnikov *et al.* 2001; Bachant *et al.* 2002; Nathan *et al.* 2006). Overexpression of it suppresses defects in chromosome condensation and segregation, pointing towards a role in regulating these processes (Meluh and Koshland 1995; Strunnikov *et al.* 2001). This function is conserved in the analogous enzymes in *C. elegans* and humans (Mukhopadhyay *et al.* 2010a; Pelisch *et al.* 2014).

1.9.4.2.2.2 *The ULP2 knockout mutant*

A *ULP2* knockout mutant has a very distinct phenotype: Apart from abnormal cell morphology and a severe growth- and sporulation defect, *ulp2-Δ* exhibits elevated levels of chromosome loss and delayed recovery after DNA-damage induced cell-cycle checkpoint arrest. What is more, that strain is highly sensitive to various stresses like hydroxyurea, temperature and DNA-damaging agents (Li and Hochstrasser 2000a; Schwienhorst 2000; Strunnikov *et al.* 2001; Bachant *et al.* 2002; Schwartz *et al.* 2007). Another very prominent feature of the *ulp2* knockout is the accumulation of high-molecular weight (HMW) SUMO conjugates, so big they hardly penetrate the resolving gel upon SDS-PAGE analysis (Bylebyl *et al.* 2003).

Like its mammalian orthologs SENP6 and SENP7, Ulp2 has been found to be capable of dismantling long poly-SUMO chains (Bylebyl *et al.* 2003; Lima and Reverter 2008;

Mukhopadhyay *et al.* 2006). Indeed, previous studies established a correlation between loss of SENP6 or Ulp2 and a failure to disassemble poly-SUMO chains (Bylebyl *et al.* 2003; Mukhopadhyay *et al.* 2006).

1.9.4.2.2.3 *Ulp2 domain architecture and functions*

Apart from its catalytic domain, Ulp2 has large C- and N-terminal non-catalytic domains. Utilizing truncation mutants, the CTD has been identified as a requirement for efficient depolymerization of large poly-SUMO conjugates (Kroetz *et al.* 2009). However, that mutant showed an only minor growth defect, suggesting that factors other than the HMW SUMO species also account for the growth defects of *ulp2*- Δ cells, or that such conjugates can be tolerated to some extent. It has been suggested that, in addition to SUMO chain deconjugation, the growth-regulating roles of Ulp2 involve removal of SUMO from specific target proteins (Kroetz *et al.* 2009). Very recently, a study using a quantitative mass spectrometry approach to analyze the effects of *ulp1* and *ulp2* mutations on the intracellular sumoylation pattern found that Ulp2 has a highly specific desumoylation activity *in vivo*, while Ulp1 exhibits a broader specificity towards many substrates (de Albuquerque *et al.* 2016). This fortified previous findings, which indicated that Ulp2 has critical functions in the depolymerization of poly-SUMO modification on specific substrates (Bylebyl *et al.* 2003; Kroetz *et al.* 2009).

In general, Ulp-class SUMO proteases have extensive, poorly conserved N-terminal non-catalytic domains (NTDs). These NTDs are associated with subcellular localization and regulation of activity (Hickey *et al.* 2012; Kroetz *et al.* 2009). Previous studies showed that the NTD of Ulp2 is necessary and sufficient for nuclear localization of the enzyme (Kroetz *et al.* 2009). It contains two short nuclear-localization signal (NLS)-like motifs, either of which alone is sufficient to sustain nuclear localization and function of Ulp2 (Kroetz *et al.* 2009). Indeed, in that study it was found that a single 7-amino acid long NLS makes the entire NTD obsolete. Fusing it to a corresponding Δ NTD mutant of Ulp2 restored Ulp2 *in vivo* functionality almost completely, suggesting that the low sequence conservation of the NTDs might be due to the fact that only the NLS in this part of the protein are relevant for its proper cellular function (Kroetz *et al.* 2009).

Both the NTD and CTD of Ulp2 are predicted to lack stable tertiary fold to large extents (Kroetz *et al.* 2009). Intrinsically disordered protein regions are frequently implicated in low-affinity but high-specificity protein-protein interactions (Dyson *et al.* 2005). Ulp2 non-catalytic domains contain three predicted SIMs: one in the NTD, and two in the CTD (Kroetz

et al. 2009). One of the two C-terminal SIMs is located directly adjacent to the catalytic domain and has already been subject to several studies (Baldwin *et al.* 2009; Kroetz *et al.* 2009). Still, the specific function of any of the three motifs is unknown.

1.9.4.2.3 Wss1

The list of SUMO-specific proteases in budding yeast would not be complete without mentioning Wss1. Originally, weak suppressor of smt3-33 (Wss1) was identified as a suppressor of the temperature sensitive phenotype produced by an L26S SUMO mutation (Biggins *et al.* 2001), and has been implicated in the response to genotoxic stress (O'Neill *et al.* 2004).

For a short period of time, Wss1 was regarded as the possible missing link between SUMO- and ubiquitin metabolisms, as it exhibited some deubiquitination activity to ubiquitin-SUMO mixed species and depolymerized SUMO chains *in vitro*, and physically associated with the 26S proteasome (Mullen *et al.* 2010). However, these findings were under debate ever since they had been published, and further studies could not confirm the SUMO- or ubiquitin- isopeptidase activity (Su *et al.* 2010; Stinglee *et al.* 2014; Balakirev *et al.* 2015). As it turns out, rightfully so. In 2014, Wss1 was newly classified as a DNA-dependent protease involved in repair of DNA-protein crosslinks (Stinglee *et al.* 2014). A later study identified Wss1 as an inactive metalloprotease under normal conditions that is activated by single-strand DNA upon genotoxic stress via a cysteine-switch regulatory mechanism. Downregulation of Wss1 activity was found to be mediated by autoproteolysis. Contrasting the aforementioned study, it was shown to have a SUMO ligase-like activity and to promote poly-sumoylation of proteins with which it interacts. This includes Cdc48. Indeed, Wss1 forms a ternary complex with the AAA ATPase Cdc48 and the adaptor protein Doa1. Upon DNA damage, this complex is recruited to already sumoylated targets and promotes elongation of their SUMO chains (Balakirev *et al.* 2015). Taken together, Wss1 seems to be a highly interesting protein, but in terms of activity profile it is not to be named in one line with the Ulp.

1.10 Thesis objectives

The main interest of this work was to characterize Ulp2 on the level of the molecule. Data on the enzyme itself was scarce, since it was fractious as a study object. However, in order to assume structure-function relationships, this hurdle had to be overcome.

This study set out to analyze the following aspects:

- 1) What are the requirements for a SUMO chain to serve as a Ulp2 target?

- 2) How does Ulp2 process a target chain? Randomly or in an ordered manner?
- 3) What is the molecular/structural basis on which the Ulp2/SUMO interactions are based?
- 4) What is the basis of the proteolysis defect in *ulp2-Δ*?
- 5) How do its preferences and mechanistic conditions influence Ulp2's activity *in vivo*?

Previous work had shown that the absence of Ulp2 causes a severe proteolysis defect in *S. cerevisiae*, adding up to an already highly interesting phenotype of the *ulp2-Δ* mutant. This was the starting point for further functional characterization of Ulp2 *in vivo*, which is addressed in the last part of this work.

2 Material and Methods

2.1 Material

2.1.1 *Escherichia coli* strains

Tab.1: *E. coli* strains used in this study.

Strain	Genotype/relevant genotypic characteristics	Source
XL1 Blue	recA1 endA1 gyrA96 thi-1 hsdR17 supE44 relA1 lac [F' proAB lacIqZΔM15 Tn10 (Tetr)]	Stratagene
BL21-CodonPlus	<i>E. coli</i> B F ⁻ dcm ompT hsdS(rB ⁻ mB ⁻) gal λ(DE3)[pLysS Camr]	Novagene
BL21(DE3)	<i>E. coli</i> str. B F ⁻ ompT gal dcm lon hsdS _B (rB ⁻ mB ⁻) λ(DE3 [lacI lacUV5-T7 gene 1 ind1 sam7 nin5]) [malB ⁺] _{K-12} (λ ^S)	Novagene

2.1.2 *Saccharomyces cerevisiae* strains

Tab.2: *S. cerevisiae* strains used in this study.

Strain	Relevant genotype	Source
JD47-13C	<i>MATa leu2-Δ1 trp1-Δ63 his3-Δ200 ura3-52 lys2-801 ade2-101</i>	Dohmen <i>et al.</i> (1995)
yJE1	<i>MATa ulp2-Δ::HIS3 smt3-KallR::TRP1</i>	This work
yJE2	<i>MATa pdr5-Δ::nat smt3-HA ulp1-I615N</i>	This work
MS84	<i>MATa pdr5-Δ::nat smt3-HA</i>	lab collection
MS87	<i>MATa pdr5-Δ::nat ulp2-Δ::HIS3 smt3-HA</i>	lab collection
MS91	<i>MATa pdr5-Δ::nat smt3-HA wss1::hygB</i>	lab collection
yKU1	<i>MATa ulp2-Δ::HIS3</i>	lab collection
sul25-2	<i>MATa ulp2-Δ::HIS3 uba2-ts9</i>	lab collection
smt3-KallR	<i>MATa smt3-KallR::TRP1</i>	Erica Johnson

2.1.3 Plasmids

Tab.3: Plasmids used in this study.

Plasmids for yeast are described as such. For all others, the description indicates the recombinant protein(s) encoded in them. TEVp.r.s. = TEV protease recognition site; His₆ = hexahistidine tag; T = terminator; P = promoter; CYC1 = cytochrome c-1; CUP1 = metallothionein.

Plasmid name	Description	Source
pACYC-Duet-Aos1p/Uba2p	His ₆ -Aos1, Uba2-Stag	J. Wohlschlegel (Wohlschlegel <i>et al.</i> 2006)
pRSF-Duet-Ubc9/Smt3p	His ₆ -Smt3, Ubc9-Stag	J. Wohlschlegel (Wohlschlegel <i>et al.</i> 2006)
pRSF-Duet-Ubc9/Smt3p-K11R,K15R,K19R	His ₆ -Smt3(K11R,K15,K19R), Ubc9-Stag	M. Schnellhardt
pHUp41	His ₆ -Ubp41	R. Baker
pMAF17	P _{CUP1} -UB-R-e ^K -HA-Ura3-T _{CYC1} ; yeast expression plasmid	M. Froehlich
pMAF60	P _{CUP1} -UB-V ₇₆ -e ^K -DHFR-2xHA-T _{CYC1} ; yeast expression plasmid	M. Froehlich
PCA129	P _{CUP1} -PRS316-stp-102-3xHA-T _{CYC1} ; yeast expression plasmid	C. Andreasson
pLS1	FLAG-Smt3-ΔN17Smt3(M0)-3xΔN17Smt3-eGFP-HA-His ₆	L. Schürholz
pLS2	FLAG-Smt3-ΔN17Smt3(M1)-3xΔN17Smt3-eGFP-HA-His ₆	L. Schürholz
pLS3	FLAG-Smt3-ΔN17Smt3(M2)-3xΔN17Smt3-eGFP-HA-His ₆	L. Schürholz
pLS5	FLAG-Smt3-ΔN17Smt3(M4)-3xΔN17Smt3-eGFP-HA-His ₆	L. Schürholz
pLS6	FLAG-Smt3-ΔN17Smt3(M5)-3xΔN17Smt3-eGFP-HA-His ₆	L. Schürholz
pLS7	FLAG-Smt3-ΔN17Smt3(M6)-3xΔN17Smt3-eGFP-HA-His ₆	L. Schürholz
pJE2	FLAG-Ubiquitin-1xΔN17Smt3-eGFP-HA-His ₆	This work
pJE3	FLAG-Ubiquitin-2xΔN17Smt3-eGFP-HA-His ₆	This work
pJE4	FLAG-Ubiquitin-3xΔN17Smt3-eGFP-HA-His ₆	This work
pJE5	FLAG-Ubiquitin-4xΔN17Smt3-eGFP-HA-His ₆	This work
pJE6	FLAG-Smt3-eGFP-HA-His ₆	This work
pJE7	FLAG-Smt3-ΔN17Smt3-eGFP-HA-His ₆	This work
pJE8	FLAG-Smt3-2xΔN17Smt3-eGFP-HA-His ₆	This work
pJE9	FLAG-Smt3-3xΔN17Smt3-eGFP-HA-His ₆	This work
pJE10	FLAG-Smt3-4xΔN17Smt3-eGFP-HA-His ₆	This work
pJE12	MBP~TEVp.r.s.~Ulp2-FLAG	This work
pJE14	FLAG-eGFP-HA-His ₆	This work
pJE18	MBP~TEVp.r.s.~Ulp1-FLAG	This work
pJE20	FLAG-Smt3(G98A)-4xΔN17Smt3-eGFP-HA-His ₆	This work
pJE22	FLAG-5xΔN17Smt3-eGFP-HA-His ₆	This work
pJE23	MBP~TEVp.r.s.~Ulp2(C624A)-FLAG	This work
pJE26	FLAG-Smt3(G98A)-ΔN17Smt3(G98A)-3xΔN17Smt3-eGFP-HA-His ₆	This work
pJE28	FLAG-Smt3(G98A)-His ₆	This work
pJE30	FLAG-Smt3(G98A)-ΔN17Smt3(G98A)-His ₆	This work
pJE31	FLAG-Smt3(G98A)-2xΔN17Smt3(G98A)-His ₆	This work
pJE32	FLAG-MBP-4xΔN17Smt3-eGFP-HA-His ₆	This work
pJE33	FLAG~TEVp.r.s.~Smt3-4xΔN17Smt3-eGFP-HA-His ₆	This work
pJE34	FLAG-SUMO1-4xΔN17Smt3-eGFP-HA-His ₆	This work
pJE37	FLAG-2xUbiquitin-4xΔN17Smt3-eGFP-HA-His ₆	This work
pJE38	FLAG-3xUbiquitin-4xΔN17Smt3-eGFP-HA-His ₆	This work
pJE42	FLAG-SUMO2-4xΔN17Smt3-eGFP-HA-His ₆	This work
pJE43	FLAG-Smt3(G98A)-Ubiquitin-3xΔN17Smt3-eGFP-HA-His ₆	This work
pJE44	FLAG-Smt3(G98A)-SUMO2-3xΔN17Smt3-eGFP-HA-His ₆	This work
pJE45	FLAG-Smt3(M0)-4xΔN17Smt3-eGFP-HA-His ₆	This work
pJE50	FLAG-Smt3(M2)-4xΔN17Smt3-eGFP-HA-His ₆	This work
pJE51	FLAG-Smt3(MEnd)-4xΔN17Smt3-eGFP-HA-His ₆	This work
pJE54	FLAG-Smt3-ubiquitin-3xΔN17Smt3-eGFP-HA-His ₆	This work

pJE55	FLAG-Smt3-SUMO2-3xΔN17Smt3-eGFP-HA-His ₆	This work
pJE56	FLAG-Smt3(M1)-4xΔN17Smt3-eGFP-HA-His ₆	This work
pJE69	FLAG-Smt3(M4)-4xΔN17Smt3-eGFP-HA-His ₆	This work
pJE70	FLAG-Smt3(M5)-4xΔN17Smt3-eGFP-HA-His ₆	This work
pJE71	FLAG-Smt3(M6)-4xΔN17Smt3-eGFP-HA-His ₆	This work
pJE76	FLAG-Smt3-ubiquitin-1xΔN17Smt3-eGFP-HA-His ₆	This work
pJE82	FLAG-SUMO2(Smt3 motifs M1, M5, MEnd)-4xΔN17Smt3-eGFP-HA-His ₆	This work
pJE83	FLAG-ubiquitin(Smt3 motifs M1 & M5 inserted in loop)-4xΔN17Smt3-eGFP-HA-His ₆	This work
pJE91	FLAG-3xSUMO2-eGFP-HA-His ₆	This work
pJE95	5'ΔULP1(I615N)-T _{ULP1} ; integrative yeast plasmid	This work
pJE100	FLAG-Ubi-MBP-4xΔN17Smt3-eGFP-HA-His ₆	This work
pJE101	MBP-Ubc9	This work
pJE102	MBP~TEVp.r.s.~Ulp2(411-774)-FLAG	This work
pJE103	MBP~TEVp.r.s.~Ulp2(411-693)-FLAG	This work
pJE104	MBP~TEVp.r.s.~Ulp2(1-774)-FLAG	This work
pJE105	MBP~TEVp.r.s.~Ulp2(411-1034)-FLAG	This work
pJE108	MBP~TEVp.r.s.~Ulp2(411-693;C624A)-FLAG	This work
pJE111	MBP~TEVp.r.s.~Ulp2(411-710)-FLAG	This work
pJE114	MBP~TEVp.r.s.~Ulp2(411-1034;C624A)-FLAG	This work
pJE115	MBP~TEVp.r.s.~Ulp2(1-774;C624A)-FLAG	This work
pJE116	MBP~TEVp.r.s.~Ulp2(411-1034; SIM2 mutated)-FLAG	This work
pJE117	MBP~TEVp.r.s.~Ulp2(1-774; SIM2 mutated)-FLAG	This work
pJE119	MBP~TEVp.r.s.~Ulp2(411-774; SIM2 mutated)-FLAG	This work
pJE120	MBP~TEVp.r.s.~Ulp2(411-774; C624A)-FLAG	This work
pJE127	MBP~TEVp.r.s.~(209-774)-FLAG	This work
pJE128	FLAG-Smt3-ΔN17Smt3(M2)-ΔN17Smt3-eGFP-HA-His ₆	This work
pJE130	FLAG-Smt3-ΔN17Smt3(M6)-ΔN17Smt3-eGFP-HA-His ₆	This work
pJE132	FLAG-SUMO2-2xΔN17Smt3-eGFP-HA-His ₆	This work
pJE133	FLAG-Smt3(M2)-2xΔN17Smt3-eGFP-HA-His ₆	This work
pJE134	FLAG-Smt3(M6)-2xΔN17Smt3-eGFP-HA-His ₆	This work
pJE135	FLAG-Smt3-SUMO2-ΔN17Smt3-eGFP-HA-His ₆	This work
pJE138	MBP-FLAG-TEVprotease(S219A)	This work
pJE144	MBP~TEVp.r.s.~Ulp2(411-710)-3xGly-His ₆	This work
pJE159	FLAG-Smt3-ΔN17Smt3-ΔN17Smt3(M0)-3xΔN17Smt3-eGFP-HA-His ₆	This work
pJE160	FLAG-Smt3-ΔN17Smt3-ΔN17Smt3(M1)-3xΔN17Smt3-eGFP-HA-His ₆	This work
pJE161	FLAG-Smt3-ΔN17Smt3-ΔN17Smt3(M2)-3xΔN17Smt3-eGFP-HA-His ₆	This work
pJE162	FLAG-Smt3-ΔN17Smt3-SUMO2-3xΔN17Smt3-eGFP-HA-His ₆	This work
pJE163	FLAG-Smt3-ΔN17Smt3-ΔN17Smt3(M4)-3xΔN17Smt3-eGFP-HA-His ₆	This work
pJE165	FLAG-Smt3-ΔN17Smt3-ΔN17Smt3(M5)-3xΔN17Smt3-eGFP-HA-His ₆	This work
pJE166	FLAG-Smt3-ΔN17Smt3-ΔN17Smt3(M6)-3xΔN17Smt3-eGFP-HA-His ₆	This work
pJE167	FLAG-Smt3(D61R)-4xΔN17Smt3-eGFP-HA-His ₆	This work
pJE168	FLAG-Smt3(S62A)-4xΔN17Smt3-eGFP-HA-His ₆	This work
pJE169	FLAG-Smt3(K54A)-4xΔN17Smt3-eGFP-HA-His ₆	This work
pJE171	FLAG-Smt3-ΔN17SUMO2(M6)-3xΔN17Smt3-eGFP-HA-His ₆	This work
pJE172	FLAG-Smt3(K54E)-4xΔN17Smt3-eGFP-HA-His ₆	This work
pJE173	FLAG-Smt3(K58A)-4xΔN17Smt3-eGFP-HA-His ₆	This work
pJE174	FLAG-Smt3(K58E)-4xΔN17Smt3-eGFP-HA-His ₆	This work
pJE175	FLAG-Smt3(E59A)-4xΔN17Smt3-eGFP-HA-His ₆	This work
pJE176	FLAG-Smt3(D61A)-4xΔN17Smt3-eGFP-HA-His ₆	This work
pJE177	FLAG-Smt3-ΔN17Smt3(D79K)-3xΔN17Smt3-eGFP-HA-His ₆	This work
pJE178	FLAG-Smt3-ΔN17Smt3(Q75D)-3xΔN17Smt3-eGFP-HA-His ₆	This work
pJE179	FLAG-Smt3-ΔN17Smt3(Q75A)-3xΔN17Smt3-eGFP-HA-His ₆	This work

pJE180	FLAG-Smt3- Δ N17Smt3(D74A)-3x Δ N17Smt3-eGFP-HA-His ₆	This work
pJE181	FLAG-Smt3- Δ N17Smt3(E78R)-3x Δ N17Smt3-eGFP-HA-His ₆	This work
pJE182	FLAG-Smt3- Δ N17Smt3(D79A)-3x Δ N17Smt3-eGFP-HA-His ₆	This work
pJE183	FLAG-Smt3- Δ N17Smt3(A73E)-3x Δ N17Smt3-eGFP-HA-His ₆	This work
pJE184	FLAG-Smt3- Δ N17Smt3(D74K)-3x Δ N17Smt3-eGFP-HA-His ₆	This work
pJE189	FLAG-Smt3- Δ N17 ₁₇ Smt3(MEnd)-3x Δ N17Smt3-eGFP-HA-His ₆	This work

2.1.4 Material

2.1.4.1 Chemicals and consumables

Tab. 4: Chemicals and consumables used in this study.

Name	Supplier
5-FOA	Carl Roth, Karlsruhe, Germany
Acetic acid	Carl Roth, Karlsruhe, Germany
Adenine	AppliChem, Darmstadt, Germany
Agar	MP Biomedicals, Illkirch, France
Agarose	Sigma-Aldrich, Steinheim, Germany
Amylose resin	New England Biolabs, Frankfurt a. M., Germany
Ampicillin	Sigma-Aldrich, Steinheim, Germany
Anti-FLAG M2 affinity resin	Sigma-Aldrich, Steinheim, Germany
Blotting paper	VWR Internationals, Lutterworth, UK
Bovine serum albumin	Sigma-Aldrich, Steinheim, Germany
Bromophenol Blue	SERVA Electrophoresis, Heidelberg, Germany
Calcium chloride	Acros Organics, Geel, Belgium
Chloramphenicol	Sigma-Aldrich, Steinheim, Germany
Crystallization plates	TTP-Labtech, Hertfordshire, UK
Coomassie Brilliant Blue R250	SERVA Electrophoresis, Heidelberg, Germany
Copper sulfate	Merck, Darmstadt, Germany
Cycloheximide	Sigma-Aldrich, Steinheim, Germany
D-(+)-Glucose	Carl Roth, Karlsruhe, Germany
D-(+)-Maltose	Sigma-Aldrich, Steinheim, Germany
Di-ammonium hydrogen citrate	Sigma-Aldrich, Steinheim, Germany
Dimethyl sulfoxide	Carl Roth, Karlsruhe, Germany
Disodium hydrogen phosphate	Carl Roth, Karlsruhe, Germany
Dithiothreitol	AppliChem, Darmstadt, Germany
Mixed dNTP	New England Biolabs, Frankfurt a. M., Germany
DNA ladder	New England Biolabs, Frankfurt a. M., Germany
DNA staining solution	SERVA Electrophoresis, Heidelberg, Germany
Drop/chromatography columns	Bio-Rad, California, USA
D-Sorbitol	SERVA Electrophoresis, Heidelberg, Germany
EDTA	Carl Roth, Karlsruhe, Germany
Ethanol	VWR Internationals, Fontenay-sous-Bois, France
E.Z.N.A. Plasmid Mini Kit 1	Omega Bio-tek, Norcross, Georgia
FLAG peptide	Sigma-Aldrich, Steinheim, Germany
Glass beads ($\varnothing = 0.1-0.11\text{mm}$)	Sartorius, Goettingen, Germany
Glass beads ($\varnothing = 0.4-0.5\text{ mm}$)	Sartorius, Goettingen, Germany
Glycerol	Carl Roth, Karlsruhe, Germany

Glycine	AppliChem, Darmstadt, Germany
HEPES	AppliChem, Darmstadt, Germany
Hydrochloric acid	Merck, Darmstadt, Germany
Hydrogen peroxide	Sigma-Aldrich, Steinheim, Germany
Hygromycine	Carl Roth, Karlsruhe, Germany
Imidazole	Sigma-Aldrich, Steinheim, Germany
Isopropanol	VWR Internationals, Fontenay-sous-Bois, France
Isopropyl-beta-D-thio-galactoside	Formedium, Hunstanton, England
Kanamycine	Formedium, Hunstanton, England
L-Arginine	Carl Roth, Karlsruhe, Germany
L-Histidine	Merck, Darmstadt, Germany
L-Isoleucine	Sigma-Aldrich, Steinheim, Germany
Lithium Acetate	Sigma-Aldrich, Steinheim, Germany
L-Leucine	AppliChem, Darmstadt, Germany
L-Lysine	Carl Roth, Karlsruhe, Germany
L-Methionine	Merck, Darmstadt, Germany
L-Phenylalanine	Merck, Darmstadt, Germany
L-Threonine	Carl Roth, Karlsruhe, Germany
L-Tryptophane	Carl Roth, Karlsruhe, Germany
Luminol	Sigma-Aldrich, Steinheim, Germany
L-Uracil	Sigma-Aldrich, Steinheim, Germany
Magnesium chloride	Carl Roth, Karlsruhe, Germany
Methanol	VWR Internationals, Fontenay-sous-Bois, France
MG132	Sigma-Aldrich, Steinheim, Germany
Nickel-Sepharose™ high performance	GE Healthcare, Uppsala, Sweden
Nitrocellulose membrane	GE Healthcare, Uppsala, Sweden
Nourseothricin	Jenabioscience, Jena, Germany
NucleoSpin® Gel and PCR Clean-up Kit	Macherey-Nagel, Dueren, Germany
Nutrient broth	Difco, Meylan cedex, France
PAGE Ruler Plus	Thermo Fisher Scientific, Massachusetts, USA
p-coumaric acid	Sigma-Aldrich, Steinheim, Germany
PD-10 columns	GE Healthcare, Uppsala, Sweden
PEG 3350	Sigma-Aldrich, Steinheim, Germany
Peptone	BD, Le Pont de Claix, France
Potassium chloride	Acros Organics, Geel, Belgium
Potassium dihydrogen phosphate	VWR Internationals, Leuven, Belgium
Potassium hydroxide	Merck, Darmstadt, Germany
Protease inhibitor cocktail (“cOmplete“)	Roche Applied Science, Mannheim, Germany
Protein Assay Dye Reagent	Bio-Rad, Munich, Germany
Protein LoBind Tubes	Eppendorf, Hamburg, Germany
Rotiphorese® Gel 30 (37,5:1)	Carl Roth, Karlsruhe, Germany
Skimmed milk powder	Carl Roth, Karlsruhe, Germany
Sodium acetate	AppliChem, Darmstadt, Germany
Sodium chloride	AppliChem, Darmstadt, Germany
Sodium dihydrogen phosphate	Merck, Darmstadt, Germany
Sodium dodecyl sulfate	Carl Roth, Karlsruhe, Germany
Sodium hydroxide	Merck, Darmstadt, Germany
Spin-column concentrators	Merck, Darmstadt, Germany
Syringe filters	Pall Corporation, Cornwall, UK
Sucrose	Merck, Darmstadt, Germany

Super RX medical X-ray films	Fujifilm, Duesseldorf, Germany
TCEP	Sigma-Aldrich, Steinheim, Germany
TEMED	AppliChem, Darmstadt, Germany
Tris	Carl Roth, Karlsruhe, Germany
Tryptone	Formedium, Hunstanton, England
Tween 20	AppliChem, Darmstadt, Germany
Yeast extract powder	Formedium, Hunstanton, England
Yeast nitrogen base (w/o amino acids)	Formedium, Hunstanton, England

2.1.4.2 Electrical equipment

Tab. 5: Electrical equipment used during this work.

Instrument	Manufacturer
ÄKTAprime chromatography machine	Amersham Biosciences (now: GE Healthcare), Uppsala, Sweden
AGFA Curix 60 machine	AGFA, Mortselsel, Belgium
Agarose gel electrophoresis chamber	Peqlab, Erlangen, Germany
Blue light box	Clare Chemical Research, Ross on Wye, UK
Centrifuges	Beckman Coulter, Krefeld, Germany; Eppendorf, Hamburg, Germany
DynaPro NanoStar	Wyatt Technology, California, USA
Electrophoresis power supply	Amersham pharmacia biotech (now: GE Healthcare), Uppsala, Sweden
FE20/EL20 pH meter	Mettler Toledo, Erfstadt, Germany
HiLoad™ 16/60 Superdex™ 200 column	GE Healthcare, Uppsala, Sweden
Gradient thermocycler	Biometra, Goettingen, Germany
MAR345 image-plate detector	marXperts, Hamburg, Germany
Microscope	Zeiss, Oberkochen, Germany
MicroMax-007 HF rotating-anode generator	VariMax HF, Rigaku, Japan
Mosquito Crystallization Robot	TTP-Labtech, Hertfordshire, UK
Nanodrop 2000 Spectrophotometer	Thermo Fisher Scientific, MA, USA
Oxford Cryostream 700	Oxford Cryosystems, Oxford, England
Rocking platform	Biometra, Goettingen, Germany
Roller mixer	CAT M. Zipperer, Ballrechten-Dottingen, Germany
Shaking incubator	Infors, Einbach, Germany New Brunswick Scientific, Edison, USA
SDS-PAGE running chamber	Bio-Rad, California, USA
Semi-dry blotter	Bio-Rad, California, USA
Spectrophotometer	Pharmacia biotech (now: GE Healthcare), Uppsala, Sweden
Tabletop centrifuge	Eppendorf, Hamburg, Germany
Thermal shaker	Eppendorf, Hamburg, Germany
Thermocycler	Biometra, Goettingen, Germany
UV light source	Syngene, Cambridge, UK
Vortex	Scientific Industries, New York, USA

2.1.5 Enzymes

Tab. 6: Enzymes used in this study.

Name	Supplier
AcTEV™ Protease	Invitrogen
β-glucuronidase	Sigma-Aldrich
DNaseI	Roche Applied Science
DreamTaq DNA polymerase	Thermo Fisher Scientific
Fast Digest AgeI	Thermo Fisher Scientific
Fast Digest BamHI	Thermo Fisher Scientific
Fast Digest EcoRI	Thermo Fisher Scientific
Fast Digest HindIII	Thermo Fisher Scientific
Fast Digest KpnI	Thermo Fisher Scientific
Fast Digest MssI	Thermo Fisher Scientific
Fast Digest MunI	Thermo Fisher Scientific
Fast Digest NsiI	Thermo Fisher Scientific
Fast Digest PstI	Thermo Fisher Scientific
Fast Digest SacI	Thermo Fisher Scientific
Fast Digest XbaI	Thermo Fisher Scientific
Lysozyme	Sigma-Aldrich
Phusion DNA polymerase	New England Biolabs
T4 DNA ligase	New England Biolabs

2.1.6 Antibodies

Tab.7: Antibodies used in this study.

Antibody	relevant characteristics	Host animal	Dilution	Source
α-HA-tag (3F10)	monoclonal	rat	1:5,000	Sigma-Aldrich
α-FLAG M5	monoclonal	mouse	1:2,000	Sigma-Aldrich
α-Smt3	polyclonal	rabbit	1:10,000	M. Miteva, 2007
α-ubiquitin (P4D1)	monoclonal	mouse	1:2,000	Santa Cruz Biotechnology
α-MBP	monoclonal	mouse	1:10,000	New England Biolabs
α-Cdc11	polyclonal	rabbit	1:5,000	Santa Cruz Biotechnology
α-Tpi1	polyclonal	rabbit	1:20,000	R. J. Dohmen, 1991
α-rat	horseradish peroxidase (HRP)-coupled	goat	1:5,000	Abcam
α-rabbit	HRP-coupled	donkey	1:5,000	GE Healthcare
α-mouse	HRP-coupled	goat	1:5,000	Sigma-Aldrich

2.1.7 Media

2.1.7.1 Media for *E. coli*

For cultivation of *E. coli* cells, lysogeny broth (LB) was prepared according to the following recipe:

1 % (w/v) tryptone
0.5 % (w/v) yeast extract
1 % (w/v) NaCl

To eventually obtain solid medium, 2 % (w/v) agar was added, as well. The medium was sterilized by autoclaving.

Antibiotics stocks were prepared at the following concentrations:

100 mg/ml ampicillin (in ddH₂O)
35 mg/ml chloramphenicol (in ethanol)
50 mg/ml kanamycine

The ampicillin and kanamycine stocks were sterilized by passing them through 0.22- μ m syringe filters. Antibiotic stock solutions were stored at -20 °C, and added to the medium when required right before use.

2.1.7.2 Media for *S. cerevisiae*

2.1.7.2.1 Standard yeast media

For routine growth of *S. cerevisiae* either yeast peptone medium containing glucose (YPD) or synthetic dextrose (SD) medium was used. The compositions were as described elsewhere (Dohmen *et al.* 1995). In brief, the recipes were as follows:

YPD: 1 % yeast extract
2 % peptone
2 % glucose

SD: 0.67 % yeast nitrogen base (YNB) without amino acids
2 % glucose
20 mg/l Adenine
20 mg/l L-Arginine
60 mg/l L-Isoleucine
40 mg/l L-Lysine
10 mg/l L-Methionine
60 mg/l L-Phenylalanine
50 mg/l L-Threonine

Tryptophane, histidine, leucine and uracil served as auxotrophic markers and were therefore only added if appropriate (meaning: not used as a selection marker). In those cases, they were added to the following final concentrations: 10 mg/l l-histidine, 60 mg/l l-leucine, 40 mg/l l-tryptophan, 20 mg/l uracil.

In order to obtain solid medium, the mixes additionally contained agar at a final concentration of 2 %.

The individual components of each medium (except for yeast extract and peptone, which were prepared as one stock) were prepared separately, sterilized and then mixed to obtain the final medium. The amino acid stocks, as well as adenine and uracil stocks, were sterilized by sterile filtration using 0.22- μ m syringe filters; the rest was sterilized by autoclaving.

Antibiotics stocks were prepared in ddH₂O at the following concentrations: 500 mg/ml kanamycine, 50 mg/ml nourseothricin, 400 μ g/ml hygromycine, filter-sterilized, and then stored at -20 °C until needed.

2.1.7.2.2 Special yeast media

For crossing of yeast strains, special media were used as follows:

Pre-sporulation medium: 5 % glucose
3 % nutrient broth
1 % yeast extract
2 % agar

Sporulation medium: 0.1 % yeast extract
1 % potassium acetate
2 % agar

5-FOA-containing medium: the appropriate solid medium supplemented with
1 mg/ml 5-fluoroorotic acid (5-FOA)

2.2 Methods

2.2.1 Cell cultivation

2.2.1.1 Standard conditions

2.2.1.1.1 Escherichia coli

Unless stated differently, *Escherichia coli* cells were grown at 37 °C. In case of cultivation in liquid medium, the cultures were shaken at 160-180 rpm. Where applicable, ampicillin (Amp) was added to the growth medium at a concentration of 100 µg/ml and/or kanamycine (Kan) was added to a final concentration of 50 µg/ml. When *E.coli* strain BL21-CodonPlus was used, chloramphenicol (Cam) was added to a final concentration of 25 µg/ml.

2.2.1.1.2 Saccharomyces cerevisiae

Unless stated differently, *Saccharomyces cerevisiae* cells were grown at 30 °C. Temperature sensitive strains were cultivated at 25 °C in preparation of the actual experiment. When grown in liquid medium, cells were agitated at 180 - 200 rpm. Where applicable, antibiotics were added to final concentrations as follows: 500 µg/ml kanamycine (kan), 100 µg/ml nourseothricin (nat), 400 µg/ml hygromycine (hygB).

2.2.1.2 Special conditions

2.2.1.2.1 Protein expression in E.coli

All recombinant proteins generated in the course of this work were expressed in *E. coli* BL21-CodonPlus cells, with the exception of Ubc9, which was expressed in BL21(DE3)

cells. For all constructs featuring MBP, the growth medium was supplemented with 1 % glucose.

In general, cells were grown to an optical density at 600 nm (OD_{600}) of ~0.5 - 0.7, before cultures were briefly cooled on ice and expression was induced by addition of isopropyl-beta-D-thio-galactoside (IPTG). The final concentrations of IPTG were as follows:

- Smt3- and/or GFP-containing constructs: 0.5 mM
- MBP-Ulp2-FLAG: 1 mM
- MBP-Ulp1-FLAG: 0.5 mM
- All other MBP fusion constructs (including truncated Ulp2): 0.3 mM

Further fermentation was allowed at 18 °C for ~20 h in case of the MBP fusion constructs; Smt3- and GFP-containing proteins were expressed at 30 °C for 3.5 h.

One exception was the expression of Ubp41, which was induced at $OD_{600} = 0.8$ by addition of IPTG to a final concentration of 0.4 mM. Ubp41 was expressed at 30 °C for 6 h.

2.2.1.2.2 Growth assays of *S. cerevisiae*

Most assays involving *S. cerevisiae* were based on monitoring the presence/abundance of specific proteins under certain growth conditions over time. In these cases, cultivation deviated from the standard procedure. To test stability of certain proteins, their degradation rates in the cell were monitored by inhibiting global translation once a certain cell density was reached. To this end, YPD or the appropriate SD medium was inoculated at $OD_{600} = 0.2$ with cells of the strain of interest derived from a fresh overnight culture. In case of monitoring proteins expressed from plasmids, the medium was supplemented with 100 µg/ml $CuSO_4$.

Cells were grown to $OD_{600} \sim 0.8$, then 30 ml per condition to be tested were harvested by centrifugation at 3,900xg for 5 min at room temperature, followed by resuspension in 6.6 ml YPD containing 0.5 mg/ml cycloheximide. If the assay asked for proteasome inhibition or vacuole inhibition, the pellet was resuspended in 6.3 ml YPD supplemented with 20 µM MG132 or 1 mM phenylmethylsulfonyl fluoride (PMSF), respectively, and the cultures were incubated for 30 min before cycloheximide was added. Control cultures contained the same volume dimethyl sulfoxide (DMSO). If a temperature sensitive strain was used, it was cultivated at 25 °C until it reached an OD_{600} of ~0.8. Cells were pelleted, resuspended in YPD and then cultivated at 37 °C for at least 45 min before cycloheximide was added.

At defined time points, 1-ml samples were withdrawn from the culture, and immediately mixed with ice-cold sodium azide (NaN₃) to reach a final concentration of 10 mM NaN₃. Cells were pelleted by centrifugation at 11,000xg for 1.5 min, at room temperature in a tabletop centrifuge. The supernatant was removed using a vacuum pump. The pellet was snap-frozen, and stored at -20 °C until further treatment.

2.2.2 Biomolecular techniques

2.2.2.1 DNA isolation

2.2.2.1.1 Isolation of plasmid DNA from *E. coli*

E. coli cells bearing the plasmid of interest were cultivated in 5 ml LB+Amp medium for 12-16 hours with agitation. Cells were harvested by centrifugation, and plasmid DNA was extracted using E.Z.N.A. Plasmid Mini Kit 1 in accordance with the supplier's manual.

2.2.2.1.2 Isolation of genomic DNA from *E. coli*

In order to obtain carrier DNA that would aid yeast transformation, genomic DNA was extracted from *E. coli* XL1 Blue cells. To this end, the cells were grown in 5 ml LB medium for at least 12 hours shaking. Cells were harvested by centrifugation. The obtained pellet was resuspended in 250 µl Solution I of the aforementioned E.Z.N.A. Plasmid Mini Kit 1, but in this case Solution I did not contain RNaseI. The downstream steps were performed as outlined in the manufacturer's guidelines for the usual application. After elution, the resultant DNA was subjected to ethanol precipitation as follows: The elution was mixed with 350 µl isopropanol and then subjected to centrifugation at 30,000xg for 2 min at 4 °C. The supernatant was discarded and 1 ml of 70 % ethanol was added without mixing. After incubation at -20 °C for at least 12 h, the sample was spun down at 30,000xg for 2 min at 4 °C. The supernatant was discarded and residual ethanol was removed by incubation at 60 °C for 10 min. Then, the DNA was resuspended in 100 µl elution buffer by incubation of the solution at 99 °C for 10 min followed by 3 min of vigorous vortexing.

2.2.2.2 PCR amplification

All oligonucleotides were purchased either from Sigma-Aldrich or Integrated DNA Technologies (IDT) in a dried form and resuspended in ddH₂O. A full list of primers used in

this work is provided at the end of the text (pages 115 - 117; Tab. 9). To amplify DNA *in vitro*, polymerase chain reaction was performed. For thermocycling, either a regular, or a gradient thermocycler was used, depending on the pair of primer used.

Afterwards, the resultant DNA fragments were extracted from the reaction mix using NucleoSpin® Gel and PCR Clean-up kit (Macherey-Nagel) following the manufacturer's instructions. Optimal primer annealing temperatures were calculated using the free online tool "NEB Tm calculator" provided by New England Biolabs.

After cloning, all constructs were confirmed by sequencing done by GATC Biotech. (Especially the strategy followed to generate the various Ulp2 substrates is described *en detail* in Eckhoff & Dohmen, 2015. For more information than the general description provided here, please consult that publication.)

2.2.2.2.1 ...for cloning purposes

DNA fragments meant for downstream genetic applications were generated using the proofreading DNA polymerase Phusion (NEB). A typical 50- μ l reaction mix contained the following components:

- 10 μ l 5x HF buffer (supplied with the polymerase; NEB)
- 2.5 μ l 10 μ M forward primer
- 2.5 μ l 10 μ M reversed primer
- 1 μ l 10 mM dNTP mix (containing 10 mM of each dATP, dGTP, dTTP, dCTP)
- 0.5 μ l template DNA
- 0.5 μ l Phusion DNA polymerase
- 33 μ l ddH₂O

If necessary, DMSO was added to the reaction to final concentrations ranging from 4 % to 10 %.

In a typical thermocycling program denaturation for 3 min at 98 °C was followed by 22 cycles of the following progression: 30 sec denaturation at 98 °C, 30 sec of annealing at the appropriate temperature, elongation at 72 °C for 30 sec per 1 kb. The program was ended with a single, final elongation period of 5 min at 72 °C.

If two PCR products had to be fused, or if point mutations or medium-sized insertions were introduced, overlap PCR or overlap-extension PCR was applied. The technique is based on the idea of fragments priming each other, thus it is crucial to include overlapping sequences of adequate length (calculated annealing temperature should be ≥ 50 °C) in the reversed primer of the 5'-fragment and in the forward primer of the 3'-fragment. The approach involves a two-step procedure after the fragments, which are supposed to be fused, have been individually amplified and purified.

Agarose gel electrophoresis allowed for an accurate enough estimation of the amount of each fragment in its solution. The procedure was then as follows:

- 3 μ l 5x HF buffer (supplied with the polymerase; NEB)
- 1 μ l fragment 1
- x μ l fragment 2 (approximately the same amount as fragment 2)
- 0.3 μ l 10 mM dNTP mix
- 0.15 μ l Phusion DNA polymerase
- 15-x μ l ddH₂O

Components were mixed and subjected to thermocycling after an initial denaturation for 3 min at 98 °C, there were 8 cycles of 30 sec denaturation at 98 °C, 3 min of annealing at 48 °C, followed by elongation at 72 °C for 30 sec per 1 kb. In this step, the two fragments primed each other. In the second step, the fused fragments were amplified by adding the following mix to the initial reaction mix after thermocycling was completed:

- 9 μ l 5x HF buffer (supplied with the polymerase; NEB)
- 3 μ l 10 μ M forward primer used in amplification of the 5'-fragment
- 3 μ l 10 μ M reversed primer used in amplification of the 3'-fragment
- 0.9 μ l 10 mM dNTP mix (containing 10 mM of each dATP, dGTP, dTTP, dCTP)
- 0.4 μ l Phusion DNA polymerase
- 29 μ l ddH₂O

The second round of thermocycling typically consisted of 17 repeats of 30 sec denaturation at 98 °C, 30 sec of annealing at the appropriate temperature, and elongation at 72 °C for 30 sec per 1 kb. The program was ended with a single, final elongation period of 5 min at 72 °C.

2.2.2.2.2 ...for screening purposes

To test for successful cloning, PCR reactions were performed on the basis of the clones without prior DNA extraction. If *E. coli* cells were to be tested, single colonies were each resuspended in 30 μ l sterile ddH₂O, and 5 μ l of this suspension were used as template DNA in the reaction mix. If *S.cerevisiae* cells were to be tested, tiny amount of cell material of single colonies were placed in individual PCR tubes, and then subjected to 1 min of microwaving at 900 W followed by 5 min incubation on ice before the PCR mix was added. A typical 25- μ l reaction contained the following ingredients:

- 2.5 μ l 10x buffer (supplied with the polymerase; Thermo Fisher Scientific)
- 1.25 μ l 10 μ M forward primer
- 1.25 μ l 10 μ M reversed primer
- 0.5 μ l 10 mM dNTP mix
- 0.5 μ l DreamTaq DNA polymerase
- ddH₂O to a final volume of 25 μ l

The thermocycling program consisted of initial denaturation for 10 min at 95 °C, followed by 35 cycles of the following sequence of steps: 30 sec denaturation at 95 °C, 30 sec of annealing at the appropriate temperature, elongation at 72 °C for 1 min per 1 kb (expected fragment size). The program ended with a single, final elongation period of 5 min at 72 °C.

2.2.2.3 Agarose gel electrophoresis

For DNA analysis, agarose gel electrophoresis was used. Different molecular weights/lengths of DNA fragments account for different mobility when migrating through an agarose gel to which an electric field is applied (Ross *et al.* 1964a, b). The agarose gels typically contained 1 - 2 % (w/v) agarose in TAE buffer (40 mM Tris, 20 mM Sodium acetate, 1 mM EDTA) and 0.002 % SERVA DNA stain G. Prior to loading, DNA samples were mixed 6:1 with 6x concentrated DNA loading dye [2 mM EDTA, pH 8.0, 4 % (w/v) Sucrose, 0.025 % (w/v) Bromophenol Blue]. Gels were run at a constant voltage of 140 V until sufficient separation was reached. For visualization, the DNA stain was excited using either UV light provided by a Gene Genius Bioimaging system (Syngene) if documentation was the only purpose, or using blue light from a Dark Reader (Clare Chemical Research) if the DNA fragments were meant for downstream application. In the latter case, correctly sized fragments were excised

from the gel, and then purified using NucleoSpin[®] Gel and PCR Clean-up Kit (Macherey-Nagel) as described in the supplier's manual.

2.2.2.4 DNA restriction digestion

PCR-generated DNA fragments and plasmid DNA were digested using site-specific restriction endonucleases. The enzymes were purchased from the FastDigest product line of Thermo Fisher Scientific. Reactions were set up in PCR tubes. In a typical 50- μ l reaction, the desired volume of DNA was mixed with 2 μ l of the relevant enzyme (in case of double-digest: 2 μ l of each) in the reaction buffer supplied with the endonuclease. Restriction digestion was allowed for 30 min up to 2 hours in a thermocycler at a constant temperature of 37 °C. If necessary, afterwards the enzymes were inactivated by incubation at a higher temperature as recommended by the supplier. Then, the DNA fragments were purified as described above for PCR products. If larger fragments had to be shed, the digestion mix was subjected to agarose gel electrophoresis and desired fragments were excised from the gel prior to purification.

2.2.2.5 Vector dephosphorylation

If a vector was subjected to digestion by only one restriction endonuclease to exploit a compatible-end strategy, or if the generated sticky ends of a double-digest were compatible, the vector was subjected to dephosphorylation prior to ligation with the insert. For this, after restriction digest was completed, the vector was eluted from the purification column in 15 μ l elution buffer. The eluate was mixed with 2 μ l ddH₂O, 2 μ l reaction buffer (supplied with the phosphatase), and 1 μ l thermosensitive Alkaline Phosphatase (FastAP), and then incubated at 37 °C for 1 hour. The mix was then subjected to a 5-min incubation at 80 °C, and subsequently used in downstream applications without further treatment.

2.2.2.6 Ligation of DNA fragments

To fuse DNA fragments into vectors, T4 DNA ligase was used in accordance with the supplier's guidelines. Typically, ligation was allowed for 30 min at room temperature in a 20- μ l reaction containing 400 u of enzyme (1 μ l). Later, 10 μ l of this were used to transform chemically competent *E. coli* XL1 Blue cells.

2.2.2.7 Generation of transformation-competent *E. coli* cells

To obtain transformation-competent *E. coli* cells, 100 ml LB medium (in case of BL21-CodonPlus cells: +Cam) was inoculated with 1 ml of a freshly-grown overnight culture of the desired strain. Cells were cultivated to $OD_{600} = 0.3$. Then, cultures were decanted into pre-cooled 50-ml conical plastic tubes and allowed to cool down for ~5 min on ice. Afterwards, cells were harvested by centrifugation for 10 min at 1,700xg in a centrifuge equipped with a swing-bucket rotor cooled to 4 °C. The supernatant was discarded and the pellet was resuspended in 50 ml (total volume) 0.1 M $CaCl_2$. The suspension was incubated on ice for 20 min before cells were pelleted again by centrifugation as before. The supernatant was discarded and the pellet was resuspended in 4 ml 0.1 M $CaCl_2$. For long-term storage, glycerol was added to a final concentration of 15 % and the cell suspension was aliquoted into 1.5-ml reaction tubes. The competent cells were kept at -80 °C until further usage.

2.2.2.8 Transformation of *E. coli* cells

To introduce integer plasmid DNA into *E. coli* cells, 0.5 μ l of the plasmid solution of interest was used. To transform *E. coli* cells with DNA from a ligation, 10 μ l of a 20- μ l ligation reaction were used. In either case, a 100- μ l aliquot of chemically competent cells was thawed on ice. The DNA was added and dispersed by gentle tapping of the tube. The mix was heat-shocked by incubation for 30 - 60 sec at 42 °C. The cells were briefly incubated on ice, 1 ml of LB medium was added to the tube, and recovery was allowed for 45 min at 37 °C shaking. Cells were collected by centrifugation in a tabletop centrifuge for 5 min at 800xg, and spread on an LB plate supplemented with the appropriate antibiotics.

2.2.2.9 Transformation of *S. cerevisiae* cells

To introduce DNA into *S. cerevisiae* cells, high efficiency yeast transformation as described previously (Daniel Gietz *et al.* 2002) was applied. In brief, 5 ml of the appropriate medium was inoculated at $OD_{600} = 0.2$ with the strain of interest cultivated in an overnight culture. Cells were grown to an $OD_{600} \sim 0.6 - 0.8$, and then harvested by centrifugation at 1,700xg for 5 min at room temperature. The resultant pellet was resuspended in 1 ml ddH₂O. Cells were transferred to a 1.5-ml reaction tube and pelleted by centrifugation at 1,500xg for 5 min at room temperature in a tabletop centrifuge. Cells were resuspended in 1 ml 0.1 M sterile lithium acetate, before being subjected to another centrifugation step. The resultant pellet was

resuspended in 48 μl ddH₂O, and then mixed with the following components by pipetting up and down:

250 μl 50 % (w/v) PEG-3350
35 μl 1 M LiAc
4 μl self-made carrier DNA
2 μl plasmid DNA

The transformation mix was incubated at 30 °C (in case of temperature sensitive strains: 25 °C) for 25 min, before being transferred to 42 °C for another 20 min. Cells were collected by centrifugation at 1,500xg for 5 min at room temperature, resuspended in 100 μl ddH₂O and then plated on the appropriate selective medium.

2.2.3 Genetic techniques

2.2.3.1 Mating and sporulation of *S.cerevisiae* strains

Since only a single strain used in this work was generated by crossing of strains, this description is not general.

To generate the *smt3-KallR ulp2- Δ* (yJE1) strain, cells of the *smt3-KallR* strain (obtained from Erica Johnson) were mixed with cells of yKU1 on YPD, and incubated as such for 1 day. Diploid cells were selected on SD-His-Trp medium. Cells of a single colony were then grown for three days on pre-sporulation medium before starving them for seven days on sporulation medium. Tetrad dissection was done manually using a Zeiss microscope and a self-made molecular picking rod. In preparation for that, a small amount of spores was resuspended in 50 μl of a 4 % solution of β -glucuronidase, and then incubated for 10 min at 37 °C. A fine line of the cell suspension was then drawn on a YPD plate and allowed to dry by leaving the plate open next to a flame for 5 min. After dissection, cell growth was allowed for five days at 30 °C. The final strain was selected on SD-His-Trp plates, and the mating type was determined by test crossing with the mating type determination strains KMY38 (*MAT α trp5-27*) and KMY39 (*MAT α trp5-27*).

2.2.4 Biochemical techniques

2.2.4.1 SDS polyacrylamide gel electrophoresis (SDS-PAGE)

In order to analyze protein-containing samples, they were separated electrophoretically on SDS-containing polyacrylamide gels following the original guidelines described by Laemmli (1970).

Resolving gels of different percentage were cast following these recipes:

Chemical agent	8 %	10 %	12 %
1.5 M Tris-HCl, pH 8.8	3.75 ml	3.75 ml	3.75 ml
30 % (w/v) Acrylamide / 0.7 % Bisacrylamide	4 ml	5 ml	6 ml
10 % (w/v) SDS	150 μ l	150 μ l	150 μ l
10 % (w/v) APS	150 μ l	150 μ l	150 μ l
TEMED	15 μ l	15 μ l	15 μ l
ddH ₂ O	7.1 ml	6.1 ml	5.1 ml

Stacking gels consisted of the following components:

2.5 ml Tris-HCl, pH 6.8
 1.7 ml 30 % (w/v) Acrylamide / 0.7 % Bisacrylamide
 100 μ l 10 % (w/v) SDS
 100 μ l 10 % (w/v) APS
 10 μ l TEMED
 5.6 ml ddH₂O

Gels were allowed to polymerize for at least 1.5 h before usage.

To run SDS-PAGEs the following buffers were used:

Running buffer: 25 mM Tris, 192 mM glycine, 0.1 % SDS

6x SDS-PAGE loading buffer: 0.375 M Tris-HCl, pH 6.8, 48 % glycerol, 12 % SDS, 0.6 M DTT, 0.06 % Bromophenol Blue

Unless high molecular weight-samples were separated, sodium acetate was added to the running buffer in the outer chamber to a final concentration of 100 mM. Unless in the appropriate buffer already, samples were mixed 6:1 with 6x SDS-PAGE loading buffer. To estimate protein size, a colored standard marker (PAGE Ruler) was run alongside with the samples. Proteins were allowed to migrate through the stacking gel at 120 V. Once they entered the separation gel, voltage was increased to 180 V.

2.2.4.2 Coomassie staining of proteins in SDS polyacrylamide gels

When SDS-PAGE had been performed to estimate protein yield and purity from purification (not for the purpose of immunodetection), the gel was stained with Coomassie Brilliant Blue after the run was completed. The following solutions were used:

Coomassie Brilliant Blue staining solution: 30 % methanol, 10 % acetic acid, 0.3 % (w/v)
Coomassie Brilliant Blue R250

Destaining solution: 30 % methanol, 10 % acetic acid

The gel was incubated in ~100 ml of staining solution at room temperature for ~15 min with agitation. The gel was briefly rinsed with ddH₂O, and then incubated in an excess volume of destaining solution. Destaining solution was repeatedly renewed until the dye was only held back in the protein bands.

2.2.4.3 Detection of proteins by immunoblotting (Western Blot)

Separated proteins were transferred to nitrocellulose membranes using semidry blotting. The hardware used was a Bio-Rad semidry blotter connected to a Pharmacia Biotech power supply. The standard buffer was composed as follows:

Blotting buffer: 25 mM Tris, 192 mM glycine, 0.1 % (w/v) SDS, 20 % MeOH

PBS: 1.8 mM KH₂PO₄, 10 mM Na₂HPO₄, 2.7 mM KCl, 137 mM NaCl; pH 7.4

PBS-T: PBS + 0.1 % Tween 20

Detection solution: 100 mM Tris-HCl, pH 8.5, 2.5 mM Luminol, 400 μ M p-coumaric acid, 0.02 % hydrogen peroxide

When HMW species were supposed to be transferred, the methanol concentration in the blotting buffer was reduced to 5 %. For blotting of proteins smaller than 25 kDa, the buffer was prepared without SDS.

In general, protein transfer was allowed at a constant current of 2.5 mA/cm² for 1 h. To transfer HMW species, the current was increased to 3 mA/cm² and blotting time was elongated to 1 h 40 min. To detect low molecular weight species (e.g. mono-SUMO or -ubiquitin), the blotting sandwich contained two layers of membrane, of which only the upper one was used in subsequent steps. Additionally, the transfer was stopped after 40 min and the membrane was incubated in a boiling water bath for 40 min after transfer. Before further treatment, the membrane was dried on the bench.

To prevent unspecific antibody binding, membranes were incubated in 5 % (w/v) skimmed milk powder in phosphate-buffered saline (PBS) for at least 1 h with agitation. Primary antibodies were diluted in 5 % (w/v) skimmed milk powder in PBS-T. Antibody binding was allowed overnight at 4 °C with gentle shaking. Membranes were washed 3x by incubation in an excess volume of PBS-T with agitation at room temperature for 10 min, before being incubated with the corresponding secondary antibody at room temperature with gentle shaking for 50 min. Membranes were washed 3x with PBS-T as before. For induction of HRP-produced luminescence, blots were incubated for 1 min in detection solution, which was prepared freshly right before use. Signals were documented by exposing X-ray films to the blots and developing those in an AGFA Curix 60 machine as described by the manufacturer.

2.2.4.4 Antibody removal

When detection of different antigens was necessary, antibodies were removed by incubating the respective blot three times in an excess volume of 0.2 M sodium hydroxide for 10 min at room temperature with agitation. Afterwards, the membrane was rinsed briefly with ddH₂O before being blocked and probed as described above.

2.2.4.5 Protein purification

All purification steps were carried out at 4 °C. All buffers and solutions were ice-cold. All material was pre-cooled before in contact with any protein-containing solution. All purified proteins were analyzed via Western Blot before being used in downstream applications. For estimation of protein concentration, either a spectrometric dye assay (Bio-Rad protein assay) or a nanodrop spectrophotometer was used.

2.2.4.5.1 Purification of Ulp substrates

All Ulp substrates were affinity-purified employing a two-step procedure. Each of these constructs carried an N-terminal FLAG tag and a C-terminal hexahistidine tag; both of which were employed for purification in order to obtain substrate chains at maximum purity.

The following buffers were used:

Lysis buffer: 50 mM Tris-HCl, pH 7.4, 150 mM NaCl, 10 % glycerol, 4 mM MgCl, 1x protease inhibitor mixture, 2.5 mg/ml lysozyme, 0.8 mg/ml DNaseI

Ni buffer: 50 mM Tris-HCl, pH 7.4, 500 mM NaCl, 10 % glycerol, 4 mM MgCl, 20 mM imidazole

FLAG buffer: 50 mM Tris-HCl, pH 7.4, 150 mM NaCl, 10 % glycerol, 4 mM MgCl

Protease buffer: 50 mM Tris-HCl, pH 8.0, 1 mM DTT, 0.5 mM EDTA

The OD₆₀₀ of each expression culture had been measured before harvest. For each 1 OD₆₀₀ unit of cells (corresponds to the amount of cells in 1 ml of culture with OD₆₀₀ = 1) 15 µl lysis buffer was added to the frozen pellet. Cells were carefully resuspended, aliquoted into 2-ml reaction tubes (1 ml/tube) containing 500 µl of glass beads (Ø = 0.1-0.11mm), and then incubated for 5 min at 4 °C, followed by a 5-min incubation on ice. The lysate was subjected to 4 repeats of 1 min vigorous vortexing followed by 1 min incubation on ice. Subsequent centrifugation at 30,000xg for 20 min at 4 °C cleared the crude extract from cell debris. The supernatant was recovered and supplemented with sodium chloride and imidazole to final concentrations of 500 mM and 20 mM, respectively. Per 1 ml of extract, ~400 µl equilibrated nickel-sepharose was added. Binding was allowed for ~25 min on a rotating wheel. Then, the resin was transferred to a drop column, and washed with ~15 ml Ni buffer. Proteins were

eluted with 200 mM imidazole in FLAG buffer. For elution, the resin was incubated with 1 column volume (CV) of FLAG buffer + 200 mM imidazole for 5 min before the eluate was collected. All elution fractions were pooled, and imidazole concentration was reduced to a minimum by repeated dilution and concentration of the protein solution using spin-column concentrators. Then, ~40 µl anti-FLAG M2 affinity resin was added, and binding was allowed for 2.5 h on a rotating wheel. The resin was washed in-batch 5x with 1 ml FLAG buffer, before the proteins were eluted in 2x 200 µl FLAG buffer containing 150 µg/ml FLAG peptide. Each elution step consisted of 1.5 h rotation on a wheel, subsequent centrifugation at 100xg for 1 min, followed by careful recovery of the supernatant. Pooled elutions were subjected to another centrifugation at 30,000xg for 10 min, before they were aliquoted into PCR tubes, snap-frozen in liquid nitrogen, and then stored at -80 °C until usage.

To produce substrates without N-terminal FLAG tag, elution from anti-FLAG resin was done enzymatically. To this end, to the respective resin 400 µl protease buffer was added. Depending on the construct, 1 unit of AcTEVTM Protease or 10 nM of Ubp41 was added, and cleavage was allowed for 8 h while rotating. In case of the migration standards for mono-SUMO, FLAG-Smt3 and ΔN17Smt3, cleavage by TEV protease was prolonged to 16 h. After collection of these elutions, a fresh 1 unit of TEV protease was added to them, and cleavage was allowed for 8 more hours.

2.2.4.5.2 Purification of sumoylated Ubc9

To obtain authentic Smt3 chains, the reconstituted sumoylation pathway in *E. coli* described by Wohlschlegel *et al.* (2006) was used. An MBP-tagged version of Ubc9 introduced to the system allowed for purification of authentically sumoylated Ubc9 via amylose resin.

Amylose buffer: 50 mM Tris-HCl, pH 7.5, 150 mM NaCl, 17 % glycerol

Lysis of the expression cells was done as described above for the artificial substrates. The cleared crude extract was mixed with 500 µl amylose resin (50 µl/ml of extract) and incubated for 1 h on a rotating wheel. The resin was then washed in a drop column with a total volume of amylose purification buffer. Specifically bound proteins were eluted with 10 mM maltose in amylose purification buffer. The final pooled eluate was treated and stored as described for the Ulp substrates.

2.2.4.5.3 Purification of Ubp41

The Ubp41 variant used in this study carried a hexahistidine tag.

Unlike all other expression cultures harvested in the course of this study, the Ubp41-expressing cells were not washed with PBS. Instead, the pellet was resuspended in 15 μ l of lysis buffer per absorbance unit of cells, and the suspension was then stored at -20 °C.

Lysis buffer: 50 mM Na₂HPO₄/NaH₂PO₄, pH 7.5, 300 mM NaCl, 12 mM imidazole, 10 mM DTT, 4 mM MgCl₂, 30 % glycerol

After ~16 h at -20 °C, the suspension was thawed on ice, 1x protease inhibitor, 2.5 mg/ml lysozyme, 0.8 mg/ml DNaseI and 1 mM PMSF were added, and glass bead lysis and extract clearance were performed as described above for the Ulp substrates (2.2.4.5.1). The supernatant was recovered and mixed with 500 μ l of equilibrated nickel-sepharose beads. The downstream procedure matched the purification protocol described under 2.2.4.5.1 for nickel-based purification, except that all buffers additionally contained 30 % glycerol and 1 mM DTT.

2.2.4.5.4 Purification of full-length Ulp2

To obtain pure full-length Ulp2, MBP-Ulp2-FLAG was purified via its FLAG tag.

The following buffers were used:

Lysis buffer: 50 mM Tris-HCl, pH 7.4, 150 mM NaCl, 10 mM DTT, 4 mM MgCl, 1 mM EDTA, 1x Protease inhibitor mixture, 2.5 mg/ml lysozyme, 0.8 mg/ml DNaseI

Buffer M: 50 mM Tris-HCl, pH 7.4, 150 mM NaCl, 1 mM DTT

Lysis procedure and subsequent clearance of cell debris was done as described for the Ulp substrates.

Lysis procedure and subsequent clearance of cell debris was done as described for the Ulp substrates (2.2.4.5.1). To each 5 ml of lysate, 40 μ l of anti-FLAG M2 resin was added, and binding was allowed for 1 h while rotating. After that, resin beads were washed in batch 5x with 1 ml of Buffer M. Specifically bound proteins were eluted by incubating the resin with 100 μ l Buffer M containing 100 μ g/ml FLAG peptide for 1 h on a rotating wheel.

2.2.4.5.5 Purification of the Ulp2 active domain

While for all other proteins used in the course of this study small amount were sufficient, crystallization required a large-scale approach for purification of the active domain of Ulp2. To this end, MBP-Ulp2(411-710)-3xGly-His₆ fusion construct with a TEV protease recognition site inserted between MBP and Ulp2 was employed.

The following buffers were used:

Lysis buffer: 50 mM Tris-HCl, pH 7.4, 150 mM NaCl, 2 mM DTT, 10 % glycerol, 4 mM MgCl₂, 1 mM EDTA, 1x Protease inhibitor mixture, 1 mg/ml lysozyme, 0.2 mg/ml DNaseI

Buffer Amy: 50 mM Tris-HCl, pH 7.4, 150 mM NaCl, 2 mM DTT, 10 % glycerol

Buffer On: 10 mM HEPES-KOH, pH 7.0, 150 mM NaCl, 1 mM DTT

Ni* Buffer: 10 mM HEPES-KOH, pH 7.0, 1 M NaCl, 1 mM DTT, 20 mM imidazole

Buffer Sto: 10 mM HEPES-KOH, pH 7.0, 100 mM NaCl, 10 mM DTT

Final buffer: 10 mM HEPES-KOH, pH 7.0, 100 mM NaCl, 1 mM TCEP

Cell pellets were grinded to a fine powder using mortar and pestle. Both tools were pre-cooled with liquid nitrogen, and while grinding every 2-3 min liquid nitrogen was scooped into the mortar to keep the powder frozen. The powder was transferred to pre-cooled 50-ml tubes. Per 1 gram of powder, 5 ml of lysis buffer was added. The mix was incubated on a roller mixer until the powder was completely dissolved in the lysis buffer. Subsequent centrifugation at 30,000xg for 20 min at 4 °C cleared the crude extract from cell debris. The supernatant was mixed with 1 ml amylose resin per 20 ml extract. Binding was allowed for 2.5 h on a roller mixer. Afterwards, the resin was transferred to a drop column and washed with 20 CV of Buffer Amy. Proteins were eluted in 5 CV of Buffer Amy supplemented with 20 mM maltose. All elution fractions were pooled, and the buffer was exchanged to Buffer On using PD-10 columns as described in the supplier's manual. The protein solution was diluted 1:4 in Buffer On, and to each 50 ml, freshly purified MBP-FLAG-TEV protease was added to a final concentration of ~1 μM. Cleavage was allowed for at least 15 h on a roller mixer. Afterwards, the mix was passed through a 0.22-μm filter. The solution was

supplemented with 20 mM imidazole. To each 50 ml of protein solution, 1 ml of equilibrated nickel-sepharose was added. Binding was allowed for ~20 min on a roller mixer. The resin was washed in drop columns with 20 CV of Ni* Buffer. Proteins were eluted in 10-15 CV of Ni* Buffer containing 250 mM imidazole. Buffer was exchanged to Buffer Sto using PD-10 columns.

The protein solution was then subjected to gel filtration via a HiLoad™ 16/60 Superdex™ 200 (GE Healthcare) column connected to an ÄKTAprime machine featuring a fractionator. Fractions containing the protein of interested were tested for monodispersity using a DynaPro NanoStar DLS instrument (Wyatt Technology) in accordance with the supplier's guidelines. Monodispers fractions were pooled and concentrated to 3 mg/ml in spin-concentrators (30 kDa cut-off).

2.2.4.5.6 Purification of TEV protease

TEV protease N-terminally tagged with MBP was purified using amylose resin. The purification via amylose resin, including lysis etc., was done as described above for the Ulp2 active domain (2.2.4.5.5). The enzyme was purified freshly every time.

2.2.4.6 *In vitro* desumoylation assay

Desumoylation assays were carried out in 1.5-ml Protein LoBind Tubes (Eppendorf). Unless stated differently, crude extract from *E. coli* containing the respective recombinantly expressed Ulp were used. The extracts were prepared as described under 2.2.4.5.1 for the substrates. Substrates and lysates were diluted in activity test buffer (ATB).

ATB: 10 mM Tris-HCl, pH 8.0, 150 mM NaCl, 10 mM DTT, 1 mM EDTA

The amount of substrate necessary to produce a sufficiently detectable signal was estimated by Western Blot for each substrate individually.

Each set-up contained the following:

- 6 µl extract (diluted or undiluted)
- 2 µl substrate (diluted or undiluted)
- 12 µl ATB

Unless indicated differently, cleavage was allowed at 30 °C for 2 h. Then, reaction mixtures were subjected to centrifugation at 30,000xg for 5 min at 4 °C. Seventeen microliters of supernatant were mixed with 6x SDS-PAGE loading buffer and boiled for 5 min. Cleavage products were then analyzed by SDS-PAGE and immunodetection.

Deubiquitination assays were carried out likewise, except for the reaction mix containing 2 μ l of purified Ubp41 (amount was not defined) instead of Ulp2 (lysate).

2.2.4.7 Ulp2 binding assay

The entire assay was done at 4 °C. The following buffers were used:

Buffer A: 50 mM Tris-HCl, pH 7.4, 150 mM NaCl, 17 % glycerol, 1 mM DTT

Buffer B: 50 mM Tris-HCl, pH 7.4, 150 mM NaCl, 17 % glycerol, 1 mM DTT, 1 mg/ml BSA

Crude extract of *E. coli* cells expressing MBP-Ulp2(C624A)-FLAG was prepared as described under 2.2.4.5.1 for the substrates. The extract was diluted 1:3 in Buffer A. For each 1 ml of undiluted lysate, 50 μ l amylose resin was added, and binding was allowed for 1.5 h on a roller mixer. For controls, another aliquot of amylose resin was treated identically but without addition of lysate. Resins were collected by centrifugation at 500xg for 1 min, transferred to a 1.5 ml reaction tube, and washed in batch: Once with 10 CV of Buffer A, then 4 times with 10 CV of Buffer B. With the last washing step, the resin was split into 20- μ l aliquots in 1.5-ml Protein LoBind Tubes. To each tube, 200 μ l Buffer B was added. Substrate was added to a final concentration of ~100 nM to each aliquot of resin with or without immobilized Ulp2(C624A). Binding was allowed for 1.5 h on a rotating wheel. Subsequently, beads were collected by centrifugation at 500xg for 1 min and washed once with 1 ml of Buffer B, followed by transfer to fresh tubes and washing twice with Buffer A. Bound proteins were collected by adding 40 μ l of SDS-PAGE loading buffer to each tube and boiling for 5 min. Binding was analyzed by SDS-PAGE and immunodetection.

To assay the substrate MBP-4xSmt3-GFP, the same protocol was followed, but anti-FLAG M2 resin (10 μ l/tube) was used instead of amylose resin. Instead of substrates featuring a FLAG tag, their equivalents not carrying a FLAG tag were employed.

2.2.4.8 Preparation of crude extracts from *S. cerevisiae*

Depending on what was supposed to be detected, different extraction methods were employed. However, the extraction buffer was always the same:

Extraction buffer: 60 mM Tris-HCl, pH 6.8, 5 % glycerol, 2 % SDS, 4 % β -mercaptoethanol, 0.0025 % (w/v) Bromophenol Blue

For SUMO detection, pellets were resuspended in 400 μ l 0.1 M NaOH, and incubated for 5 min at room temperature. Cells were then pelleted again by centrifugation at 16,000xg for 1.5 min. The liquid was discarded. Each pellet was resuspended in 100 μ l extraction buffer and immediately incubated at 99 °C for 3 min. To each suspension, 50-80 μ l glass beads (\emptyset = 0.4-0.5 mm) were added, and each tube was subjected to 1 min of vigorous vortexing, followed by another 3 min of boiling at 99 °C. Then, the samples were subjected to centrifugation at 16,000xg for 3 min, and the supernatant was recovered into fresh tubes.

For all other objectives, the respective pellets were each resuspended in 100 μ l extraction buffer and immediately incubated at 99 °C for 5 min. Samples were spun down at 16,000xg for 3 min, and the supernatant was transferred to fresh tubes.

2.2.5 Crystallization and crystal analysis

2.2.5.1 Crystallization and data collection

Crystals of Ulp2(411-710) were obtained at 4 °C employing the sitting-drop vapour-diffusion technique. The reservoir solution contained 0.2 M di-ammonium hydrogen citrate and 20 % (w/v) PEG 3350. Single crystals appeared after 7 days from a 2:1 ratio of protein solution to reservoir solution. Crystals were cryo-protected in reservoir buffer containing 20 % glycerol and snap-frozen in liquid nitrogen prior to diffraction analysis.

Initial data were collected in-house using a Rigaku MicroMax-007 HF rotating-anode generator equipped with HighFlux mirrors and a MAR345 image-plate detector at 100 K using an Oxford Cryostream 700. A total of 180 degrees of data was collected with an image width of 0.2 degrees and an exposure time of 120 seconds. For phasing, a sulphur-SAD experiment was performed at the Swiss Light Source (Paul-Scherrer-Institute, Villigen, Switzerland) at beamline X06DA equipped with a Pilatus 2M detector (Dectris, Switzerland). Conditions employed were according to a published procedure (Weinert *et al.* 2015). The wavelength was set to 2.0664 Å corresponding to an energy of 6.00 keV. The frame width was set to 0.05 degrees with an exposure time of 0.05 seconds. Beam attenuation was set to 21.7 % resulting in an estimated radiation dose of 0.5 MGy per 360 degrees. Data were collected in four 720 degrees sweeps with a chi angle of the PRIGo goniostat (Waltersperger *et al.* 2015) of 0, 10, 20, and 30 degrees, respectively.

2.2.5.2 Data processing, structure determination and refinement

Native data were processed using *XDS* and scaled with *XSCALE* (Kabsch 2010). The structure was solved by single-wavelength anomalous dispersion using phases computed by the *phenix.autosol* routine of the *PHENIX* package (Adams *et al.* 2011; Read *et al.* 2011). Experimental electron density was interpreted to build a model for the Ulp2 catalytic domain using *SHELX*. The model was refined using iterative cycles of computation by *phenix.refine* (Afonine *et al.* 2012) and manual modeling in *Coot* (Emsley *et al.* 2010).

3 Results

To avoid confusion, in this section the generalized term “SUMO” will be substituted by the precise name of the actual protein (e.g. “Smt3”).

3.1 Characterizing Ulp2 cleavage mechanism

3.1.1 Ulp2 dismantles poly-Smt3 chains in a sequential manner

In 2000, Ulp2 was described for the first time. Apart from genetic, *in vivo* analysis, the SUMO specificity of the protease was determined in a cleavage assay using recombinantly expressed GST-Ulp2 and a His₆-ubiquitin-Smt3-HA construct (Li and Hochstrasser 2000a). The authors of that study reported on a very low *in vitro* activity. In order to gain insight into the processing mode, however, the enzyme of interest must be able to process a substrate to completion. Consequently, a different approach was needed for this study. Testing the original GST-Ulp2 fusion, it proved to be rather insoluble, yielding only little amounts of usable material (data not shown). Maltose binding protein (MBP), a frequently used purification tag of ~42 kDa, has previously been characterized to have positive effects on solubility and folding of its fusion partner (Fox *et al.* 2003). An N-terminal MBP tag indeed overcame the above mentioned solubility problems. An MBP-Ulp2-FLAG construct fulfilled the activity requirements of this study. Notably, C-terminally untagged, S-tagged or His₆-tagged versions were inferior (data not shown). For comparison, an analogous construct was prepared for Ulp1.

In order to investigate on preference and cleavage site selectivity, a set of test substrates was designed (Figure 5). In each of them, a linear chain of Smt3 moieties was linked to enhanced GFP (eGFP). Apart from being a well-characterized protein (Tsien 1998), GFP is reasonably stable, compact due to its β -barrel fold (Stepanenko *et al.* 2013), and also readily trackable by its fluorescence during purification. For simplicity, the here-used eGFP will be abbreviated to GFP in the following text. Mimicking isopeptide bonds, the individual members of the Smt3 chains were fused in a head-to-tail manner.

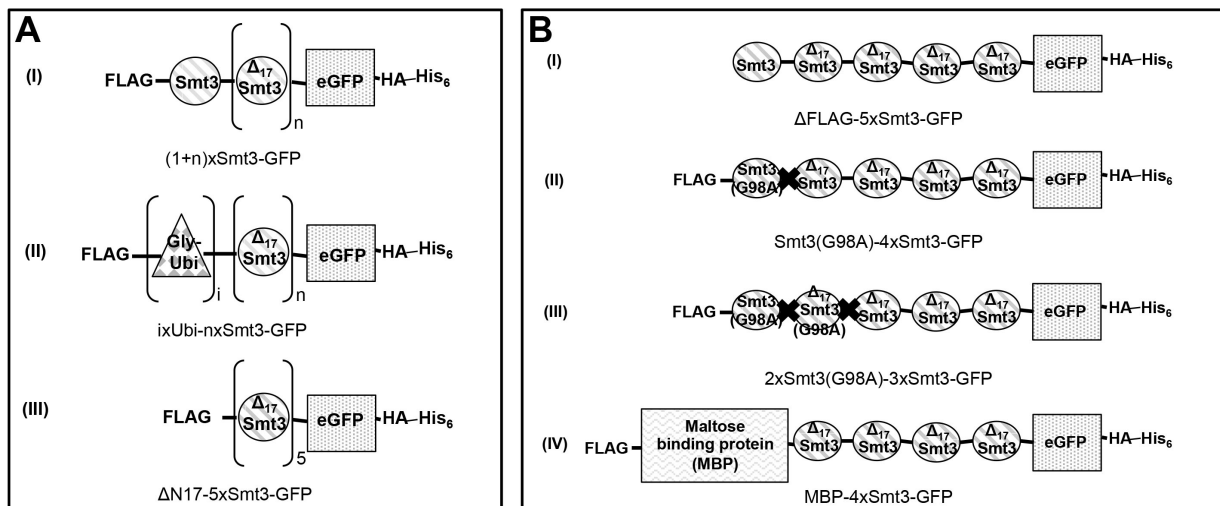


FIGURE 5: Schematic representation of test substrate design. Enhanced green fluorescent protein (eGFP) served as an anchor protein to which Smt3/ubiquitin(ubi) chains were attached. Each construct was equipped with an HA-tag and a hexahistidine (His_6) tag at the C-terminus. With one exception [B(I)], all constructs additionally had an N-terminal FLAG tag in place of the starting methionine residue. Smt3 units were fused in a head-to-tail manner. To mimic natural Smt3-linkages, all but the most distal Smt3 moiety were N-terminally truncated, lacking the first 17 amino acid residues ($\Delta\text{N17Smt3}$ = aa 18-98). The constructs' abbreviations used in the further course of this paper are given under each illustration. **A**, General constructs. $n = 0-4$; $i = 1-3$; constructs featuring (I) Smt3 chains of different length, and with (II) ubiquitin-capped Smt3 chains of different length. Ubiquitin moieties were fused head-to-tail. Each ubiquitin molecule was led by an extra glycine (Gly) residue, which served as a spacer. (III) Control molecule with 5 identical ($\Delta\text{N17Smt3}$) chain members. **B**, Constructs with different levels of N-terminal obstruction. Constructs were used to evaluate importance of an accessible distal end of a substrate-attached SUMO chain for Ulp2 activity. Black cross = uncleavable peptide bond (G98A). Modified from Eckhoff & Dohmen (2015).

As mentioned earlier, Smt3 features three canonical lysine residues, K11, K15 and K19, and most Smt3-Smt3 linkages are formed via one of them. To take account of that, all acceptor molecules in a chain were truncated by the first 17 amino acids (ΔN17), thereby imitating the kinked links. All substrates were equipped with an N-terminal FLAG tag and a C-terminal hexahistidine tag, both of which serving purification purposes. The former was additionally used for analysis for it allowed detection of the first Smt3 moiety. An HA tag between GFP and His_6 was standardly utilized to obtain assay results.

A detailed description can be found in the methods section, but in brief, a 5xSmt3-GFP substrate was incubated with various dilutions of crude extract from MBP-Ulp2-FLAG-expressing *E. coli* cells. Using purified Ulp2 for the assay as a standard was inopportune, since purification came at large costs in terms of both material as well as enzymatic activity. To ensure that no compound of the lysate was falsifying the assay output, and that there was no unspecific cleavage, a MBP-Ulp2(C624A)-FLAG construct was prepared. Mutating the active cysteine to alanine renders the enzyme inactive. Crude extract from *E. coli* cells expressing this version of Ulp2 was used as a negative control in each desumoylation assay. Indeed, these lysates did not have an impact on the integrity of the tested substrates (Fig. 6A).

That means, any observed cleavage activity in the other samples can be assigned to the respective Ulp.

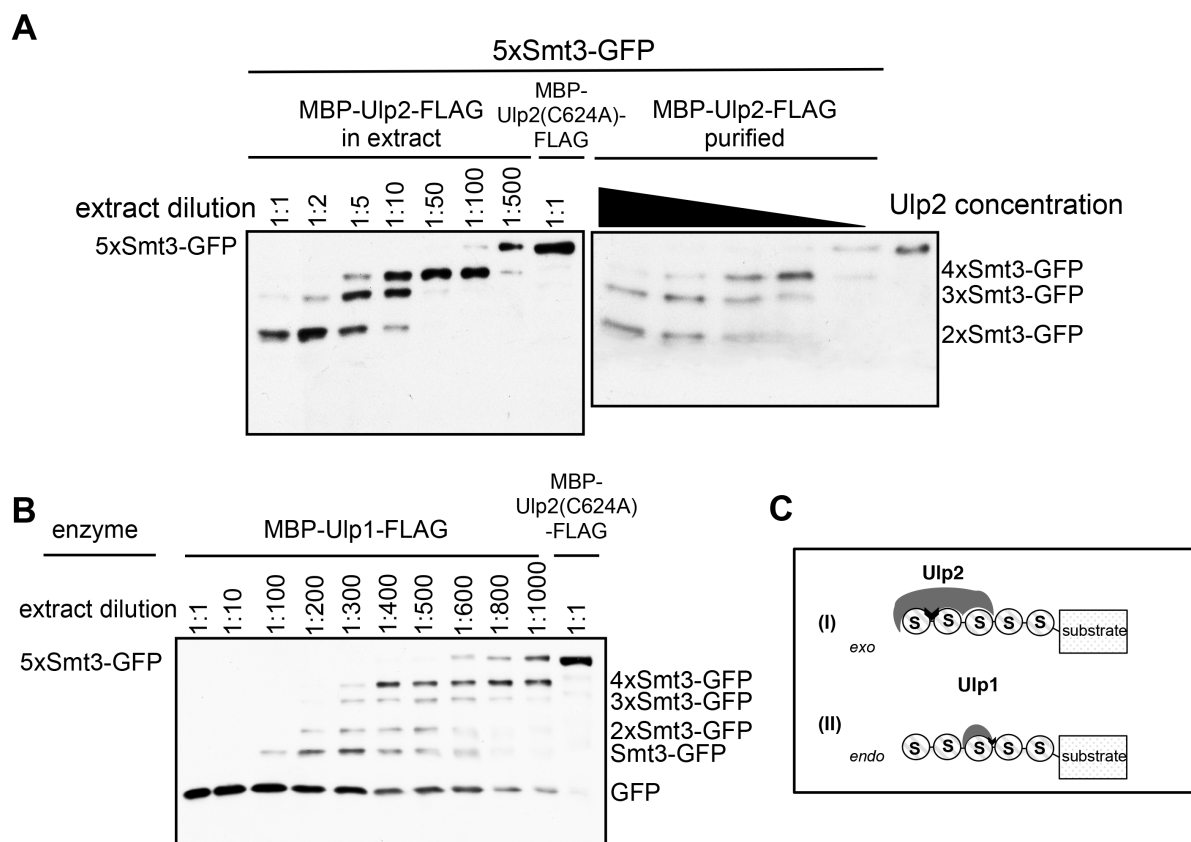


FIGURE 6: Ulp2 liberates single Smt3 moieties from the distal end of a substrate-attached Smt3 chain. 5xSmt3-GFP substrates were incubated with *E. coli* lysates containing Ulp1 or Ulp2 diluted in activity test buffer ("1:1" = undiluted lysate). A lysate that contained the inactive (inact.) variant of Ulp2(C624A) was used as a control. Substrates were incubated with different dilutions of Ulp-containing lysates for 2 h at 30 °C. Reaction products were then analyzed by SDS-PAGE and anti-HA Western blotting. Full-length substrate is labeled on the *left-hand side* of each blot, cleavage products are labeled on the *right*. **A**, Analysis of Ulp2 activity profile using either *E.coli* lysate containing MBP-Ulp2-FLAG or purified MBP-Ulp2-FLAG. Purified MBP-Ulp2-FLAG was diluted in activity test buffer (ATB). A control sample contained only ATB instead of enzyme solution (right lane). 5xSmt3-GFP substrate was treated with dilutions of MBP-Ulp2-FLAG (1:1, 1:2, 1:5, 1:10, 1:100) for 2 h at 30 °C. **B**, Analysis of Ulp1 activity profile. **C**, Schematic representation of mechanistic differences between Ulp2 and Ulp1. Ulp2 binds to the first three consecutive Smt3 units and works by cleaving single Smt3 units off the end of a chain (*exo*). Ulp1 requires only a single Smt3 molecule to bind a target and can cleave randomly after any Smt3 moiety inside of the chain (*endo*). Figure modified from Eckhoff & Dohmen (2015).

As also reported from other studies, Ulp1 exhibited a comparatively high activity *in vitro*. This was taken into account by using higher dilutions of the extract containing recombinant Ulp1. Even though of inferior levels, Ulp2 activity was sufficient to process the substrates to completion, thereby allowing for assaying its cleavage profile. Ulp2 exhibited an ordered sequential processing activity, dismantling the most distal Smt3 moiety first, then the next in line, etc. (Fig. 6A). This diverges from what has been described for SENP6, for which an indiscriminate, stochastic cleavage mode has been reported (Békés *et al.* 2011).

In contrast to Ulp2, Ulp1 produced a rather distributive cleavage pattern, indicating that it randomly cleaves any isopeptide linkage within a given Smt3 chain (Fig. 6B). These results suggest drastically different cleavage mechanisms for the two Ulp1s, with Ulp2 employing an *exo* mechanism to break down Smt3 chains, whereas Ulp1 operates by a stochastic (*endo*) mode, not showing any preference about which isopeptide bond of a substrate-attached Smt3 chain to cleave first (Fig. 6C). However, due to its very high activity level *in vitro*, from a dilution series as shown in Fig. 6B, one cannot with reasonable certainty exclude the possibility that Ulp1 actually acts as an *exo* enzyme, but high processivity made the cleavage pattern suggest an *endo* mechanism. To address this issue, the most distal Smt3 moiety of 5xSmt3-GFP was followed over time when incubated with Ulp1, making use of the substrate's N-terminal FLAG tag.

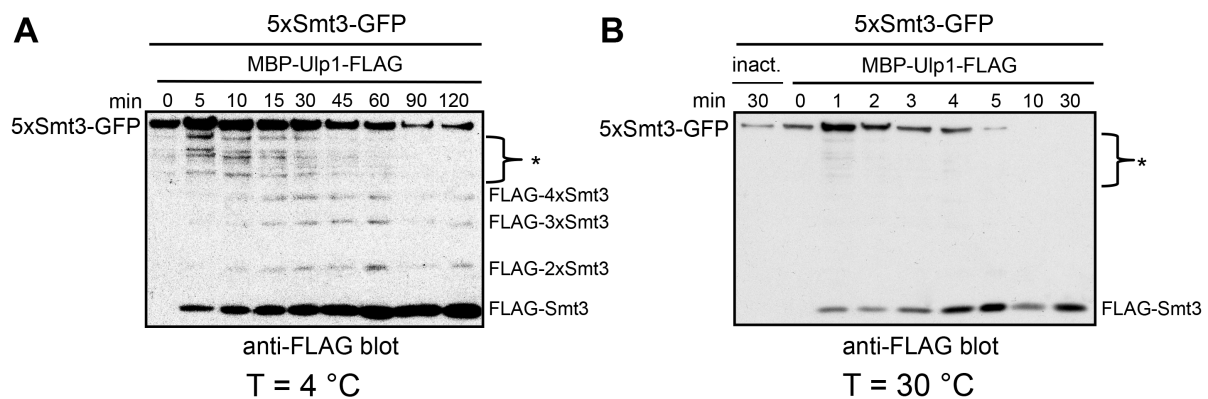


FIGURE 7: Ulp1 removes poly-Smt3 from a substrate chain. Purified 5xSmt3-GFP was incubated with a 1:2,000 dilution of lysate containing MBP-Ulp1-FLAG. Dilutions were prepared using reaction buffer. At the indicated time points, samples were withdrawn and reaction was stopped by addition of SDS-PAGE loading buffer and subsequent boiling. Then, reaction mixtures were separated by SDS-PAGE and subjected to Western blot detection of FLAG tag. Extract-derived or unspecific bands are indicated by asterisk (*). The full-length substrate is indicated on the *left-hand side* of each blot, cleavage products are indicated on the *right*. **A**, Assay was performed on ice. **B**, Assay was performed at 30 °C; inact. = sample contained undiluted extract containing MBP-Ulp2(C624A)-FLAG. Modified from Eckhoff and Dohmen (2015).

Of note, only drastically reducing reaction velocity by performing the assay on ice allowed for detection of released oligo-Smt3 chains (Fig. 7A). At 30 °C, no such intermediates were detectable (Fig. 7B). Apparently, reaction was too fast at that temperature. These findings indicate two things: Firstly, Ulp1 indeed works via an *endo* mechanism. Secondly, it seems to be highly processive, and after the first cut rapidly dismantles a chain down to monomeric Smt3.

The band pattern obtained from tracking the GFP-containing leaving group hinted towards Ulp2 cleaving off one unit of Smt3 at a time. To verify this, Smt3 chain cleavage was monitored over time tracking the FLAG tag attached to the most distal moiety of the substrate

Since all but the first unit of Smt3 were truncated, it was necessary to check whether featuring the first 17 amino acids (with the exception of the first methionine) conferred any bias to the enzyme's preference. To this end, a substrate was tested in which also the most distal chain member was a truncated version (5x Δ N17Smt3-GFP). As shown in Fig. 9, deletion of the N-terminus of the distal Smt3 moiety did not affect the cleavage pattern observed for Ulp2.

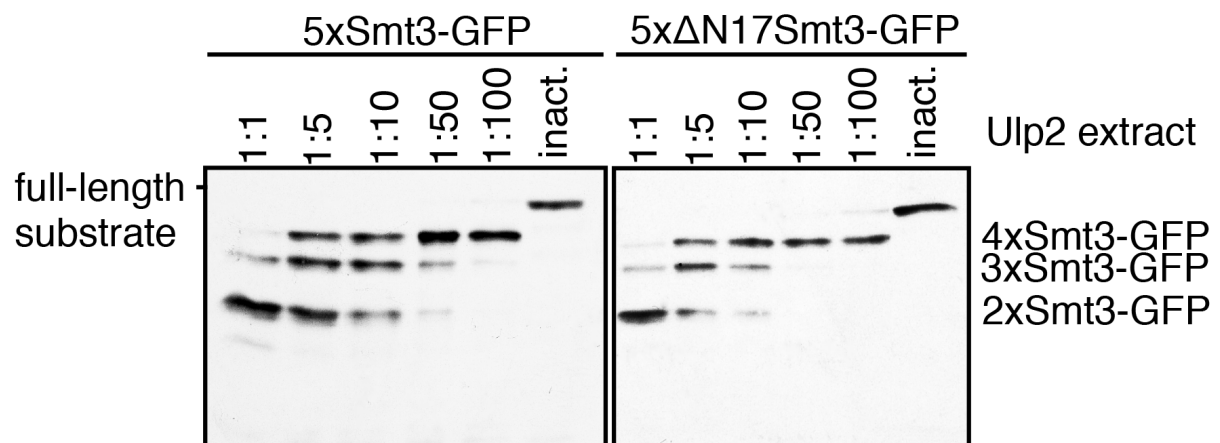


FIGURE 9: Ulp2 does not discriminate between full-length Smt3 and N-terminally truncated (Δ N17) Smt3. Comparison of band patterns derived from Ulp2-mediated processing of substrates harboring Smt3 chains led either by full-length Smt3 or by N-terminally truncated (Δ N17) Smt3. These 5xSmt3-GFP substrates were incubated with *E. coli* lysates containing Ulp2 diluted in activity test buffer ("1:1" = undiluted lysate). As a control, a lysate was used that contained the inactive (inact.) C624A variant of Ulp2. Substrates were incubated with different dilutions of Ulp2-containing lysates for 2 h at 30 °C. Reaction products were then analyzed by SDS-PAGE and anti-HA Western blotting. Sizes of full-length substrates are indicated on the *left* of the blots, product sizes are labeled on the *right*. Modified from Eckhoff & Dohmen (2015).

Any measure taken to ensure that artificial substrates are as close to authentic ones as possible cannot conceal the fact that they are still not natural. In order to test whether linear head-to-tail fusions are suitable models for native Smt3 chains, thus allowing accurate analysis of Ulp mechanisms, a previously described *in vivo* sumoylation system reconstituted in *E. coli* was utilized to obtain a substrate decorated with authentic Lys-linked Smt3 chains (Wohlschlegel *et al.* 2006). Ubc9, the SUMO-E2 enzyme, catalyzes its own sumoylation in yeast cells (Klug *et al.* 2013). Exploiting this feature, it was made the anchor protein in the *E. coli*-based system to generate polysumoylated Ubc9 (Fig. 10 A&B). When the system was supplied with Smt3 in which the three canonical acceptor sites (K11, 15 and 19) were rendered unusable for chain formation by exchanging Lys with Arg (R), the chains were markedly shorter. This gives solid hint that the polysumoylated Ubc9 carries chains whose linkages have been formed preferentially via one of the major acceptor lysines in Smt3. Similar to what was observed for the artificial substrates, Ulp2 processed the native chains

attached to Ubc9 sequentially starting from the distal end (Fig. 10C). Hence, one can say that the GFP-anchored head-to-tail fusions are a feasible model, and that the mechanistic conclusions drawn from those assays well reflect what is true for Ulp2 activity towards authentic K-linked Smt3 chains.

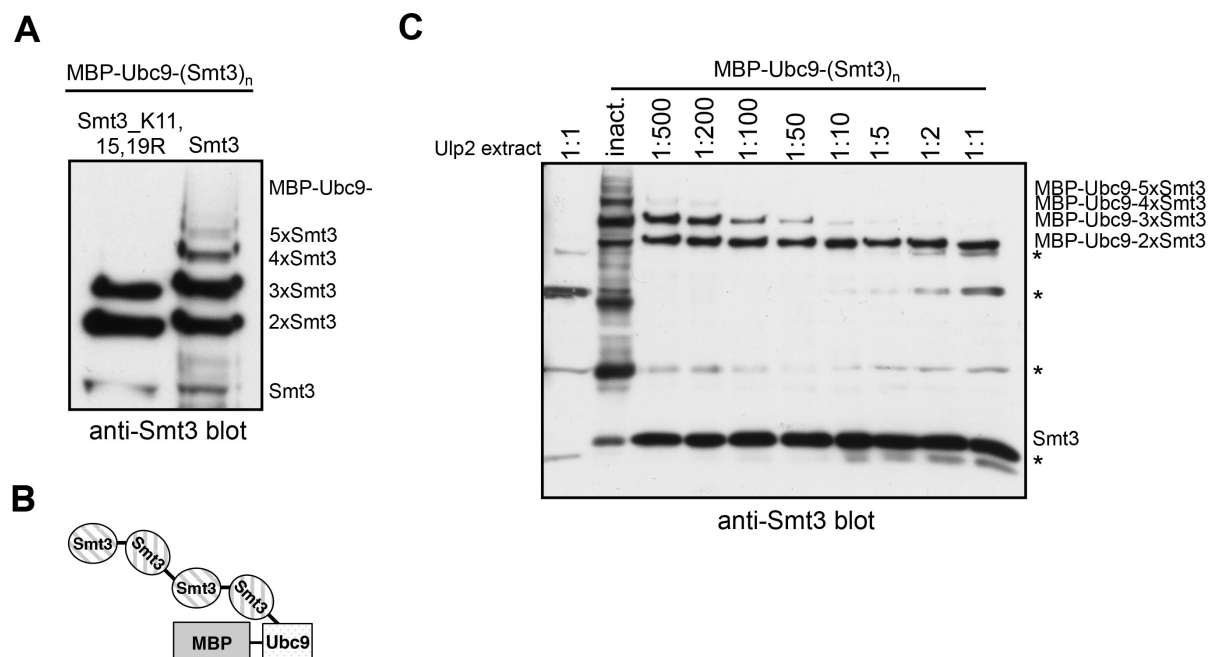


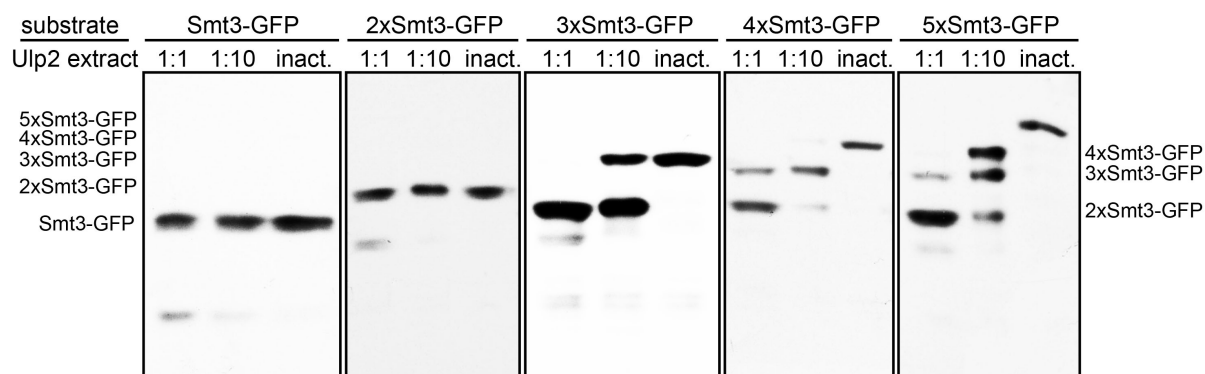
FIGURE 10: Ulp2 dismantles authentic, K-linked poly-Smt3 chains from their distal ends. **A**, MBP-Ubc9 conjugated to Smt3 was produced utilizing an *E. coli*-based *in vivo* sumoylation system. Isopeptide bonds in larger Smt3 chains are formed primarily via the canonical acceptor lysines K11,15,19. **B**, Schematic representation of test substrate obtained from reconstituted sumoylation system in *E. coli* (in this example: MBP-Ubc9-4xSmt3). **C**, MBP-Ubc9 conjugated to poly-Smt3 chains of different lengths was incubated with *E. coli* lysate containing Ulp2 diluted in activity test buffer ("1:1" = undiluted lysate). As a control, lysate containing the inactive (inact.) variant of Ulp2(C624A) was used. Substrates were incubated with different dilutions of Ulp2-containing lysates for 2 h at 30 °C. Reaction products were then analyzed by SDS-PAGE and immunodetection of Smt3. Lysate-derived signals are indicated by asterisk (*). Modified from Eckhoff & Dohmen (2015).

3.1.2 Three linked Smt3 moieties are the minimum Ulp2-target requirement

Previous studies identified Ulp2 as an enzyme processing poly-Smt3 chains (Bylebyl *et al.* 2003). Considering this and the data presented above, it was of interest to determine the requirements on an Smt3 chain to be recognized as a target by Ulp2. To address this, substrates featuring 1-5 Smt3 moieties were assayed. As it turned out, neither mono- nor di-Smt3 were efficiently cleaved by Ulp2 (Fig. 11A). For all other substrates, the reaction stopped at the stage of two Smt3 moieties attached to GFP. This indicates that Ulp2 needs a minimum of three linked units of Smt3 to efficiently process a substrate chain. To verify this, ubiquitin-capped substrates were tested likewise. This set confirmed that mono- or di-Smt3 does not serve as a Ulp2 target, and that cleavage only occurs when the chain contains at least

three linked units of Smt3 (Fig. 11B). In addition, assaying the ubiquitin-capped substrates established that, in terms of substrate recognition by Ulp2, ubiquitin moieties could not replace Smt3 in a chain.

A



B

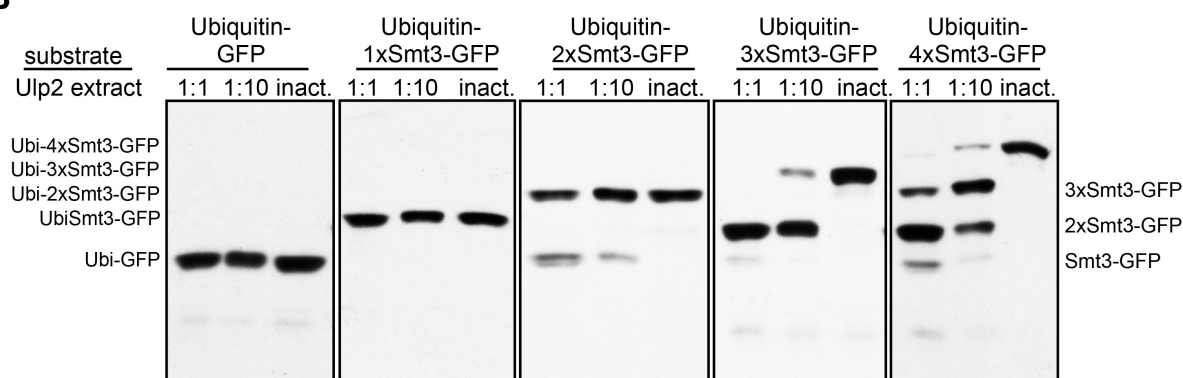


FIGURE 11: Ulp2 preferentially acts on substrates with chains composed of three or more Smt3 units. The indicated substrates were incubated with *E. coli* lysates containing MBP-Ulp2-FLAG diluted in activity test buffer. Undiluted lysate containing the inactive variant Ulp2(C624A) was used as a control. Purified Smt3 chains consisting of 1 to 5 Smt3 moieties linked to GFP-HA (**A**) or purified ubiquitin-capped substrates consisting of 0 to 4 Smt3 units linked to GFP-HA (**B**) were subjected to digestion by MBP-Ulp2-FLAG in *E. coli* lysate for 2 h at 30 °C. Reaction products were analyzed by SDS-PAGE and anti-HA Western blotting. Sizes of full-length substrates are indicated on the *left* of the blots, product sizes are labeled on the *right*. Modified from Eckhoff & Dohmen (2015).

3.1.3 Efficient cleavage by Ulp2 requires free access to N-terminal region or surrounding surfaces of the distal Smt3 moiety

Ulp2's clear preference for the distal end of an Smt3 chain gave rise to the question whether disabling free access to the N-terminus would interfere with cleavage, and if so, to which extent this would be inhibitory or changing the cleavage pattern. To investigate this, various substrates with different N-termini were prepared. To begin with, the standard 5xSmt3-GFP substrate, which carries an N-terminal FLAG tag, was compared to a version that lacks that tag (Δ FLAG-5xSmt3-GFP). As shown in Fig. 12A, if at all, the FLAG tag had a minor effect on processing by Ulp2. However, obstructing the distal end with one or two units of

3xSmt3-GFP function as intrinsic inhibitors by trapping the enzyme. In another variant, the first Smt3 is replaced by MBP (MBP-4xSmt3-GFP). The 42-kDa-protein caused a massive drop in cleavage efficiency, as well (Fig 12B). Interestingly, the obstruction effect was less severe than in case of two consecutive units of Smt3(G98A). Since 2xSmt3(G98A) featuring a combined molecular weight of ~23 kDa, this is disproportional to the size of the blocking species.

In summary, these findings demonstrated that cleavage of an Smt3 chain is obliged to start at the most distal unit, and obstructing this moiety significantly impairs processing of that chain by Ulp2. In contrast to that, none of the obstructing species could hamper chain cleavage by Ulp1 (Fig. 12c).

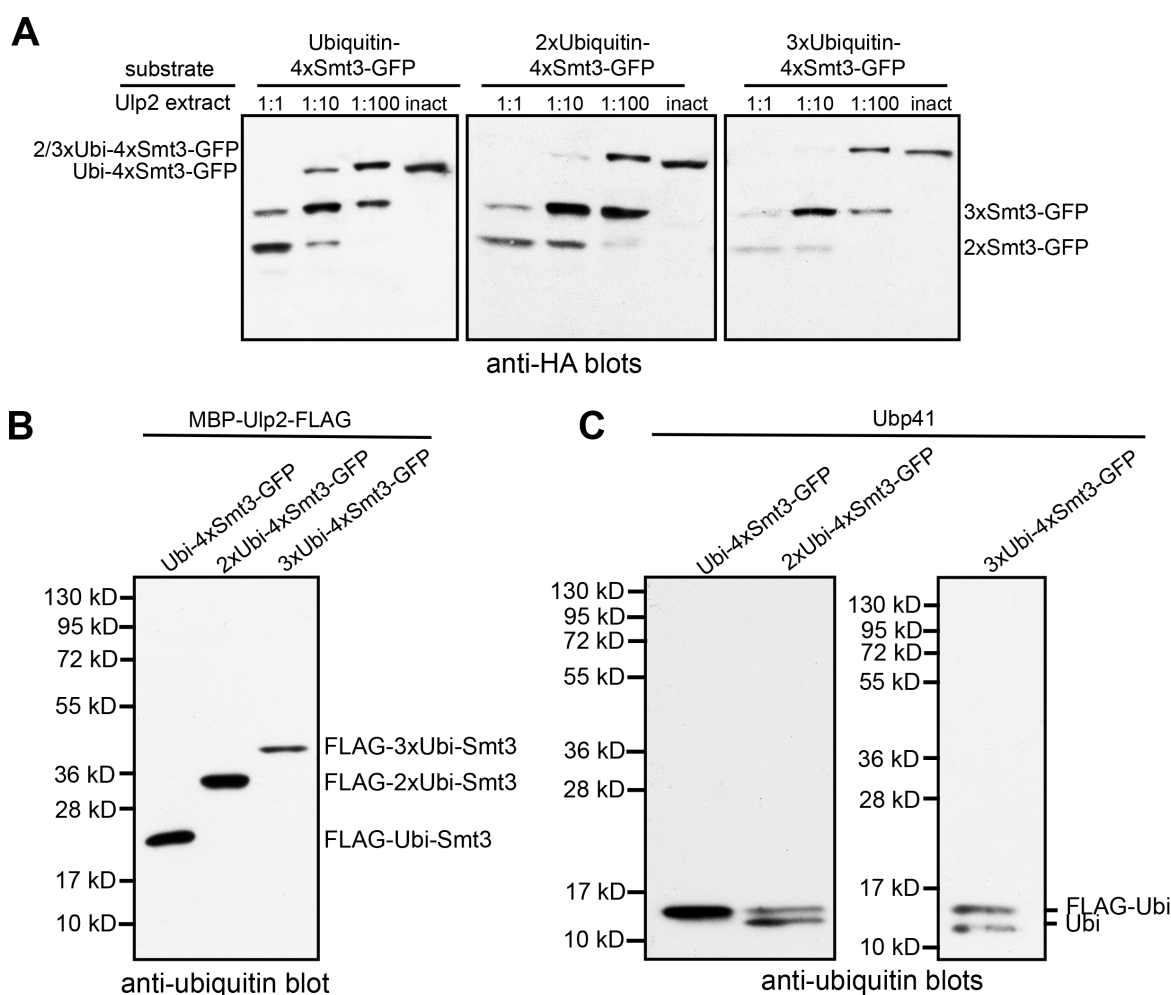


FIGURE 13: Multiple units of ubiquitin at the distal end of an Smt3 chain do not interfere with processing of an Smt3 chain by Ulp2. Ubi = ubiquitin. **A**, The indicated substrates were incubated with *E. coli* lysates containing MBP-Ulp2-FLAG diluted in activity test buffer for 2 h at 30 °C. An undiluted lysate containing the inactive variant Ulp2(C624A) was used as a control (inact.). Reaction products were analyzed by SDS-PAGE and anti-HA Western blotting. Sizes of full-length substrates are indicated on the *left-hand side* of each blot, products are labeled on the *right*. **B**, As in **A**, but anti-ubiquitin Western blotting was used, and the blot does not include control samples. **C**, Same as **B**, but using purified Ubp41 instead of Ulp2 lysate. Modified from Eckhoff & Dohmen (2015).

Unlike what was found for uncleavable Smt3 and MBP, capping Smt3 chains with ubiquitin had only a mild, if any, inhibitory effect on target processing by Ulp2 (Fig. 13A).

Surprisingly, attaching one, two or even three units of ubiquitin to 4xSmt3-GFP did not interfere with cleavage. Apparently, Ulp2 tolerates a sufficiently flexible appendix such as one to three ubiquitin moieties. On a side note, confirming previous findings (Li and Hochstrasser 2000a), Ulp2 did not show any activity towards ubiquitin (Fig. 13B). In contrast, the ubiquitin-specific protease Ubp41 could readily cleave off the ubiquitin molecules in a control experiment (Fig. 13C).

3.1.4 Ulp2 needs at least three consecutive Smt3 moieties to capture a target

Having established three units as the minimum length of an Smt3 chain to serve as a Ulp2 target, the obvious next question was whether this preference was due to the enzyme's inability to bind to shorter chains. To this end, a binding test was designed that made use of the inactive variant of Ulp2, Ulp2(C624A). While being unable to process a substrate, the single-site mutation apparently did not affect the enzyme's binding abilities. In the assay, MBP-Ulp2(C624A)-FLAG was immobilized on amylose resin via its MBP tag, and then incubated with different substrates. Control samples confirmed that none of the substrates bound to pure amylose resin (Fig. 14); hence, all observed signals are specific and due to Ulp2-substrate interaction.

The assay displayed that Ulp2 indeed needs three units of Smt3 to efficiently bind a target (Fig. 14). Interestingly, affinity did not seem to increase for chains longer than three members, suggesting a binding mode that involves three Smt3 binding sites on Ulp2, which have to be simultaneously occupied in order to achieve full cooperative binding. On a side note, capping chains with uncleavable Smt3 did not interfere with the ability of Ulp2 to bind to them (Fig. 14B). Testing whether this holds true for MBP-4xSmt3-GFP, too, required modification of the assay. Instead of amylose, anti-FLAG resin was utilized to immobilize the enzyme, and the usual substrates were swapped for analogous ones without FLAG tags. As shown in Fig. 14C, an MBP-led chain is still captured by Ulp2, albeit less efficient than an uncapped one.

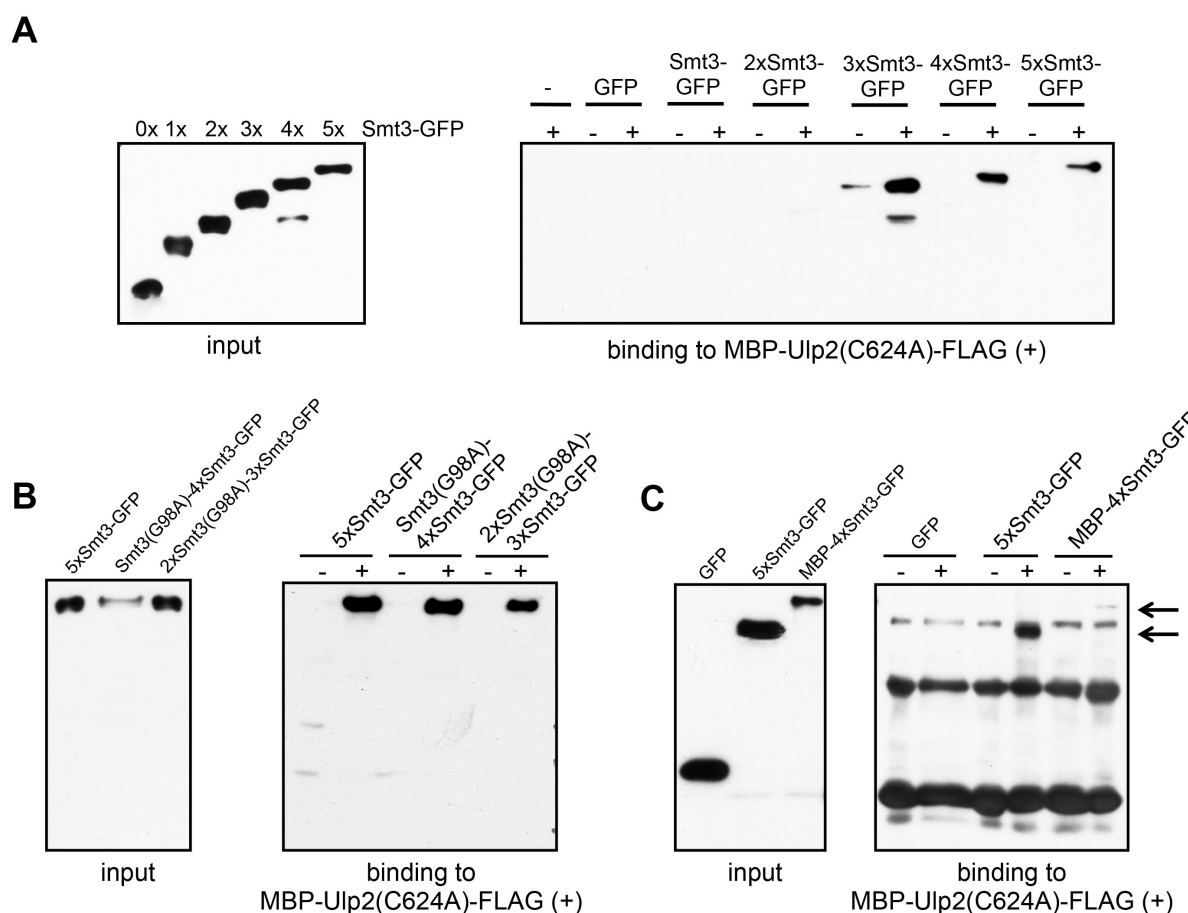


FIGURE 14: Ulp2 binds to Smt3 chains featuring at least three members. Input: Volumes of each substrate preparation equal to the volumes used in the binding assays were analyzed by SDS-PAGE and anti-HA Western blotting. **A**, MBP-Ulp2(C624A)-FLAG was immobilized on amylose resin, and subsequently incubated with ~100 nM of substrates with chains of different lengths (+). As a control, the same amount of each substrate was incubated with pure amylose resin (-). After 1.5 h, unbound proteins were washed off, and boiling in SDS-PAGE loading buffer eluted specifically bound proteins. Seventy-five percent of each elution volume were analyzed by SDS-PAGE and anti-HA Western blotting. **B**, Assessing the ability of Ulp2 to bind to Smt3 chains capped by one or two units of Smt3(G98A). Same procedure as for **A**. **C**, Assessing the ability of Ulp2 to bind to Smt3 chains capped by MBP. Basically same procedure as for **A** and **B**, but instead of on amylose resin, MBP-Ulp2(C624A)-FLAG was immobilized on anti-FLAG M2 resin, and the substrates did not contain N-terminal FLAG tags. Modified from Eckhoff & Dohmen (2015).

3.1.5 The active domain of Ulp2

3.1.5.1 Characteristics of the Ulp2 mechanism are grounded in the active domain

In the last decade, desumoylation enzymes and their cleavage behavior have been the focus of several studies. For instance, DeSI-1 and SENP2 have been identified to cleave isopeptide bonds rather stochastically (Shin *et al.* 2012; Lima and Reverter 2008). Since SENP2 belongs to the Ulp1-family of proteases, this is not surprising and goes well in line with the *endo* mode of Ulp1 presented above. Interestingly, however, both Ulp2-family SENPs (SENP6 and

SENp7) have been reported to cleave SUMO-SUMO linkages randomly, as well (Békés *et al.* 2011; Lima and Reverter 2008). Notably, those findings were based on analysis done with the active domains only. Ulp2 is a large protein in which the non-catalytic domains comprise the major part of the molecule. Of its 1034 amino acid residues, only 283 are counted to the active domain (UD), which lies between serine-411 and lysine-693. A previous *in vivo* study identified the N-terminus to be necessary and sufficient for nuclear localization of Ulp2, while its C-terminus was found to be required for efficient depolymerization of large poly-Smt3 conjugates (Kroetz *et al.* 2009). Against the background of Ulp2's *exo* mechanism presented in this work, especially the latter finding gave rise to the question, whether the non-catalytic domains arrange the UD on Smt3 chains in a way that only allows ordered, sequential desumoylation. To investigate on this, the UD alone [MBP-Ulp2(411-693)-FLAG] was analyzed via the same activity assay as the full-length enzyme before. Surprisingly, the cleavage pattern was indistinguishable from the one that had been found for full-length Ulp2 (Fig. 15A). Also the binding preferences of the truncated version were the same as those of wild type (Fig 15B). In conclusion, features of the UD define both the *exo* mechanism and the preference for Smt3 chains of more than three members. The non-catalytic domains do not take part in that.

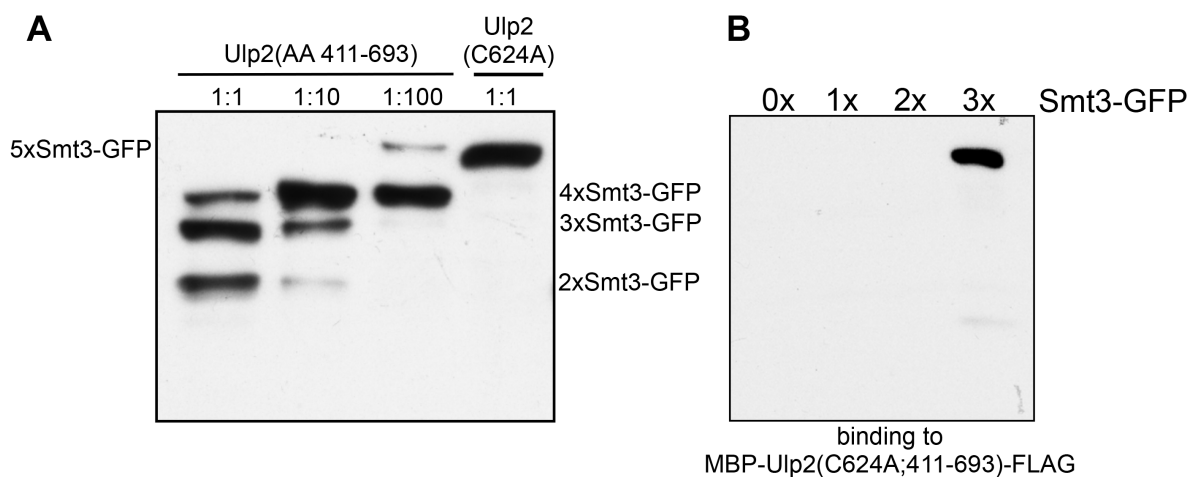


FIGURE 15: The UD alone exhibits the same preferences as full-length Ulp2. *A*, 5xSmt3-GFP was incubated with *E. coli* lysates containing MBP-Ulp2(411-693)-FLAG diluted in activity test buffer for 2 h at 30 °C. An undiluted lysate containing the inactive, full-length variant MBP-Ulp2(C624A)-FLAG was used as a control. Reaction products were analyzed by SDS-PAGE and anti-HA Western blotting. The full-length substrate is indicated on the *left-hand side* of the blot, cleavage products are indicated on the *right*. *B*, MBP-Ulp2(C624A;411-693)-FLAG was immobilized on amylose resin, and subsequently incubated with ~100 nM of substrates with chains of different lengths. After 1.5 h, unbound proteins were washed off, and boiling in SDS-PAGE loading buffer eluted specifically bound proteins. Seventy-five percent of each elution volume were analyzed by SDS-PAGE and anti-HA Western blotting. *Left* panel was modified from Eckhoff & Dohmen (2015).

3.1.5.2 A SIM close to the active domain might be controlled by the NTD

The UD has been reputed to be hard to recombinantly express in an active form. For this reason, setting out to analyze it, several differently truncated versions of the full-length enzyme were prepared and tested in parallel. In the course of that, an interesting feature of Ulp2 was discovered. Among the mutants, two variants, Ulp2(411-774) and Ulp2(411-1034), were able to completely dismantle an Smt3 chain (Fig. 16A).

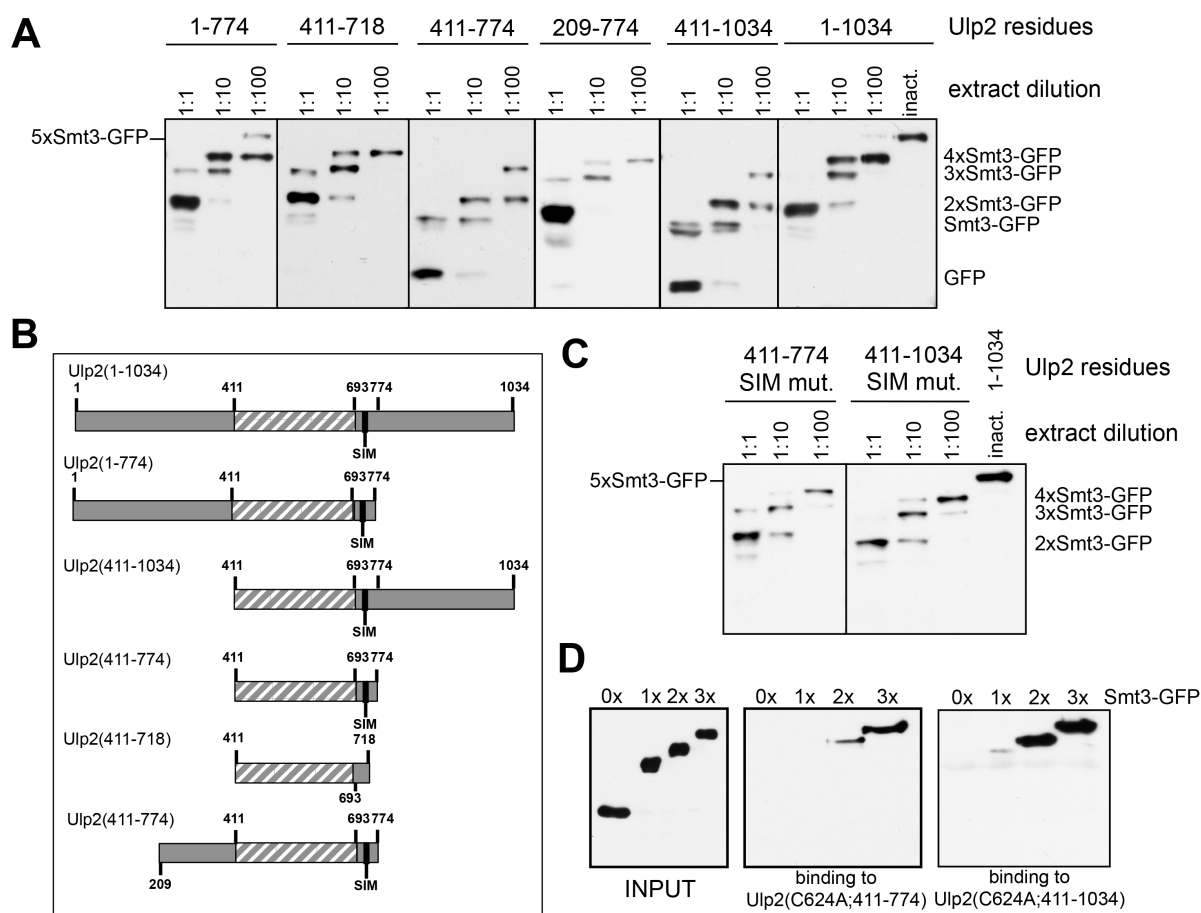


FIGURE 16: The UD alone exhibits the same preferences as full-length Ulp2. **A**, 5xSmt3-GFP was incubated with *E. coli* lysates containing different truncation variants of Ulp2 framed by MBP and FLAG tag diluted in activity test buffer for 2 h at 30 °C. An undiluted lysate containing the inactive, full-length variant MBP-Ulp2(C624A)-FLAG was used as a control. Reaction products were analyzed by SDS-PAGE and anti-HA Western blotting. The full-length substrate is indicated on the *left-hand side* of the blot, cleavage products are indicated on the *right*. **B**, Schematic representation of Ulp2 domain arrangement and truncation mutant designs. Numbers indicate corresponding position of residues in the respective compartment. Striped = UD. **C**, As for **A**, but with lysate of Ulp2 truncation variants in which the SIM was mutated (DDDDEEIQII → DDDDEEAQAA). **D**, Input: Volumes of each substrate preparation equal to the volumes used in the binding assays were analyzed by SDS-PAGE and anti-HA Western blotting. Inactive (C624A) Ulp2 truncation variants were immobilized on amylose resin, and subsequently incubated with ~100 nM of substrates with chains of different lengths. After 1.5 hours, unbound proteins were washed off, and boiling in SDS-PAGE loading buffer eluted specifically bound proteins. Seventy-five percent of each elution volume were analyzed by SDS-PAGE and anti-HA Western blotting.

Those mutants lacked the N-terminal non-catalytic domain and their C-terminus exceeded the UD. Sequence analysis revealed that both of them contained a certain SIM (see Figure 16B for a schematic representation), which had already been reported on (Kroetz *et al.* 2009) and been subject to some *in vivo* analysis (Baldwin *et al.* 2009). This motif resides in the borders of D719 and E729. To test whether the SIM was causing the gain of function, corresponding variants were prepared, in which the hydrophobic residues were exchanged by alanine (DDDDEEIQII → DDDDEEAQAA). As shown in Figure 16C, in these mutants wild type behavior was restored. This confirmed that the SIM provoked the untypical cleavage activity. Of note, all truncation mutants were equally well expressed, ruling out the possibility that expression levels were part of the explanation. Also their activity levels were comparable. Ulp2(411-774) and Ulp2(411-1034) were able to efficiently process mono- and di-sumoylated substrates, whereas the other variants, like the full-length enzyme, did not (data not shown). Irritatingly, the ability to recognize mono-Smt3 as a target cannot be entirely explained by elevated binding abilities. While the gain-of-function mutants were able to capture 2xSmt3-GFP in a binding test, they did not bind to monosumoylated GFP (Fig. 16D). Since Ulp2(209-774) did not show divergent cleavage activity (Fig. 16A), an element in the region between aspartate-210 and asparagine-410 must have some kind of controlling impact on the SIM. Since the *in vivo* relevance of this feature is questionable, the investigations on this stopped at this point.

3.1.6 Ulp2 hardly recognizes SUMO2

As discussed earlier, unlike yeast, humans express four different forms of SUMO, some of which are highly different in sequence. These differences account for the paralogue-specificity of the various SENPs. Smt3 shares about 48 % sequence homology with SUMO1, and is ~42 % identical to SUMO2. Ulp2 has been known to recognize SUMO1 (Li and Hochstrasser 2000a), but it was unclear whether it would process SUMO2, as well. To test this, a SUMO2-led version of the standard substrate was prepared (SUMO2-4xSmt3-GFP) and incubated with Ulp2. As shown in Fig. 17A and 17B, SUMO2 has an inhibitory effect on the reaction and is hardly trimmed off by Ulp2.

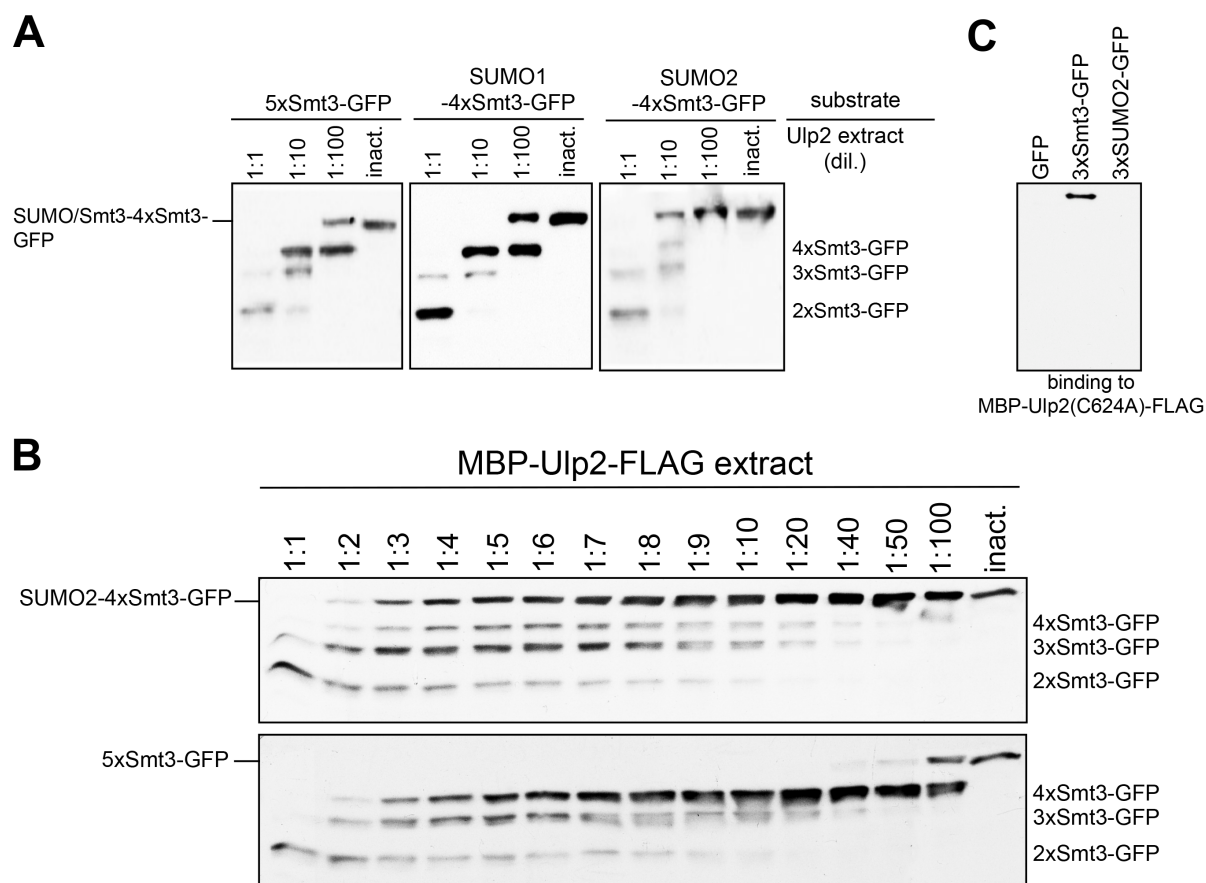


FIGURE 17: Ulp2 does not bind to SUMO2 and hardly processes it when it is part of an Smt3 chain. A, Substrates composed of 4x Δ N17Smt3-GFP led by either Smt3, SUMO1 or SUMO2 were incubated with *E. coli* lysates containing MBP-Ulp2-FLAG diluted in activity test buffer for 2 h at 30 °C. An undiluted lysate containing the inactive variant Ulp2(C624A) was used as a control. Reaction products were analyzed by SDS-PAGE and anti-HA Western blotting. The full-length substrate is indicated on the *left-hand side* of the blot, cleavage products are indicated on the *right*. **B,** As for **A**, but without SUMO1 and with higher resolution due to a higher number of dilutions. **C,** MBP-Ulp2(C624A)-FLAG was immobilized on amylose resin, and subsequently incubated with ~100 nM of substrates with chains of different composition. After 1.5 h, unbound proteins were washed off, and boiling in SDS-PAGE loading buffer eluted specifically bound proteins. Seventy-five percent of each elution volume were analyzed by SDS-PAGE and anti-HA Western blotting.

Indeed, the enzyme preferentially cut after the second chain member, which is the first unit of Smt3 in the chain. This result was supported by the finding that Ulp2 cannot capture a 3xSUMO2-GFP substrate in a binding assay (Fig. 17C). Apparently, Ulp2 hardly recognizes SUMO2 as a target.

3.1.7 Ulp2 recognizes different surface areas of each of its three binding partners in trimeric Smt3

The finding of Ulp2 not processing SUMO2 offered a great opportunity to identify the sites in Smt3 that are relevant for interaction with the enzyme. Since the structures of Smt3 and SUMO2 are superimposable with high accuracy (Fig. 18), it was possible to mutate defined

In brief, adjacent differing residues were grouped together and subsumed as “motifs”. Figure 19A shows which region corresponds to which motif name. This nomenclature will be used in the entire following text. (On a side note, the odd numbering is due to the development of this sub-study and shall not be of any disturbance.) Additionally, “motif” will be abbreviated to “M” from now on.

The respective sequence stretches in Smt3 were exchanged by the corresponding sequence of SUMO2, creating sets of mutants carrying these mutations in either the first (= most distal), the second, or the third moiety of an Smt3 chain linked to GFP (see Fig. 19B for schematic representation). Assaying the binding ability of Ulp2 to Smt3 chains of different length (Fig. 11), had given a hint towards Ulp2 featuring three different binding sites for Smt3, and that all three sites had to be occupied in order to cleave the most distal member in a chain. If that hypothesis was correct, different regions of Smt3 should be relevant in the first three moieties counted from the distal end to cleave off the first one. As shown in Fig. 20, this, in fact, was the case. While Smt3(M1), Smt3(M5) and Smt3(MEnd) at the distal end were dismantled less efficiently than wild-type Smt3 (Fig. 20A&D), these mutations did not negatively affect cleavage when present in the second or third moiety. In contrast, Smt3(M6) was readily cleaved off, but in the second Smt3 unit this patch caused limited processing of the most distal chain member (Fig. 20B). Of note, initial data for this set [Smt3-Smt3(M)-3xSmt3-GFP] of motif mutants (with the exception of the SUMO2 insertion mutant) were raised by Lea Schürholz, a Bachelor student, who did this test in the course of her Bachelor thesis (2015) using full-length Ulp2 under supervision of the author of this work. For this work, some of the constructs were newly cloned, expressed and purified.

Last but not least, M0 and M4 are only relevant in the third position (Fig. 20C). A structural representation of the sites is given in Figure 23. On a side note, due to experimental problems, MEnd could not be tested for the third position. This mutant will be tested as soon as possible. For each set of mutants, a chain containing a SUMO2 moiety in the position of focus was tested alongside the motif variants. The inhibitory effect provoked by this substrate set the standard for what was considered a relevant motif. Of note, processing by Ulp1 was not limited by the mutations in the different positions (Fig. 21). The interaction points between Ulp1 and Smt3 have been determined in a previous crystallization study (Mossessova and Lima 2001), and, of course, variants in which these residues were affected were not or hardly cleaved off by the enzyme. However, the respective Smt3 chain members were merely skipped and did not cause any further relevant effect, as expected considering the *endo* mode by which Ulp1 works.

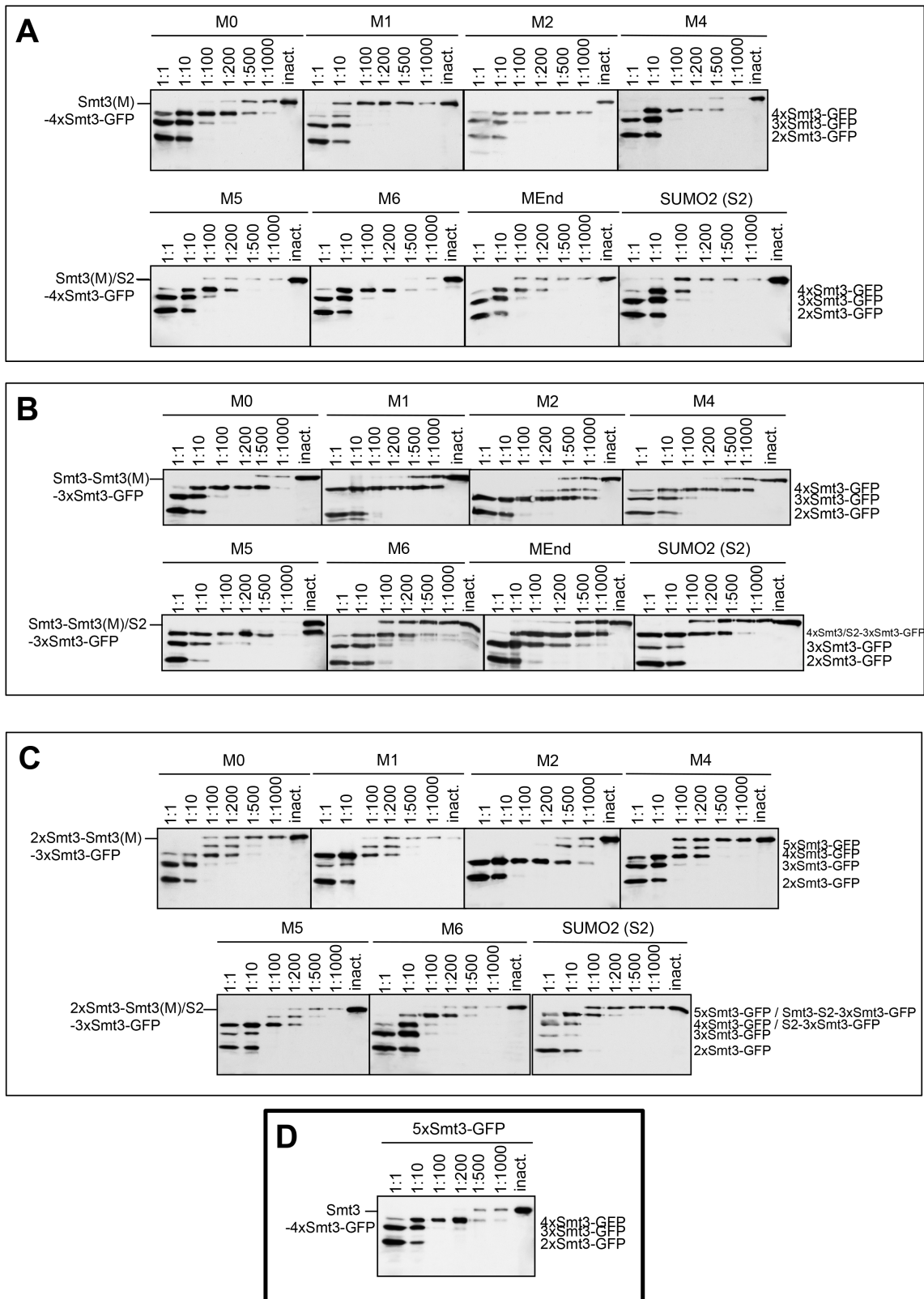


FIGURE 20: Different regions in the three first Smt3 moieties are important for cleavage of the distal unit. *A*, Substrates, in which the most distal Smt3 moiety was mutated or was SUMO2, were incubated with *E. coli* lysates containing MBP-Ulp2(411-710)-FLAG diluted in activity test buffer for 2 h at 30 °C. An undiluted lysate containing the inactive variant Ulp2(C624A) was used as a control. Reaction products were analyzed by SDS-PAGE and anti-HA Western blotting. The full-length substrate is indicated on the *left-hand side* of the blot, cleavage products are indicated on the *right*. *B*, As for *A*, but here the second moiety was mutated. *C*, As for *A*, but here the third moiety was mutated. *D*, As for *A*, but using the benchmark substrate.

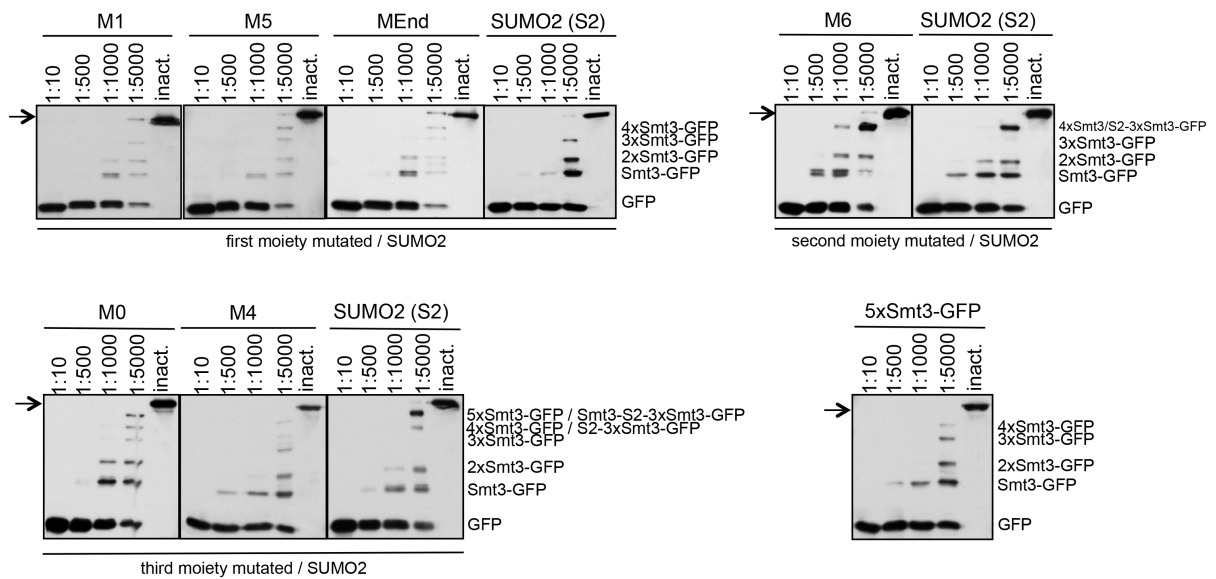


FIGURE 21: Ulp1 cleavage pattern is not affected by motif exchanges. Substrates that had been identified as conspicuous in the motif screen with Ulp2 were incubated with *E. coli* lysates containing MBP-Ulp1-FLAG diluted in activity test buffer for 2 h at 30 °C. An undiluted lysate containing the inactive variant of Ulp2 was used as a lysate control. Reaction products were analyzed by SDS-PAGE and anti-HA Western blotting. The arrow on the *left-hand side* of each blot indicates the size of the full-length substrates, cleavage products are indicated on the *right*.

The importance of M1, M5 and MEnd for the most distal moiety, and of M6 for the second Smt3 chain member was verified by exchanging the respective stretches of sequence in SUMO2 and testing a corresponding substrate chain [SUMO2(M1,M5,MEnd)-4xSmt3-GFP/Smt3-SUMO2(M6)-3xSmt3-GFP].

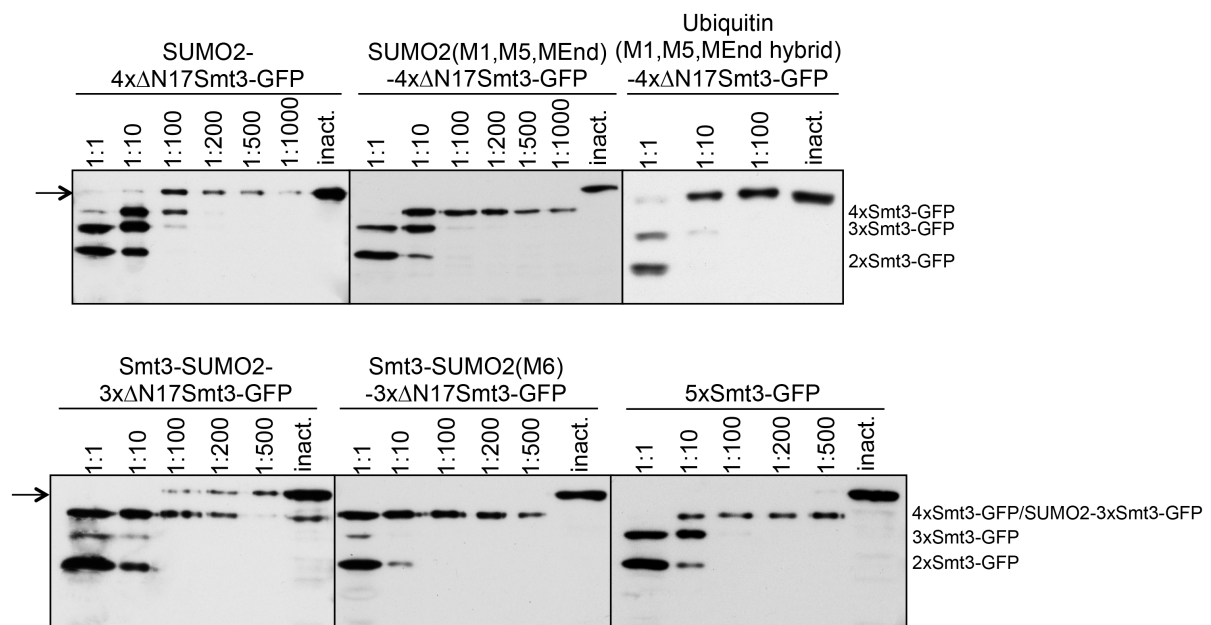


FIGURE 22: Exchanging the relevant motifs renders SUMO2 a Ulp2 target. Substrates as labeled were incubated with *E. coli* lysates containing MBP-Ulp2(411-710)-FLAG diluted in activity test buffer for 2 h at 30 °C. An undiluted lysate containing the inactive variant Ulp2(C624A) was used as a control (inact.). Reaction products were analyzed by SDS-PAGE and anti-HA Western blotting. Arrows on the *left-hand side* of the blots indicates the full-length substrate, cleavage products are indicated on the *right*.

Indeed, the respective mutations offset the blocking effect of SUMO2 (Fig. 22). For the third copy, this test is –due to time reasons- still pending.

It should be mentioned that the relevant residues in the most distal unit alone are not enough to define a Ulp2 target. When inserted into a susceptible loop of ubiquitin (between Thr9 and Gly10; 2 additional glycine residues on each side of the insert as linker), whose C-terminus is modified to match Smt3 (LRLRGG → REQIGG), M1 and M5 did not make the resultant hybrid a Ulp2 target (Fig. 21, upper rightmost panel). Interestingly, however, this mutant has an inhibitory effect on processing, whereas wild-type ubiquitin is readily tolerated, as shown above (Fig. 13). However, since such a hybrid mutant is highly adventurous, it shall not be subject to any further speculation here.

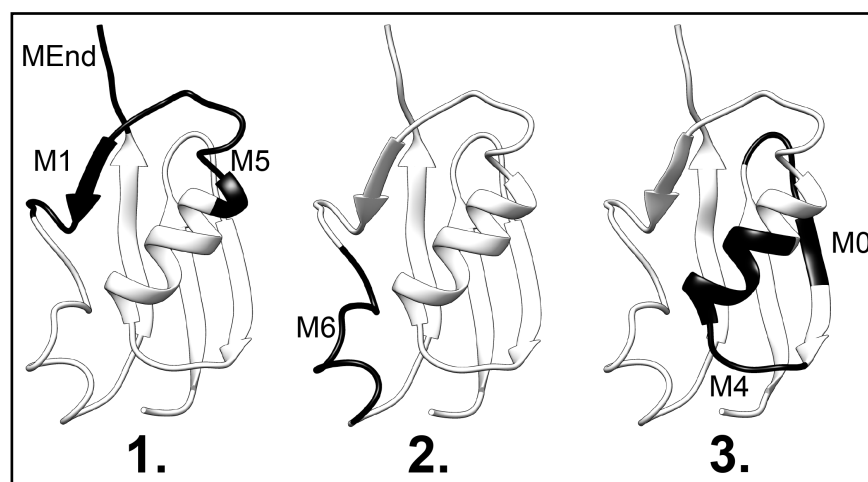


FIGURE 23: Structural representation of the sites in Smt3 relevant for binding to Ulp2 depending on their position in a chain. Graphics were prepared in Chimera (Pettersen *et al.* 2004) using PDB 1L2N in *ribbon* representation. Relevant regions are depicted in black; 1. = most distal moiety. Motifs were named as defined above.

If mutations in the second chain member affect cleavage of the most distal Smt3 moiety by lowering the binding affinity of the enzyme to the chain, a corresponding substrate should be captured less efficiently than wild type in a binding assay. Indeed, a three-membered Smt3 chain featuring M6 mutation in the second unit is poorly bound compared to either the positive control or a chain in which M6 is mutated in the most distal moiety instead (Fig. 24). As expected, Ulp2 bound neither to SUMO2-2xSmt3-GFP nor to Smt3-SUMO2-Smt3-GFP. Smt3-Ubi-Smt3-GFP was hardly captured, as well. This test further supports the idea, that there are three different binding sites in the UD, and that all three have to be occupied simultaneously to achieve full cooperative binding.

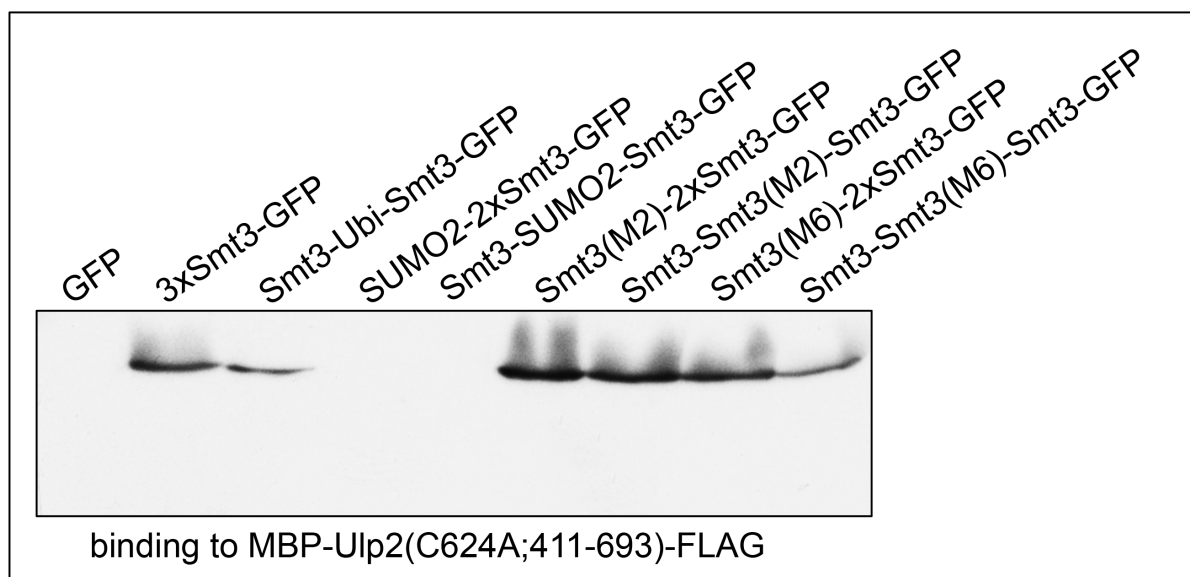


FIGURE 24: Binding behavior of UD to various substrates containing mutated Smt3, Ubi or SUMO2. MBP-Ulp2(C624A;411-693)-FLAG was immobilized on amylose resin, and subsequently incubated with ~100 nM of substrates featuring chains of different composition. After 1.5 h, unbound proteins were washed off, and boiling in SDS-PAGE loading buffer eluted specifically bound proteins. Seventy-five percent of each elution volume were analyzed by SDS-PAGE and anti-HA Western blotting. *NOTE:* Elevated affinity to M2-containing substrates is addressed in section 3.1.7.1, but since samples were loaded in that order (the M2 substrates being not on the outside) the picture was not cut.

The motif screen identified the regions of Smt3 involved in interaction with Ulp2. As shown above, Ulp2 treats SUMO1 like Smt3. Hence, motif residues differing between SUMO2 and Smt3, but were the same (or very similar, e.g. D and E) in SUMO1, could be excluded from further analysis. This left a total of ten sites for the most distal moiety and five for the second moiety. The third chain member has not been subject to further analysis, yet. As the aforementioned co-crystal of Ulp1 and Smt3 (Mossessova and Lima 2001) identified several interaction points between the binding partners that fall into the borders of the herein defined motifs M1 and MEnd, these regions -for now- were not analyzed in more detail. That left five candidate residues for each, M5 and M6: K54, K58, E59, D61, and S62 in the most distal moiety, A73, D74, Q75, E78, and D79 in the second unit. To narrow down the number of interaction points, single-site mutants for each of these were prepared and tested. In addition to an alanine scan, eight out of the ten were also either exchanged by the corresponding residue in SUMO2 (as done for Q75) or by an oppositely charged amino acid. The two exceptions were S62 and A73. For these sites, only A73E and S62A were tested.

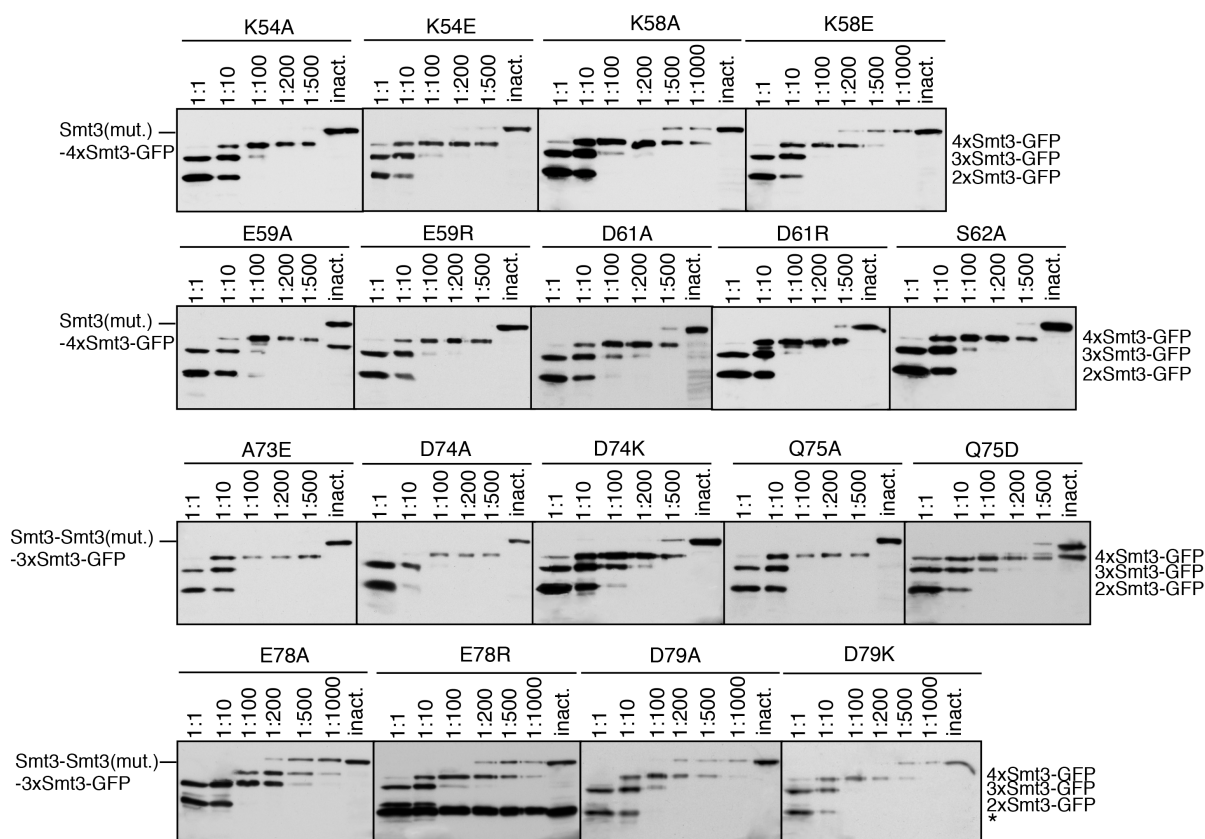


FIGURE 25: Single-site mutants in the M5 or M6 area of Smt3 do not have a strong inhibitory effect.

Substrates containing point mutations as labeled above the blots were incubated with *E. coli* lysates containing MBP-Ulp2(411-710)-FLAG diluted in activity test buffer for 2 h at 30 °C. An undiluted lysate containing the inactive, full-length variant MBP-Ulp2(C624A)-FLAG was used as a control. Reaction products were analyzed by SDS-PAGE and anti-HA Western blotting. The full-length substrate is indicated on the *left-hand side* of the blot, cleavage products are indicated on the *right*. Unspecific bands are indicated by asterisk (*).

As it turned out, single-site mutations in the assayed sites of Smt3 have only a small, if any, impact on processing by Ulp2 (Fig. 25). For K58, a small reduction in cleavage can be observed in the higher extract-dilutions, but on the whole, exchanging single amino acids did not provoke an effect detectable with the assay at hand. Apparently, at least double mutants would be necessary to identify individual crucial residues.

Noted in the margin, the activity assays were performed with a highly active extract of *E. coli* cells expressing the truncated form of Ulp2 MBP-Ulp2(411-710)-FLAG. Even though, the blocking effects were more pronounced when the tests were done with lysate containing the inherently less active full-length enzyme (data not shown), this choice made sense with respect to the results presented in the next section (3.2).

3.1.7.1 Exchanging four defined residues in Smt3 creates a version to which Ulp2 exhibit a very high affinity

In the course of the interaction-point study, it was found that exchanging (maximally) four residues in a certain area of Smt3, significantly elevates the affinity of both Ulp2 and Ulp1 for this molecule. Specifically, these were the mutations N86E, I88T, A91V, and H92F in the region M2. In cleavage assays, mutants containing the M2 mutations were highly favored over all other Smt3 units in the substrate chains (Fig. 20). This applied to Ulp1, as well (Fig. 26). When in second or third position, Ulp2 skipped the more distal units and cleaved off the M2 mutant directly (Fig. 20B and 20C). A binding test with chains carrying these mutations in the most distal or in the second unit of a three-membered chain [Smt3(M2)-2xSmt3-GFP, Smt3-Smt3(M2)-Smt3-GFP] identified a significantly enhanced affinity of the enzyme for this variant as the most plausible cause (Fig. 24). Even though not relevant for this study, this finding might be interesting for other, possibly technical, applications.

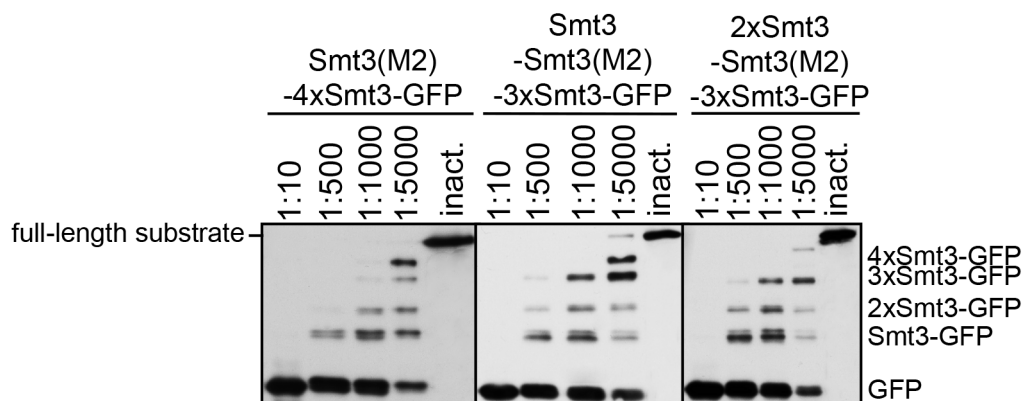


FIGURE 26: Ulp1, like Ulp2, prefers M2-containing Smt3 mutants. Substrates carrying M2 mutations in the first, second or third moiety counted from the distal end of an Smt3 chain were incubated with *E. coli* lysates containing MBP-Ulp1-FLAG diluted in activity test buffer for 2 h at 30 °C. An undiluted lysate containing the inactive variant of Ulp2 was used as a lysate control. Reaction products were analyzed by SDS-PAGE and anti-HA Western blotting. Size of the full-length substrates is indicated on the *left-hand side* of the blot, cleavage products are indicated on the *right*.

3.2 The crystal structure of the Ulp2 active domain

3.2.1 Crystallization of the Ulp2 active domain

As mentioned earlier, Ulp2 has large N- and C-terminal non-catalytic domains. Both are predicted to be intrinsically disordered (prediction: NTD ~40 % disordered, CTD >60 % disordered) (Kroetz *et al.* 2009). This puts significant hurdles in the way of structural investigations of the enzyme. Even small flexible regions can make crystallization attempts

fail. Domains of ~400 amino acids, which to large parts lack a stable tertiary fold, constitute an almost insurmountable challenge.

Since all mechanistically relevant features of Ulp2 are grounded in the UD (see section 3.1.5.1), structural information of that area should be sufficient to allow for more detailed analysis of the cleavage mechanism the enzyme employs. In order to achieve this, protein crystallization was applied. Even though the UD in its tightest borders (residues 411-693) showed a good level of activity, it was outperformed by the 17-amino acid longer version Ulp2(411-710) (Fig. 27), which proved to be not only sufficiently active but also more stable than Ulp2(411-693) during purification (data not shown). Both of these features were a hint towards Ulp2(411-710) being folded better than the UD in its conventional barriers. Hence, the longer version was used for crystallization attempts.

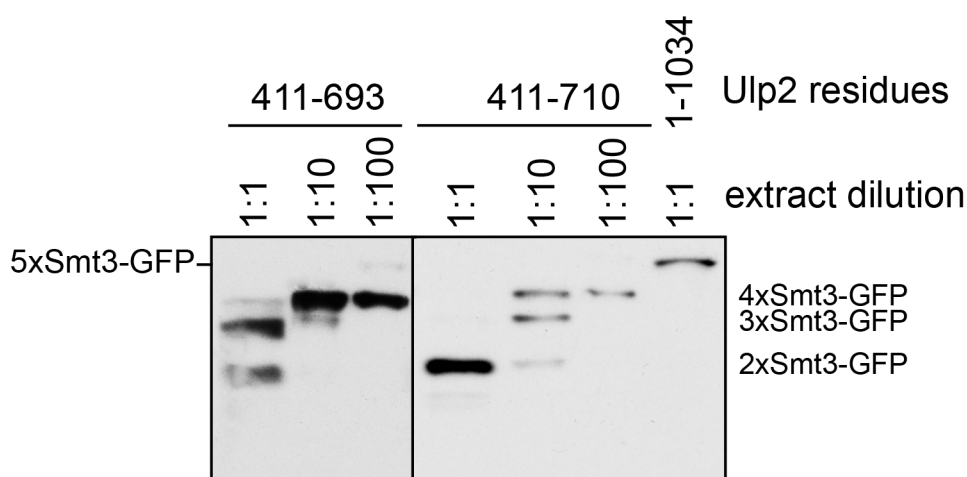


FIGURE 27: Slightly elongating the UD yields a more active construct. 5xSmt3-GFP was incubated with *E. coli* lysates containing truncation variants of Ulp2 as indicated, framed by MBP and FLAG tag, diluted in activity test buffer for 2 h at 30 °C. An undiluted lysate containing the inactive, full-length variant MBP-Ulp2(C624A)-FLAG was used as a control. Reaction products were analyzed by SDS-PAGE and anti-HA Western blotting. The full-length substrate is indicated on the *left-hand side* of the blot, cleavage products are indicated on the *right*.

For economical reasons, FLAG tag-aided purification was not an option, thus the construct so far standardly used in this study could not be utilized. Instead, a hexahistidine-tagged version of the MBP fusion was prepared. Three residues of glycine between the C-terminus of the domain and His₆ facilitated for optimal binding to the purification resin and overcame a compromise in the enzyme's activity, which had been observed for a direct fusion (data not shown). A TEV protease recognition site between MBP and UD allowed for cleavage of the solubility enhancer. Purification consisted of four steps: MBP affinity purification, followed by removal of that tag via TEV protease digestion, nickel pull-down, and gel filtration. Ulp2(411-710)-Gly₃-His₆ eluted as a single peak, and SDS-PAGE analysis did not show

degradation products (data not shown). Only monodisperse fractions were used for crystallization (DLS data not shown). As shown in Fig. 28B, the final species displayed full proteolytic activity in cleavage reactions with 4xSmt3-GFP, indicating that it maintained its proper fold during the purification process.

A single crystal was obtained under conditions as described in the methods section for the Ulp2 domain that encompassed amino acid residues 427-704. The structure contains one molecule in space group $P2_12_12_1$. Electron density maps were obtained with phases calculated using data from single-wavelength anomalous dispersion with the anomalous signal from sulfur (S-SAD). The structure was refined to 2.3 Å with an R-factor and an R_{free} of 0.1689 and 0.1965, respectively (see Tab. 8 for full information and statistics). Nineteen residues, 546-564, cannot be observed in the structure (Fig. 28A). They did not yield conclusive electron density. It is very likely they compose a flexible loop region in the UD.

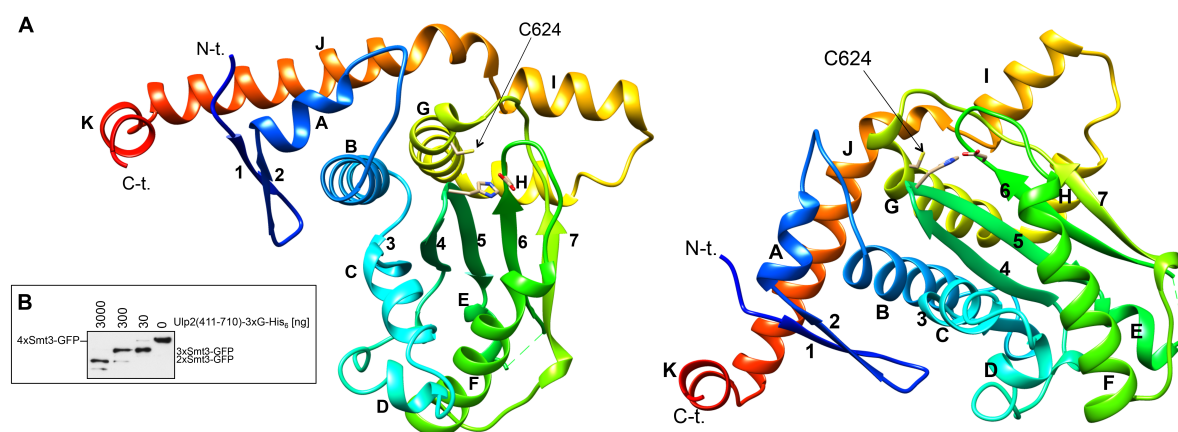


FIGURE 28: Structure of the catalytic domain of Ulp2. *A*, Two views of the UD in *ribbon* representation. N-t. = N-terminus; C-t. = C-terminus. Secondary structure elements are either lettered (α -helices) or numbered (β -strands). The catalytic triad is depicted in ball-and-stick representation; the arrow indicates the active cysteine residue (C624). The segment AA 546-564, for which no conclusive electron density was obtained, was deemed disordered and indicated as a dashed line. Graphics were prepared with Chimera (Pettersen *et al.* 2004). *B*, 4xSmt3-GFP was incubated with different amounts of purified Ulp2(411-710)-3xG-His₆ from the protein preparation that was used in crystallization for 2 h at 30 °C. Reaction products were analyzed by SDS-PAGE and anti-HA Western blotting. The full-length substrate is indicated on the *left-hand side* of the blot, cleavage products are indicated on the *right*.

3.2.2 The structure of the Ulp2 active domain underlines its classification

The secondary structure of Ulp2(427-704) includes 11 α -helices and 7 β -strands. Its active site has the central α -helix, three β -strands and the Cys-His-Asp catalytic triad typical for papain-like proteases (Drenth *et al.* 1968). Also, it features the characteristic Trp-tunnel through which the di-glycine motif of Smt3 is threaded, as already found in structures of Ulp1 and several SENP active domains (Mossessova and Lima 2001; Nayak and Muller 2014).

Table 8: Crystallographic data

a = Friedel pairs are counted as separate reflections; b = as defined by Diederichs & Karplus (1997); c = Ideal values are according to Engh & Huber (Engh *et al.* 1991); Data in parentheses indicate statistics for data in the highest resolution bin.

Data set	Native home	S-SAD
Diffraction source	Rigaku MicroMax 007 HF	Swiss Light Source X06DA
Wavelength (Å)	1.5418	2.0644
Temperature (K)	100	100
Detector	Mar345	Pilatus 2M
Space group	P2 ₁ 2 ₁ 2 ₁	P2 ₁ 2 ₁ 2 ₁
a, b, c (Å)	42.5, 55.5, 172.8	42.5, 55.6, 172.8
α, β, γ (°)	90, 90, 90	90, 90, 90
Resolution range (Å)	9.09 – 2.03 (2.58 – 2.43)	86.4 – 2.13 (2.19 – 2.13)
Total No. of reflections	157,785 (5,237)	1,625,224 (35,003)
No. of unique reflections ^a	50,094 (3,099)	18,756 (1,638)
Completeness (%)	98.3 (82.6)	98.6 (85.6)
$\langle I/\sigma(I) \rangle$	12.3 (1.76)	35.1 (4.8)
R_{meas}^b (%)	9.0 (56.6)	12.5 (60.9)
Overall B factor from Wilson plot (Å ²)	28.2	24.8
Phasing		
No. of sites		11
Resolution range (Å)		14.8 – 2.5
FOM		0.27
Refinement		
Resolution range (Å)		86.4 – 2.3 (2.4 -2.3)
Completeness (%)		98.6 (85.6)
σ cutoff		-3.0
No. of reflections, working set		34,693
No. of reflections, test set		2,780
Final R_{cryst}		0.169 (0.214)
Final R_{free}		0.197 (0.261)
No. of non-H atoms		2391
Protein		2174
Acetate		1
Water		206
Protein residues		259
R.m.s. deviations^c		
Bonds (Å)		0.002
Angles (°)		0.45
Average B factors (Å ²)		34.31
Macromolecules		33.58
Ligands		51.40
Solvent		41.53
Number of TLS groups		3
Ramachandran plot		
Most favoured /allowed (%)		97.3/2.7
Rotamer outliers (%)		0
Clashscore		2.06

Structural alignment of the UD with Ulp1 and SENP7 active domains underlined its relationship with the former, and its family affiliation with the latter (Fig. 29). Even though quite different in terms of sequence (~22 % identity), Ulp2 and SENP7 structures are a good match. While the alignment to Ulp1 is regular (r.m.s.d. of 1.102 Å over only 86 amino acids; 20 % sequence identity), the UD can be well aligned with SENP7 active domain over 148

amino acids with an r.m.s.d. of 1.066 Å. However, a conspicuous difference between the two is the presence of a helix-loop-helix element in the UD (residues 638-666; helices H and I) that is missing in SENP7. In its place, SENP7 features a simple loop (Fig. 29B).

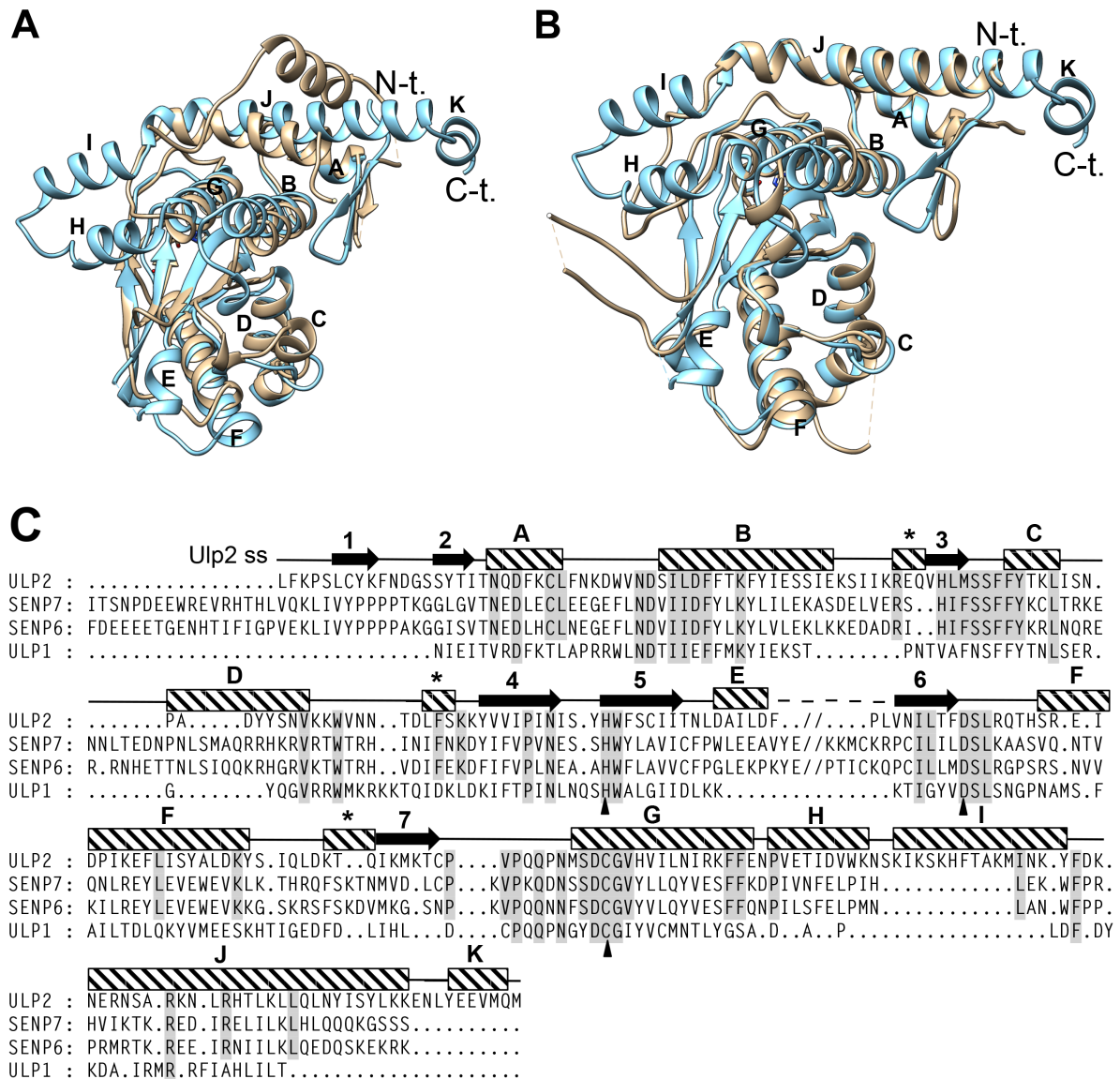


FIGURE 29: Comparison of the UD to other Ulp/SENP family members. Structural superpositions were prepared with Chimera (Pettersen *et al.* 2004). **A**, Superposition of the Ulp2 catalytic domain (blue) with Ulp1 catalytic domain (PDB 2HL8; ochre) in *ribbon* representation. Secondary structure elements of Ulp2 are either lettered (α -helices) or numbered (β -strands); N-t. = N-terminus of UD, C-t. = C-terminus of UD. Putatively disordered regions are denoted by dashed lines. **B**, Superposition of the Ulp2 catalytic domain (blue) with SENP7 catalytic domain (PDB 3EAY; ochre) in *ribbon* representation. Secondary structure elements of Ulp2 are either lettered (α -helices) or numbered (β -strands); N-t. = N-terminus of UD, C-t. = C-terminus of UD. Segments of the domains, for which no structural information is available, are depicted as dashed lines. **C**, Alignment of the sequences corresponding to the catalytic domains of Ulp2, SENP6, SENP7 and Ulp1. Gaps are indicated by dots; the missing region in the UD structure is depicted as //, signifying that the sequence is missing from the alignment. Secondary structure elements of the UD are sketched above the alignment; arrows = β -strands, striped blocks = α -helices; numbering and lettering of the respective elements as in the graphics. Helical elements of only 3 residues were not classified as α -helices and are labeled by asterisk (*). Residues conserved between all 4 or between Ulp2 and SENP6 and SENP7 are highlighted. Arrowheads below the alignment indicate residues of the catalytic triad.

3.2.3 Putative Smt3 binding sites in the Ulp2 active domain

To determine whether three Smt3 binding sites could be provided by the UD with the identified Smt3 regions involved, a model was generated for the UD in complex with three Smt3 molecules making use of available structures of Ulp1, SENP1 and SENP2 that were previously solved in complex with Smt3, SUMO1 and RanGAP1-SUMO1, respectively (PDB 1EUV/2IY1/2IO2) (Mossessova and Lima 2001; Reverter and Lima 2006; Shen *et al.* 2006a).

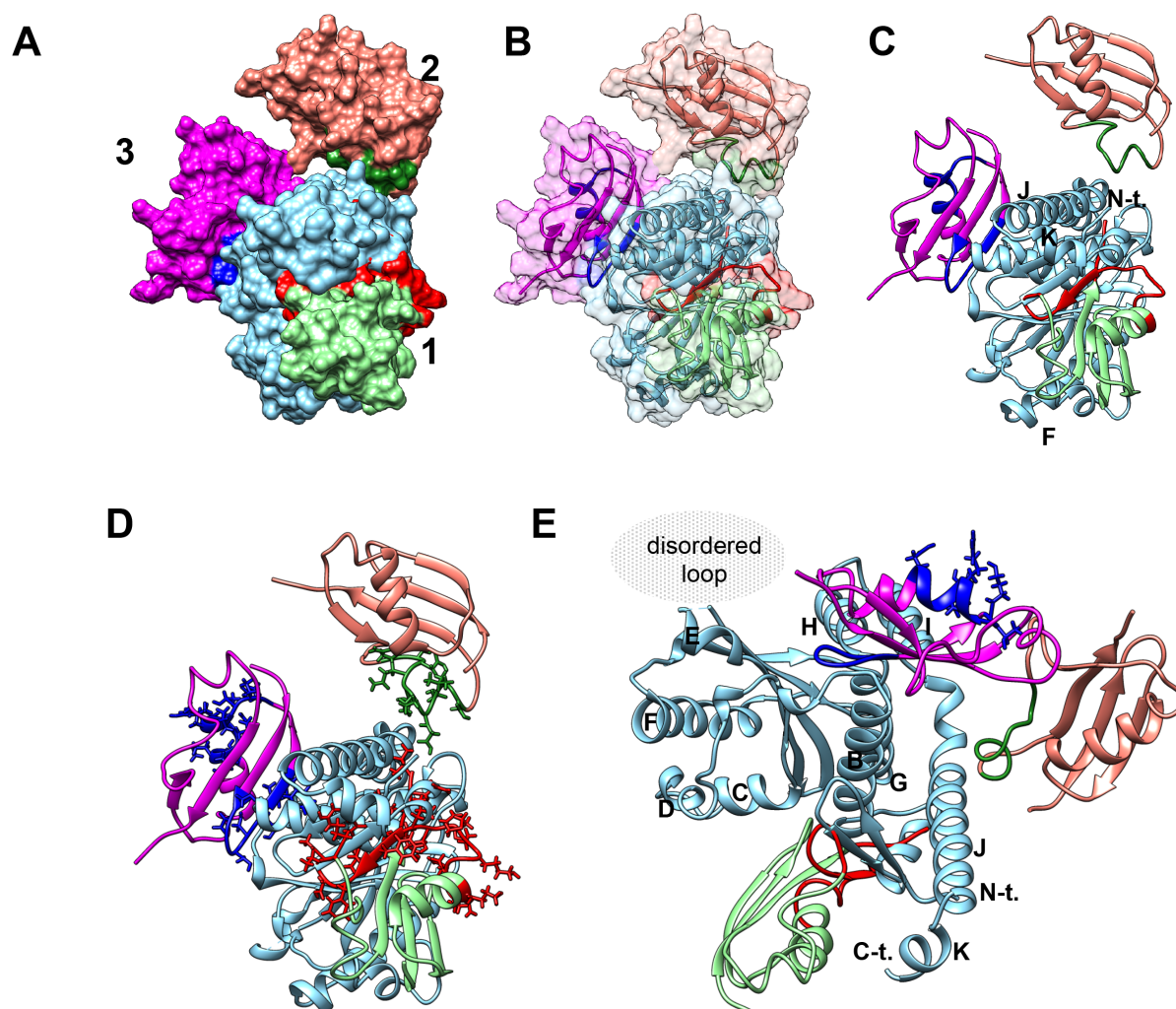


FIGURE 30: Structural models for interaction between UD and 3 linked Smt3 molecules. Graphics were prepared with Chimera (Pettersen *et al.* 2004). Light blue = active domain of Ulp2 (UD); light green and red = most distal Smt3; ocher and dark green = second Smt3; pink and dark blue = third Smt3. Red = M1, M5, MEnd; dark green = M6; dark blue = M4, M0. **A**, Surface display. Smt3 moieties are numbered (1 = most distal unit). **B**, Surface display, 80 % transparency. **C**, *Ribbon* representation of the UD and the three Smt3 moieties. For better orientation, some structural elements of Ulp2 are labeled (α -helices F, J, and K; N-t. = N-terminus) **D**, Like **C**, but the residues in the respective motives are displayed. **E**, Like **C**, but rotated to a view where M4 is in focus with the putatively disordered loop it might be in contact with. Loop is indicated as grey ellipse. For orientation, α -helices of Ulp2 are lettered.

As shown in Figure 30, it is possible to arrange three consecutive Smt3 moieties on the UD, such that all the regions identified in each of the three chain members are in contact with Ulp2. This is, provided that the unstructured segment 546-564 missing in the structure is bent such that it makes contact to the M4 surface area of the third moiety (Fig. 30E). This will be further discussed in section 4.2.4.1.

3.2.4 Electrostatic surface potential of the Ulp2 active domain

The Ulp1-Smt3 co-crystal revealed an extensive protease-substrate interface. Ulp1 contacts Smt3 not only at, but also distal from the cleavage site (Mossessova and Lima 2001). The contributing interactions were mainly of polar and charge-based nature. Interestingly, the electrostatic surface potential of the UD differs significantly from the one of Ulp1, and also from the one of the SENP7 active domain (Fig. 31). While Ulp1 and SENP7 contain large acidic (*red*) or basic (*blue*) patches in their active sites, the UD is largely neutral (*white*) in that region.

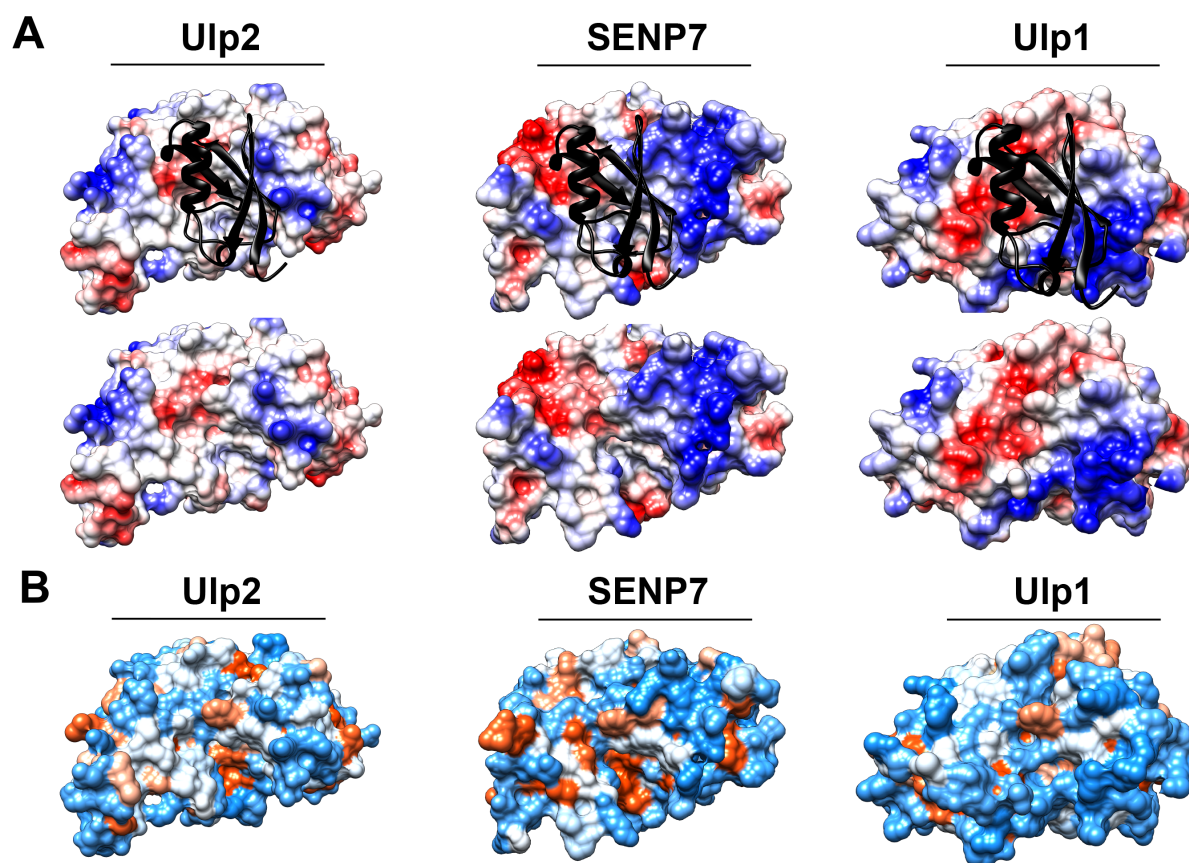


FIGURE 31: Electrostatic surface potential and surface hydrophobicity of the catalytic domains of Ulp2, SENP7 and Ulp1 are significantly different. Graphics were prepared with Chimera (Pettersen *et al.* 2004). **A**, Electrostatic surface potential of the catalytic sites of Ulp2, SENP7 (PDB 3EAY) and Ulp1 (PDB 2HL8). Black structure = Smt3, arranged there by alignment of the respective active domain with the structure of Ulp1-Smt3 (PDB1EUV). Red = negative potential, white = neutral, blue = positive potential. **B**, Hydrophobicity of catalytic sites of Ulp2, SENP7 (PDB 3EAY) and Ulp1 (PDB 2HL8). Color code is smooth transition from blue = most hydrophilic via white to orange/red = most hydrophobic.

Considering the differences between Ulp2 and SENP7 active sites, the differences in their electrostatic surface potentials would be a plausible explanation for Ulp2 not recognizing SUMO2, SENP7's preferred paralogue, despite their good structural overlap.

What is more, the UD is neither very hydrophilic (*light blue*) like the Ulp1 active site nor prominently hydrophobic (*orange-red*). A previous study on Ulp1-Smt3 interaction found strong evidence that several charged and polar residues contribute to complementary electrostatics in the interface between Ulp1 and its target. Considering the comparatively low charge density of the UD, this could be part of the explanation for the mechanistic differences between the two SUMO-specific proteases in *S. cerevisiae*. For further discussion of this, please see section 4.2.4.2.

Interestingly, the surface charge distribution in other parts of the active site is also strikingly different from the equivalent areas of Ulp1 and SENP7. Ulp2 contains an extensive basic surface where Ulp1 is patchily acidic and SENP7 exhibits mixed charges (Fig. 32). This suggests that Ulp2 is fundamentally different not only from Ulp1 but also from its protease subfamily member SENP7. It provides a significantly different surface for interactions with SUMO. Consequently, major mechanistic differences to other SUMO-specific proteases should not be surprising.

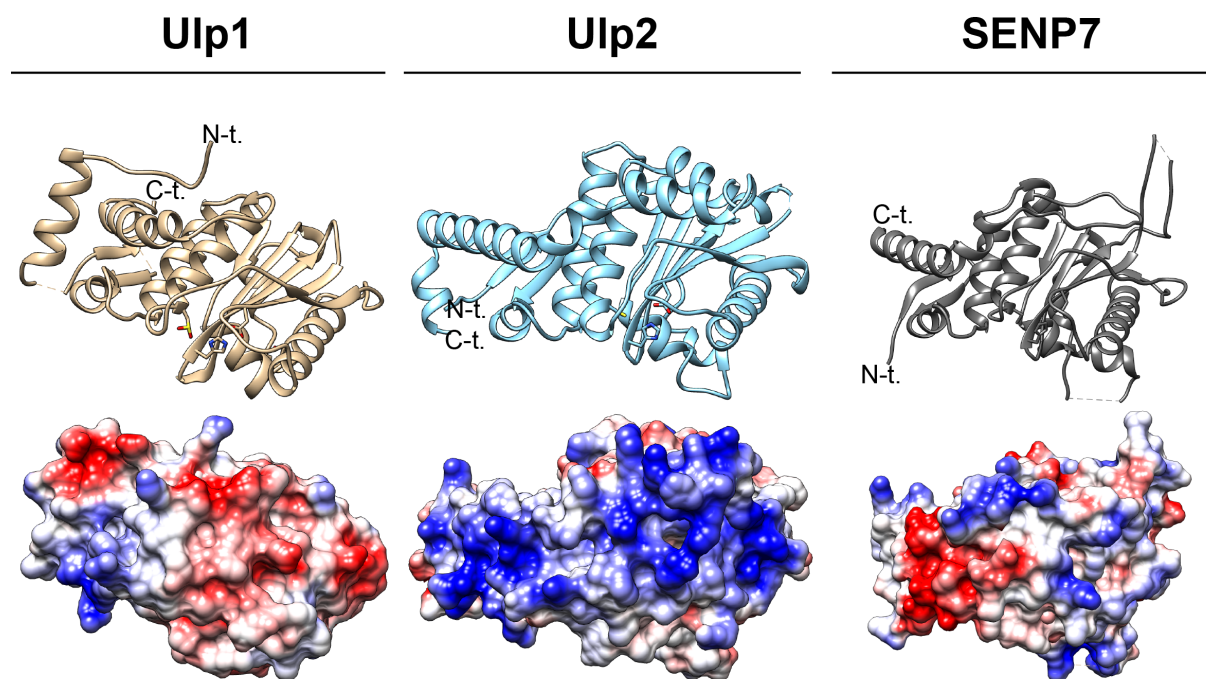


FIGURE 32: Electrostatic surface potential of the catalytic domains of Ulp2, SENP7 and Ulp1. Graphics were prepared with Chimera (Pettersen *et al.* 2004). Electrostatic surface potential of the catalytic sites of Ulp2, SENP7 (PDB 3EAY) and Ulp1 (PDB 2HL8). For orientation, structures in *ribbon* representation are displayed, as well. C-t. = C-terminus; N-t. = N-terminus.

3.3 Characterizing the relationship between Ulp2 and the proteasomal degradation system *in vivo*

Deletion of *ULP2* provokes a variety of phenotypic effects. Arguably the most prominent feature of the *ulp2-Δ* strain is the accumulation of HMW Smt3 conjugates. Similar aggregates are observed upon inhibition of the proteasome, if proteasomal subunits are mutated, or in mutants impaired in the ubiquitin conjugation machinery. This evoked the assumption that there might be a connection between absence of Ulp2, proteolysis deficiency and the ubiquitin-mediated degradation of proteins.

3.3.1 HMW Smt3 conjugates are the causing agent of a proteolysis defect in *ulp2-Δ*

Previous studies showed that *ulp2-Δ* cells are sensitive to canavanine (Miteva 2007), an arginine-analogue that leads to accumulation of misfolded proteins, which are then subjected to degradation by the UPS pathway. Since yeast mutants impaired in proteasomal degradation are significantly sensitive to canavanine, this indicated a proteolysis defect in *ulp2-Δ*. Other, unpublished data raised by former members of the *Dohmen* research group supported this finding (data not shown). In the absence of a fully functional degradation system, proteins accumulate that would usually be broken down. Hence, the turnover rate of a given proteasome substrate is a good indicator of the operational capacity of the proteasome.

Therefore, the stability of different known proteasomal substrates was tested in *ulp2-Δ* and several comparative strains. To this end, cycloheximide chases were performed.

Cycloheximide is an inhibitor of protein biosynthesis. Upon addition to the growth medium, translation is stopped, thus degradation rates of proteins of interest can be determined by monitoring their levels in the cells over time. Employing this strategy, the stability of Ub-R-e^K-HA-Ura was assessed. In this fusion construct, orotidine-5'-phosphate decarboxylase is decorated with an N-terminus that makes it prone to degradation via the UPS (N-end rule pathway of degradation, for details see (Varshavsky 2011)). In wild-type cells, this protein has a high turnover rate (Fig. 33, upper panel). However, in the absence of Ulp2 it is significantly stabilized. This stabilization is overcome by additional mutations inhibiting Smt3 chain formation, like *uba2^{ts}* or *smt3-KallR*. Likewise, Ub-V₇₆-DHFR, which is targeted to the proteasome via the ubiquitin fusion degradation (UFD) pathway (Johnson *et al.* 1995), was assayed. The results matched what was found for the N-end rule substrate (Fig. 33, middle panel). The same was true for another ubiquitin-dependent proteasome substrate, Stp1

(Fig. 33, lowest panel). These findings suggest a global proteolysis defect in the absence of Ulp2, caused by the accumulation of HMW Smt3 conjugates.

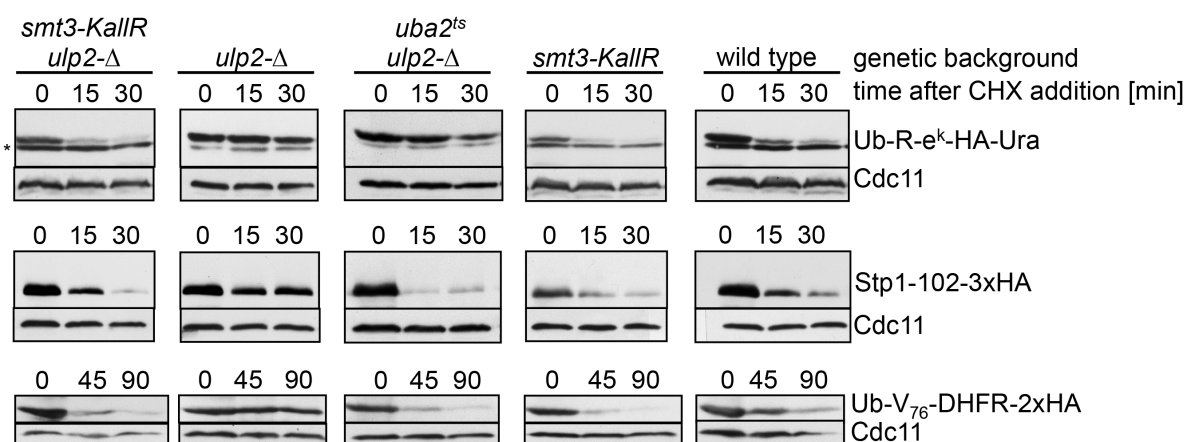


FIGURE 33: Proteasomal substrates are stabilized in the absence of Ulp2. Test substrates were expressed from the CUP₁ promoter. Indicated strains were grown in YPD containing 100 μg/ml CuSO₄ to OD₆₀₀ ~0.8. Translation was stopped by applying cycloheximide as described in section 2.2.1.2.2. Samples were analyzed by SDS-PAGE and anti-HA immunodetection. To test for differences in total protein amounts, membranes were stripped and reprobbed with anti-Cdc11 antibody. Unspecific bands are indicated by asterisk (*).

3.3.2 Ulp2 is the major player in SUMO recycling

The identification of STUBLs revealed a new function of Smt3: It can serve as a secondary degradation signal. In the face of this direct link between proteasome and Smt3 chains, the question arose whether –unlike ubiquitin- polymeric Smt3 is actually not recycled but degraded along with the protein it is attached to. Considering the similarity between ubiquitin- and SUMO cycles, Smt3 recycling was the more likely scenario. But this assumption awaited testing. To this end, cycloheximide chases were performed for different strains in the absence or presence of MG132, a proteasome inhibitor. Apart from carrying a *pdr5-Δ* mutation, which allowed MG132 to be fully effective, the test strains genomically expressed HA-tagged Smt3, to allow for better detection.

Figure 34A (first panel) shows that in the benchmark strain Smt3 was stable throughout 4.5 hours of chase time, suggesting that under normal conditions Smt3 is recycled. As discussed above, the absence of Ulp2 causes, among others effects, accumulation of HMW Smt3 conjugates and a severe proteolysis defect. This raised the question whether these two phenotypic features were related. Since a *ulp2-Δ* mutant seems to be unable to dismantle Smt3 chains to any sufficiency, Smt3 being degraded in the absence of Ulp2 was a plausible link. When the assay done for the *pdr5-Δ smt3-HA* strain was performed using the *pdr5-Δ ulp2-Δ smt3-HA* mutant, the results were indeed different: Upon translation stop, Smt3

diminished significantly over time (Fig. 34A, second panel). In contrast, Smt3 levels remained stable if the proteasome was inhibited. Inhibiting the vacuole did not have an effect. These data indicate that in the absence of Ulp2 Smt3 conjugates are subjected to degradation by the proteasome. Notably, neither a hypomorphic *ulp1-I615N* mutant, nor a *wss1-Δ* strain exhibited any variation in Smt3 levels during the assay (Fig. 34B). Therefore, Smt3 recycling seems to be—at least for the most part, if not completely—dependent on Smt3 deconjugation by Ulp2.

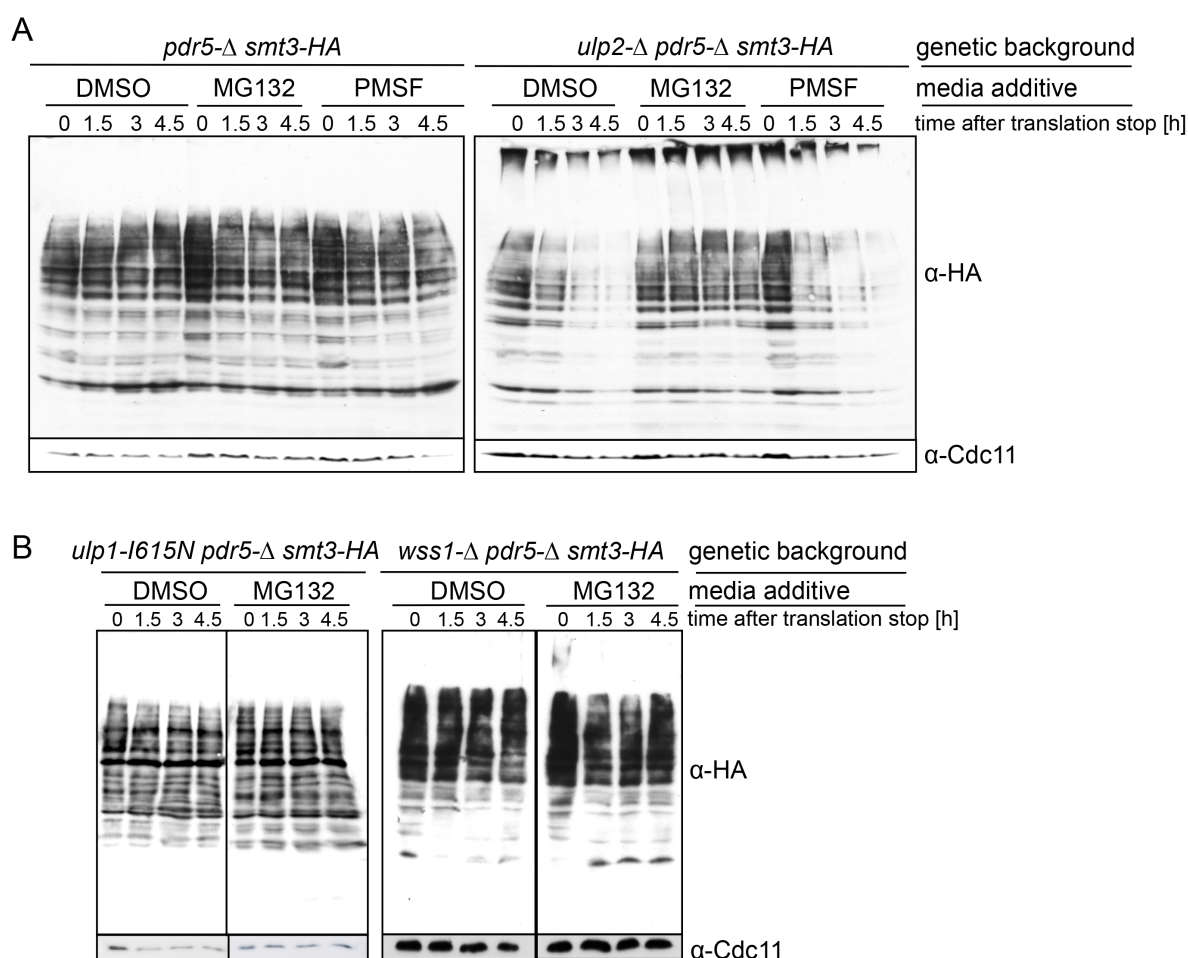


FIGURE 34: Smt3 is generally recycled, but in *ulp2-Δ* it is degraded. Indicated strains were grown in YPD to $OD_{600} \sim 0.8$. Translation was stopped by applying cycloheximide and proteasomal/vacuolar degradation was inhibited as described in section 2.2.1.2.2. Samples were analyzed by SDS-PAGE and anti-HA Western blotting. Equal sample loading was checked by reprobing blots with anti-Cdc11 antibody. **A**, Assessment of Smt3 stability in the presence of all SUMO-specific proteases (*left* panel) and in the absence of Ulp2 (*right* panel) under inhibition of the proteasomal or the vacuolar degradation pathway. **B**, Assessment of Smt3 stability in the absence of Ulp1 activity (*left* panel) and Wss1 (*right* panel), respectively.

4 Discussion

When this work was started, a reasonable amount of information concerning Ulp2 function had been obtained from *in vivo* studies. Yet, data about the enzyme itself was scarce –for good reason.

4.1 Ulp2 *in-vitro*-characterization setup

Attempts to characterize Ulp2 to more detail *in vitro* frequently failed due to the low level of activity the recombinantly expressed enzyme exhibited (Bylebyl *et al.* 2003; Li and Hochstrasser 2000b; Drag and Salvesen 2008). Therefore, this study employed new ideas, including a construct different from what had been used before, to fill that gap of knowledge. An MBP-FLAG-tag frame replaced the formerly used GST-fusion, allowing expression of Ulp2 in *E. coli* at satisfying activity levels. Several other tags and tag combinations were tested, but none of them was superior to MBP/FLAG. Large enzymes frequently pose a problem on recombinant expression. The 1034-residue Ulp2 is not an exception. Even though solubility was not a problem, generally low expression levels caused poor yield. All measures taken to increase the amount failed. This clearly had its roots in the size of the protein, as truncation mutants were expressed at much higher levels.

Luckily, it was possible to conduct the cleavage assays with crude extracts containing the recombinantly expressed enzyme without interfering/unspecific reactions or significant noise. Clearly, it would be desirable to work with purified enzymes. Unfortunately, affinity purification came at large costs, both in terms of material and in terms of protease activity. Since the application of lysate did not provoke a cleavage pattern different from when using purified Ulp2 (Fig. 6 & 28B), working with crude extracts was a feasible tribute to Ulp2's unruliness. Notably, the equally well soluble, but better expressed UD alone did not result in higher activity levels compared to the full-length enzyme, suggesting that the activity Ulp2 exhibited in the cleavage assays was the maximum one can obtain for this enzyme *in vitro*. The only obvious, larger variable that could be adjusted striving to augment this is the lysis procedure. For this work, lysozyme-aided glass bead lysis and grinding were tested, yielding equal results. It cannot be excluded that other strategies like freeze-thawing or sonication would lead to a higher-quality extracts. But the effect would probably not be striking.

Usually, test substrates were linear chains of one or several moieties of Smt3 and/or ubiquitin to enhanced GFP. This allowed for maximum flexibility concerning the composition of the chains. Subjecting authentic Smt3 chains linked to Ubc9 to digestion by Ulp2 brought the same results concerning the Ulp2 mechanism (see Fig. 10). This showed that the head-to-tail fusions were an adequate model, thus confirmed also this part of the *in vitro* system to be suitable for Ulp2 characterization.

4.2 Ulp2 mechanism

4.2.1 Ulp2 cleaves polymeric SUMO chains from their distal ends

Using an *in vitro* approach, the studies presented in this work characterized the mechanism by which Ulp2 desumoylates target proteins. The human members of the Ulp2 branch of SUMO-specific proteases, SENP6 and SENP7, had previously been analyzed and for both of them a rather stochastic mechanism had been proposed. Neither of the two seemed to exhibit a preference concerning which isopeptide bond of a SUMO chain to cleave first (Lima and Reverter 2008; Békés *et al.* 2011). The authors of the latest study, the one on SENP6, suggested that this could be a common feature of all SENPs and possibly other, non-human SUMO-specific proteases, as well. This work showed that this does, at least, not apply to Ulp2. Ulp2 clearly showed an *exo* behavior, a very strong obligation to start dismantling a poly-SUMO chain at its distal end. This was confirmed in several different tests, including monitoring the liberated species in a desumoylation assay over time (see Fig. 8) and obstructing the distal end of poly-SUMO with molecules uncleavable by Ulp2 (see Fig. 12). Its *exo* mechanism puts Ulp2 in stark contrast to the other SUMO-specific protease in budding yeast, Ulp1. In comparative tests, Ulp1 exhibited an *endo* mechanism, randomly cleaving any isopeptide bond within a poly-SUMO chain. Interestingly, the *endo* mode could only ultimately be confirmed when reaction speed was significantly lowered by performing cleavage assays with Ulp1 on ice. Only then, intermediate products could be detected (Fig. 7). This suggests that Ulp1 initially cleaves randomly within a chain, then remains bound to its end, and with a high processivity dismantles it to completion. A proper characterization of the cleavage mechanism of Ulp1 would require more tests. For this work on Ulp2, though, it was sufficient to establish its general work mode, *endo*, which deepens the differentiation of the two proteases to the mechanistic level.

4.2.2 Its *exo* behavior differentiates Ulp2 from its subfamily members

All members of the Ulp2 branch of SUMO proteases, SENP6, SENP7 and Ulp2 itself, have a preference for long polymeric chains (Bylebyl *et al.* 2003; Lima and Reverter 2008; Békés *et al.* 2011). Additionally, they share the common feature of being inactive in SUMO maturation (Li and Hochstrasser 2000a; Schwienhorst 2000; Mukhopadhyay *et al.* 2006).

Apparently, their cleavage mode puts a stop to this line of parallels (SENP6/7: rather random, Ulp2: sequential). However, major differences between family members of the subclasses of SUMO-specific proteases might not be all that surprising. As mentioned earlier, the categorization of SENPs into Ulp1-like and Ulp2-like is purely based on their domain architecture. Those with unconventional domain structure fall into the Ulp2 branch; all others are united as Ulp1-type SENPs. This very crude, single criterion leaves a lot of space for variation within the subfamilies. Hence, the many common features are indeed more surprising than the fact that there seems to be a fundamental difference between the desumoylation mechanisms employed by SENP6 and -7, and Ulp2's *exo* behavior.

In general, the catalytic domains of Ulp-class SUMO-specific proteases reside close to their C-termini (Hickey *et al.* 2012) (also see Fig. 4). In this respect, Ulp2 is noticeably different. Its active domain is almost exactly centered, framed by a 410-amino acid NTD and a CTD comprising 341 residues. This unique attribute might be an explanation for differences between Ulp2 and the other members of this class of proteases. Notwithstanding, as this work showed, the cleavage mechanism is entirely contained in the active domain. Assays using the active domain of Ulp2 did not yield results different from the findings for the full-length enzyme. So, if the intramolecular localization of the active domain accounts for distinctive features of Ulp2, they are probably not of mechanistic nature, because –at least in case of Ulp2– the bare catalytic domain by itself is decisive for the desumoylation mode.

As mentioned earlier, it should be noted that both of the studies, that gave mechanistic insight into SUMO chain cleavage by SENP6 and SENP7, were conducted using only truncated versions of the proteases (Lima and Reverter 2008; Békés *et al.* 2011). Even though the studies on Ulp2 do not suggest such a scenario, it cannot be excluded that the non-catalytic domains of the SENPs play a role in desumoylation, possibly provoking an ordered mechanism similar to Ulp2's, until the correspondent tests have been made. What is more, the results concerning mechanism in the respective studies were not at all that clear. They employed mixed-length substrates, whose cleavage pattern is naturally harder to interpret due to a variety of species present in the input already. Unfortunately, it was not possible to characterize SENP7 via the same system that was utilized for Ulp2. Neither the full-length

enzyme, nor the truncated SENP7(AA 662-984) version (the latter was used in the original study by Lima *et al.* of 2008) lent themselves to the activity assay established in this work. Different tags and tag combinations (N-terminal MBP combined with C-terminal FLAG tag, N-terminal MBP tag only, N-terminal hexahistidine tag, C-terminal hexahistidine tag) were tested, but none of the constructs exhibited sufficient cleavage activity towards a GFP-anchored SUMO2-4x Δ N11SUMO2 chain (data not shown). Also working with purified SENP7 did not change that outcome –even when following the published protocol for both purification of His₆-SENP7 and its activity test. Protein purification can be highly complex and many small, hardly controllable factors can be decisive for its failure or its success. Therefore, the reason for this rout is elusive. Still, the problem will be approached in future experiments, since only the cleavage pattern obtained from incubating a substrate-bound poly-SUMO2 chain with SENP7 can clarify whether the sequential processing activity found for Ulp2 divides the subfamily members, or whether it unites them.

4.2.3 Structure of the Ulp2 active domain

Amongst other things, this work presents the three-dimensional structure of the Ulp2 active domain. Like the other members of the Ulp/SENP family of SUMO proteases, it maintains a papain-like fold. As a result, its core and the analogous structure of Ulp1 are well superimposable. Nevertheless, there are major differences, as well. Overall, Ulp2 has more α -helical and less loop regions than Ulp1 (see Fig. 29A). Quite prominently, it contains a helix-loop-helix element (helices I and H) in a place where Ulp1 features a simple, short loop. Based on structural alignment, this part of the active domain has already been subject to some analysis and will be explored further in future experiments. Initial data already gave a hint to this being an interesting region to investigate more. However, it did not seem to be decisive for the *exo* mode: A Ulp2 mutant in which the helix-loop-helix element is replaced by the loop of Ulp1 still starts cleavage at the distal end of a poly-Smt3 chain (data not shown). Therefore, the parts of the domain crucial for engaging Ulp2 to a sequential processing mode remain to be identified. For several reasons, approaching this question via mutation screens is not a feasible strategy. Firstly, amino-acid exchange in the active domain is prone to compromising protein fold, thereby probably resulting in insoluble or inactive mutants. Secondly, a single-site mutation is probably not enough to erase Ulp2's compulsion to an *exo* mode of processing; meaning, a combination of mutations would be required. Yet, the assays developed in the course of this work are not suitable for high-throughput studies.

Consequently, developing new assays would be necessary in order to elucidate the structural determinants of the Ulp2 mechanism.

4.2.3.1 Determinants for the *exo* mode of Ulp2 are not known

The strong obligation of Ulp2 to *exo* mode suggests that it recognizes the N-terminal end or surrounding surfaces of the most distal Smt3 moiety, and that these regions are not well accessible in the other members of the chain. It could be speculated that this might be due to internal interactions between the individual Smt3 units and their neighboring moieties, resulting in some kind of quaternary structure of the poly-Smt3 chain. However, in general, SUMO chains seem to be intrinsically flexible (Békés *et al.* 2011; Keusekotten *et al.* 2014), so it is unlikely that polymeric Smt3 itself engages Ulp2 to the *exo* mode. More likely, it is dictated by a structural feature of the UD.

4.2.3.2 Ulp2 and SENP7 are well superimposable

Unsurprisingly, the UD can readily be structurally aligned with the active domain of SENP7 (see Fig. 29B). To large parts, the two are a quite accurate match. This also applies in case of the location of segment 546-564, which could not be solved in the Ulp2 structure. In the same region, the SENP7 structure features a gap of 50 residues which are disordered (Lima and Reverter 2008). In the previous text it was already mentioned that the Ulp2-like class of SUMO-specific proteases is characterized by their aberrant domain architecture, specifically insertion loops in their active domains. Apparently, these loops are highly floppy regions. These flexible elements might be a determinant for the poly-SUMO preference the members of this subfamily exhibit. Obviously, structural studies cannot clarify this, unless the respective proteases are crystallized in complex with polymeric SUMO that would possibly force the loops in a more rigid conformation.

4.2.4 Ulp2 targets polymeric Smt3 chains

Previous experiments had shown that Ulp2 cleaves poly-Smt3 chains. This work uncovered that there is a minimum length required to make polymeric Smt3 a Ulp2 target. In order to process an Smt3 chain efficiently, Ulp2 needs at least three consecutive units of Smt3 (see Fig. 11). Mono- or di-Smt3 is not recognized by the protease. What is more, Ulp2 stops processing its target at the stage of di-Smt3. The reason for that revealed a binding assay:

Ulp2 cannot bind to chains of less than three members (see Fig. 14). Notably, longer chains are not captured better than tri-Smt3, indicating that there are three Smt3 binding sites in Ulp2, which need to be simultaneously occupied in order to achieve full cooperative binding. Most possibly, binding at each of these sites alone would not be sufficiently tight. This idea goes in line with Ulp2 ending desumoylation once only two Smt3 moieties are left: If the most distal unit of poly-Smt3 is liberated, there are only two binding sites occupied, and the protease will lose its target because of insufficient affinity. A longer chain is probably, due to proximity, immediately recaptured and subjected to the next cleavage reaction. Di-Smt3, in contrast, cannot fill all three binding sites at Ulp2 and therefore no longer serves as a substrate. Binding tests with truncation mutants showed that the active domain alone already exhibits the three-units-minimum requirement (see Fig. 15). This suggests that the three Smt3 binding sites are all situated somewhere within the borders of serine-411 and lysine-693. This region does not contain any conventional SIM, so Ulp2 binds Smt3 via surfaces distinct from that. This is a feature it shares with the other members of the Ulp/SENp class of proteases. None of them bears a canonical SIM in its active domain and for those that have been structurally analyzed in complex with SUMO, all contacts were found to be different from SUMO-SIM interactions (Hickey *et al.* 2012; Mossessova and Lima 2001; Shen *et al.* 2006b).

4.2.4.1 Ulp2 recognizes different regions in the three most distal members of polymeric Smt3

In the course of this work it was found that Ulp2 hardly recognizes SUMO2 as a target (see Fig. 17). This fortunate coincidence allowed identifying the regions in Smt3 involved in Ulp2-Smt3 interaction. Regions in Smt3 could readily be mutated to their corresponding SUMO2 patches with very little, if at all, compromising of protein structure. This was confirmed by the fact that all Smt3/SUMO2 mutants were well expressed and could be as well purified as the substrates featuring exclusively wild-type Smt3 (data not shown). The same set of mutations was introduced into each of the three first moieties (counted from the distal end) of a poly-Smt3 chain. These are the Smt3 units involved in interaction with Ulp2 in the event of cleavage of the first moiety. From this resulted three libraries of variants, containing the mutations in the first, the second or the third copy of polymeric Smt3. Indeed, in each of the three, different regions are involved (see Figures 20 & 23). For the first two moieties a corresponding SUMO2 mutant confirmed this (see Fig. 22). For the third unit, that

test is pending, but will be done as soon as possible. These findings fortify the other results pointing towards three distinct Smt3 binding sites in the Ulp2 active domain. By structure modeling in *Chimera*, a possible arrangement of trimeric Smt3 on the UD was prepared. As shown in Figure 30, it is possible to place three moieties in a proximity to each other that allows isopeptide linkage in the UD with the relevant surfaces facing Ulp2. Admittedly, this is only true if the flexible segment between residues 546 and 564, which could not be displayed in the structure, is assumed to make contact to the M4 region in the third Smt3 copy. The patches relevant in that moiety are on opposite sides of the molecule. Therefore, some flexibility in the UD is prerequisite for proper binding of it, anyway. Hence, participation of a floppy loop fits well into this model. Approaching this question by creating a Ulp2 mutant lacking this loop, will probably not lead to further clarification, because a severely less active mutant (maybe due to misfolding) and a mutant that cannot properly bind the third Smt3 probably yield indistinguishable results in the assays at hand. Testing the affinity of this loop to Smt3 and Smt3(M4) is an alternative strategy worth trying.

4.2.4.2 The active site of the UD has a comparatively low surface charge

Computational analysis of the electrostatic surface potential of the UD revealed that it has a comparatively low surface charge (Fig. 31). The prominent acidic and basic patches in Ulp1 and SENP7, respectively, are largely neutralized. In addition, the area is neither very hydrophilic, like the active site of Ulp1, nor particularly hydrophobic. These features are in favor of the theory concerning cooperative binding of three Smt3 moieties to the UD. If the active site does not have the prerequisites for strong interactions to the substrate, probably surfaces elsewhere are involved. Considering that the Ulp1 active site shows a completely different picture, with dense charge and high hydrophilicity, this would explain why Ulp1 readily processes monosumoylated targets: It binds strongly even to mono-Smt3. On the other hand, also SENP7 shows a high charge density in its active site. Even though it has never been determined whether it has a minimum requirement towards target chain length, it is known to preferentially process polymeric SUMO. So the surface features in the active site might be part of the explanation for the mechanistic differences between Ulp1 and Ulp2, but should be handled with care.

4.2.4.3 Co-crystallization of Ulp2 and its target was not possible

Unfortunately, it was not possible to obtain a co-crystal of the Ulp2 active domain and a trimeric Smt3 chain. This would have made all speculations obsolete. However, none of the strategies engaged for this purpose led to success. Even though a complex between an inactive version of the Ulp2 active domain [UD(C624A)] and 3xSmt3 could be very well purified via gel filtration, it was comparatively unstable and precipitated after only four days at 4 °C (data not shown). The weak spot was UD(C624A). Apparently, the single-site mutation was enough to compromise the protease structure such that it was significantly less stable than its active variant. Using an uncleavable 3xSmt3(G98A) chain and the wild-type UD was not an option, since binding between this substrate and Ulp2 was too weak to maintain the complex during gel filtration (data not shown). In an attempt to use both favorable interaction partners, the active UD and 3xSmt3, the UD was treated with H₂O₂ to oxidize the active site cysteine prior to mixing with the substrate chain. Yet, this caused massive denaturation of the UD, leaving only a fraction of the initial protein in solution (data not shown). Experimenting with other chemical agents did not lead to success, either. For the time being, this endeavor has been suspended, but will probably be resumed sometime in the future, since only a crystal structure of the complex can ultimately answer the question of which surfaces of the UD accommodate the individual Smt3 moieties of tri-Smt3.

4.2.5 SIMs in Ulp2

4.2.5.1 The SIM close to the active site must be subject to control *in vivo*

To study the active domain of Ulp2, different truncation mutants were tested. In the course of this, it was found that a Δ NTD version (NTD = residues 1-410), unlike full-length Ulp2, targets also mono- and di-Smt3, thus is able to dismantle a poly-Smt3 chain to completion (see Fig. 16). The reason for this was tracked down to a SIM comprising the sequence between D719 and E729. It could be argued that this gain of function was due to exposure of a surface, which is buried in the protein structure under normal circumstances. But, apparently, this SIM plays a role *in vivo*. Studies on truncated versions of Ulp2 *in vivo* implicated it in HU sensitivity of the *ulp2- Δ* strain and interaction with Cdc5 (Baldwin *et al.* 2009). Therefore, there must be a mechanism in place that allows transient exposure. A mutant that lacks only half the NTD [Ulp2(209-1034)] behaves like full-length Ulp2 (Fig. 16). This indicates that there is some element between the residues 210 and 410 that controls,

possibly covers up, the SIM, but is flexible enough to be moved to allow access to this surface. Since this model requires much further investigation to be tested, and since gain-of-function mutants are always to be handled with caution, this topic was not explored further. On a side note, the Δ NTD mutants were not able to capture monosumoylated GFP in a binding assay. Still, they readily processed not only 5xSmt3-GFP to completion but also Smt3-GFP (data not shown). The reason for that is not clear. Maybe the binding was strong enough for a cleavage reaction but too weak to sustain the repeated washing in a binding assay.

4.2.5.2 Possible role of SIMs in the non-catalytic domains of Ulp2

It remains the question, which role the SIMs in the non-catalytic domains of Ulp2 play. The one adjacent to the active domain has already been discussed above. There is another one in the CTD (residues 926-934) and one in the NTD (residues 202-209) (also see Fig. 4). Neither of them has been analyzed, yet. Respective mutants did not exhibit conspicuous cleavage patterns in activity assays with the standard substrate 5xSmt3-GFP (data not shown). Intrinsically disordered protein regions are frequently found to be involved in low-affinity but high-specificity protein-protein interactions (Dyson and Wright 2005). As mentioned before, both the NTD and the CTD of Ulp2 are highly disordered. In the light of that, the SIMs together with other sequences present in these regions might direct Ulp2 to specific sumoylated target proteins. In that scenario, the other element(s) in that respective domain could then recognize the protein, while the SIM recognizes the Smt3 modification. This might be another part of the explanation why Ulp2 and Ulp1 have different substrate proteins (together with localization in the cell etc.). As mentioned earlier, *in vivo*, Ulp2 is much more specific than Ulp1. The SIM-containing disordered regions could be the reason for that. At this point, this is purely speculative. The findings presented in this work might be valuable in future experiments addressing this issue.

4.2.6 Ulp2 maintains short Smt3 chains

Interestingly, some deubiquitinating enzymes (DUBs) also seem to employ an *exo* activity towards their substrates (Komander *et al.* 2009). Namely, Usp14, the mammalian paralogue to the *S. cerevisiae* DUB Ubp6, was found to dismantle poly-ubiquitin chains from their distal ends (Hu *et al.* 2005). On the level of protein architecture, DUBs and SUMO-specific proteases are fundamentally different (Mikolajczyk *et al.* 2007; Hu *et al.* 2002; Avvakumov

et al. 2006; Renatus *et al.* 2006). Therefore, it was not possible to draw conclusions from an alignment of the active domains of Ulp2 and Usp14, since superimposition was hardly possible (data not shown). Still, in terms of cleavage mechanism, the two enzymes seem to be similar. It was suggested that the sequential processing mode Usp14 exhibits might be an editing function by which it can protect proteins decorated with short ubiquitin chains from untimely proteasomal degradation. A similar role for Ulp2 is a possible scenario. The discovery of STUbLs revealed that from a certain length on, poly-SUMO chains can ultimately lead to degradation of their anchor proteins. However, generally, mono- or di-SUMO is not sufficient to trigger this pathway (Sriramachandran and Dohmen 2014). For instance, Rnf4 requires an at least three-membered chain to efficiently recognize poly-SUMO (Tatham *et al.* 2008). Therefore, keeping chains short prevents modified proteins from degradation and also sustains the interaction platform, thus other regulatory functions, SUMO attachment to the substrate has created.

4.2.7 Ulp2 and STUbLs

This work showed that –as expected- Smt3 undergoes recycling. It is not degraded alongside with its target proteins, but liberated by Ulp2 before the substrate protein is subjected to proteasomal degradation. When monitoring Smt3 levels over time after translation stop, they remained stable under normal conditions. In contrast, in the absence of Ulp2, Smt3 diminished. This could be reversed by inhibition of the proteasome: In the presence of MG132, Smt3 was in *ulp2-Δ* as stable as in the benchmark strain (Fig. 34). Apparently, Ulp2 is the major player if not the only SUMO-specific protease in *S. cerevisiae* that is involved in recycling of Smt3. An analogous experiment with a hypomorphic *ulp1-I615N* strain did not show reduction of Smt3, indicating that it does not have an impact on this pathway. Wss1 was tested negatively, as well. As mentioned earlier, Wss1 is not predominantly a desumoylation enzyme. Still, it could not be completely excluded that it plays a role in this process. That is why it was included in this assay. As shown in Figure 34, its absence does not affect Smt3 abundance.

It must not be overlooked, that the mechanistic obligations do not allow Ulp2 to fulfill the recycling job completely. Against the background of the mechanistic studies presented in this work, it is clear that it would always leave di-Smt3 attached to the substrate. Therefore, there are two options: Either mono- or di-Smt3 is degraded alongside with its target, or there is

another, yet unknown SUMO-specific protease involved in this, cleaving off the remainders Ulp2 left. Future experiments will hopefully shed light on this.

Previous data showed that in a triple mutant that not only lacks Ulp2 but also the two STUbLs Ris1 and Hex3, Smt3 conjugates are stabilized (Maria Miteva, unpublished data). Apparently, in the absence of Ulp2, the polymeric SUMO-species are ubiquitinated and thereby filed into the UPS pathway of degradation. As mentioned above, Ulp2 seems to antagonize this. The mechanistic study presented here revealed that Ulp2 needs unimpeded access to the distal end of an Smt3 chain in order to exhibit full processing activity.

Obstructing the amino-terminus of polymeric Smt3 led to a significant reduction of cleavage efficiency (see Fig. 12). One can argue, that attaching uncleavable Smt3 or MBP to the substrate chains is not physiologically relevant. Nonetheless, the fact that a blocking species can keep Ulp2 from processing a poly-Smt3 chain is highly interesting with respect to the STUbL pathway. STUbLs bind polymeric SUMO via their various SIMs. Thereby, they are actually obstructing the chain, making it inaccessible for Ulp2. Ris1 contains 4 SIMs; the heterodimeric Hex3-Slx8 bears a total of 5 SIMs (Sriramachandran and Dohmen 2014). These SIMs allow the STUbLs to wrap up a polymeric Smt3 chain extensively. Once they attached a sufficient number of ubiquitin moieties to it, UPS shuttle factors might take over, thus also assume the blocking role. This possible model for the Ulp2-STUbL interplay is sketched in Figure 35. Notably, a similar relationship has been suggested for SENP6 and Rnf4. Amongst others, Rnf4 targets the promyelocytic leukemia (PML) protein and the inner kinetochore protein CENP-I. SENP6 was found to counteract polysumoylation of both proteins, thereby preventing their degradation via the STUbL-UPS pathway (Mukhopadhyay *et al.* 2010a; Hattersley *et al.* 2011; Mukhopadhyay *et al.* 2010b).

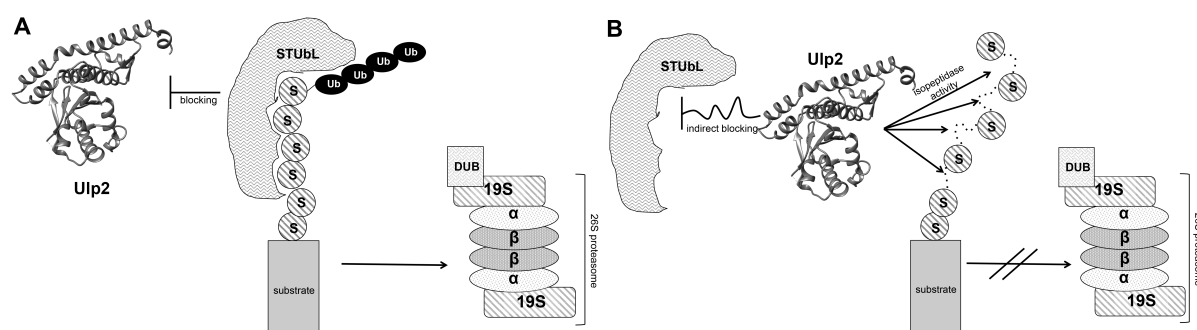


FIGURE 35: Model of possible interplay between Ulp2 and STUbLs. S = Smt3; Ub = ubiquitin. **A**, Polymeric Smt3 bound by a STUbL is obstructed, such that Ulp2 cannot process it. The STUbL decorates the Smt3 chain with several ubiquitin moieties, thereby targeting the anchor protein for degradation by the proteasome. **B**, Ulp2 keeps Smt3 chains short, hence STUbLs cannot bind to them. The degradation of the substrate via the STUbL-UPS pathway is thereby prevented.

4.2.8 Poly-ubiquitin does not interfere with target recognition by Ulp2

Blocking the N-terminus of poly-Smt3 with MBP or uncleavable Smt3 significantly reduced Ulp2's cleavage activity towards such a target. Surprisingly, attaching ubiquitin to the distal end of an Smt3 chain does not have this effect. It is readily tolerated, even when present in multiple copies. For instance, trimeric ubiquitin capping an Smt3 chain did not interfere at all with processing of that chain by Ulp2 (Fig. 13). However, it should be noted that this study utilized linear fusions of ubiquitin to Smt3 and of ubiquitin to ubiquitin. This is far from being authentic. Even more than Smt3-, ubiquitin linkages are kinked. Poly-ubiquitin is predominantly formed via K11, K48 or K63, and depending on the exact attachment sites, this can lead to a highly compact quaternary structure of the ubiquitin chain (Komander and Rape 2012). When attached to polymeric Smt3, in contrast to head-to-tail fusions, such species might be effective in hampering poly-Smt3 cleavage by Ulp2. Consequently, the results derived from the ubiquitin-capped-substrate assays should only be taken as an indication for a flexible appendix to be tolerated by Ulp2, but not be transferred to *in-vivo* poly-ubiquitin-Smt3 mixed species being equally well recognized. Actually, it is well possible that poly-ubiquitin as a firm structure might even have a blocking effect shielding polymeric Smt3 modifications against cleavage by Ulp2. Desumoylation assays utilizing authentically linked ubiquitin moieties capping 5xSmt3 anchored to GFP are an obvious way to test for this, and will probably be conducted in the near future.

4.2.9 A high-affinity Smt3 variant

In the course of this work it was found that introducing the mutations N86E, I88T, A91V, and H92F in Smt3 yielded a variant to which both Ulp2 and Ulp1 exhibited a significantly elevated affinity compared to wild-type Smt3. The mutation selection originated from the SUMO2/Smt3 motif-exchange screen. Since this sort of gain-of-function mutants was not in the focus of interest, it was not investigated further whether all four mutations were necessary for this or one or the other accounted for the effect alone. As shown in Figure 36, for instance the side chain of Ala-91 points in the opposite direction of the Ulp1 catalytic site, thus is probably irrelevant for this. Interestingly, the regions around these four residues are relatively similar, indicating that the point mutations do not create a specifically attractive patch for Ulp-Smt3 binding, but are probably directly involved in the interactions. Even though irrelevant physiologically, this finding could be interesting as a biochemical tool. The Smt3 mutant was very well expressed in *E. coli* and its stability was not compromised compared to

wild type (data not shown). Uncleavable Smt3(M2; G98A)/Smt3(M2; Δ G98) coupled to agarose or sepharose beads could serve as an affinity resin for purification of recombinantly expressed Ulp1. Other applications are conceivable. It would be worth trying whether a short fragment of Smt3 including these mutations is captured by the proteases. This would even broaden the options of application.

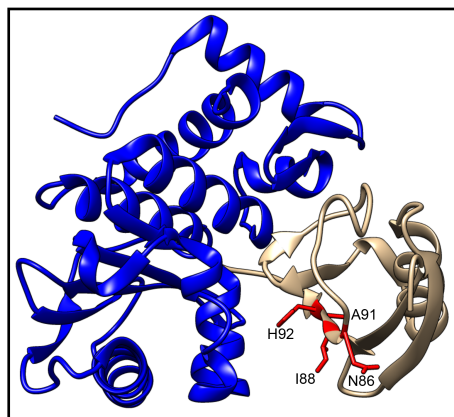


FIGURE 36: Structural model of residues possibly accounting for high-affinity binding of Ulp proteases to Smt3. Graphics were prepared with Chimera using PDB 1EUU. Blue = active domain of Ulp1; other = Smt3. Side chains of the residues of interest are displayed in red and labeled in 1-letter-code with numbers.

4.2.10 Ulp2 location

If Ulp2 takes care of Smt3 recycling, it seems reasonable to suppose that it might be located in close proximity to the 26S proteasome, possibly being in direct interaction with it. The DUB Usp14 associates with the 19S regulatory particle of the 26S proteasome (Lam *et al.* 1997). The fact that Ulp2 and Usp14 share the common feature of processing their targets sequentially starting from the distal ends, supports the idea of a similar interaction of Ulp2 with some proteasomal subunit. However, all investigations done in that respect did not point to this. In the course of this work, several variants of binding assays and interaction tests were employed to put this theory to the test. One strategy was based on co-purification of the 26S proteasome with its interaction partners as described before (Verma *et al.* 2000), the other one utilized 26S proteasomes purified from yeast and recombinant Ulp2. Neither approach led to detection of any association between the two (data not shown). Consequently, Ulp2 does not seem to interact with the proteasome. Yet, it is possible that there are mediators involved. Ulp2 may make contact to third-party proteins that in turn bind to proteasomal structures. Such an indirect interaction would probably escape notice in a binding assay as performed in the course of this work. Firstly, if there were only few molecules involved, their signal would be under the detection limit of a pull-down experiment on the basis of yeast extracts. Secondly, if the interaction between any two of the

involved proteins was rather weak, the association would be lost during an assay as done here. Purified 26S proteasomes have undergone several washing steps, possibly losing all interaction partners that are not tightly bound to them, and recombinantly expressed Ulp2 does not have any binding partners available from the outset. Consequently, a completely different approach would be necessary to address the question whether Ulp2's Smt3-recycling activity is also reflected in its molecular location. Of note, the same experiments as described in this section for Ulp2 were done for Ulp1. *Xenopus laevis* xSENP1 has been reported to specifically interact with Psmd1, a subunit of the proteasomal 19S regulatory particle (Ryu *et al.* 2014). However, none of the tests done in the course of this work suggested a similar association for Ulp1. Summing up, even though for some time Wss1 was suggested to do so (Mullen *et al.* 2010), to date there is no verified desumoylating protease directly interacting with the proteasome in *S. cerevisiae*. The details of the regulation of Smt3 recycling will be an interesting topic for future studies.

5 Outlook

At the beginning of this study, Ulp2 was hardly characterized on the molecular level. *In vivo* studies had already given a solid foundation for what its role in the cell is, and had also given some hint at its target preferences. However, due to its reluctance to recombinant expression, an in-depth characterization was missing. This work established an *in-vitro* assay system that allowed mechanistic insight. Also, solving the structure of the active domain added to the deeper understanding of Ulp2 and gave rise to new possibilities for structure-function analysis of this protease. Last but not least, *in vivo* studies focusing on a previously diagnosed proteolysis defect of the *ulp2-Δ* strain suggested a model in which Ulp2 is in an antagonistic relationship with STUbLs, competing for polysumoylated substrates.

Both, structure and *in vivo* analysis left some standing questions and opened many new interesting ones: Which structural features engage Ulp2 to an ordered, sequential processing mode? How can Ulp2 carry out its recycling-enzyme role, if it does not associate with the proteasome –or does it? Is there another, yet to be discovered, player in SUMO recycling trimming off mono- and di-SUMO from proteasome targets? Future experiments will hopefully shed light on these issues.

Twenty years ago, the existence of SUMO was discovered. Where are we going to be twenty years from now? This work added another piece to the big puzzle the SUMO network is. A puzzle, whose size one can only guess.

6 References

- Adams PD, Afonine PV, Bunkóczi G, Chen VB, Echols N, Headd JJ, Hung L-W, Jain S, Kapral GJ, Grosse Kunstleve RW, McCoy AJ, Moriarty NW, Oeffner RD, Read RJ, Richardson DC, Richardson JS, Terwilliger TC, Zwart PH (2011) The Phenix Software for Automated Determination of Macromolecular Structures. *Methods* (San Diego, Calif) 55 (1):94-106.
- Adamson AL, Kenney S (2001) Epstein-Barr Virus Immediate-Early Protein BZLF1 Is SUMO-1 Modified and Disrupts Promyelocytic Leukemia Bodies. *Journal of Virology* 75 (5):2388-2399.
- Afonine PV, Grosse-Kunstleve RW, Echols N, Headd JJ, Moriarty NW, Mustyakimov M, Terwilliger TC, Urzhumtsev A, Zwart PH, Adams PD (2012) Towards automated crystallographic structure refinement with phenix.refine. *Acta Crystallographica Section D* 68 (4):352-367.
- Avvakumov GV, Walker JR, Xue S, Finerty PJ, Mackenzie F, Newman EM, Dhe-Paganon S (2006) Amino-terminal Dimerization, NRDP1-Rhodanese Interaction, and Inhibited Catalytic Domain Conformation of the Ubiquitin-specific Protease 8 (USP8). *Journal of Biological Chemistry* 281 (49):38061-38070.
- Ayaydin F, Dasso M (2004) Distinct In Vivo Dynamics of Vertebrate SUMO Paralogues. *Molecular Biology of the Cell* 15 (12):5208-5218.
- Bachant J, Alcasabas A, Blat Y, Kleckner N, Elledge SJ (2002) The SUMO-1 Isopeptidase Smt4 Is Linked to Centromeric Cohesion through SUMO-1 Modification of DNA Topoisomerase II. *Molecular Cell* 9 (6):1169-1182.
- Balakirev MY, Mullally JE, Favier A, Assard N, Sulpice E, Lindsey DF, Rulina AV, Gidrol X, Wilkinson KD (2015) Wss1 metalloprotease partners with Cdc48/Doa1 in processing genotoxic SUMO conjugates. *eLife* 4:e06763.
- Baldwin ML, Julius JA, Tang X, Wang Y, Bachant J (2009) The yeast SUMO isopeptidase Smt4/Ulp2 and the Polo Kinase Cdc5 act in an opposing fashion to regulate sumoylation in mitosis and cohesion at centromeres. *Cell Cycle* 8 (20):3406-3419.
- Bawa-Khalfe T, Cheng J, Wang Z, Yeh ETH (2007) Induction of the SUMO-specific Protease 1 Transcription by the Androgen Receptor in Prostate Cancer Cells. *Journal of Biological Chemistry* 282 (52):37341-37349.
- Bayer P, Arndt A, Metzger S, Mahajan R, Melchior F, Jaenicke R, Becker J (1998) Structure determination of the small ubiquitin-related modifier SUMO-1. *Journal of Molecular Biology* 280 (2):275-286.
- Békés M, Prudden J, Srikumar T, Raught B, Boddy MN, Salvesen GS (2011) The Dynamics and Mechanism of SUMO Chain Deconjugation by SUMO-specific Proteases. *Journal of Biological Chemistry* 286 (12):10238-10247.
- Bencsath KP, Podgorski MS, Pagala VR, Slaughter CA, Schulman BA (2002) Identification of a Multifunctional Binding Site on Ubc9p Required for Smt3p Conjugation. *Journal of Biological Chemistry* 277 (49):47938-47945.
- Bernier-Villamor V, Sampson DA, Matunis MJ, Lima CD (2002) Structural Basis for E2-Mediated SUMO Conjugation Revealed by a Complex between Ubiquitin-Conjugating Enzyme Ubc9 and RanGAP1. *Cell* 108 (3):345-356.
- Biggins S, Bhalla N, Chang A, Smith DL, Murray AW (2001) Genes involved in sister chromatid separation and segregation in the budding yeast *Saccharomyces cerevisiae*. *Genetics* 159 (2):453-470.

- Bohren KM, Nadkarni V, Song JH, Gabbay KH, Owerbach D (2004) A M55V Polymorphism in a Novel SUMO Gene (SUMO-4) Differentially Activates Heat Shock Transcription Factors and Is Associated with Susceptibility to Type I Diabetes Mellitus. *Journal of Biological Chemistry* 279 (26):27233-27238.
- Borden KL, Boddy MN, Lally J, O'Reilly NJ, Martin S, Howe K, Solomon E, Freemont PS (1995) The solution structure of the RING finger domain from the acute promyelocytic leukaemia proto-oncoprotein PML. *The EMBO Journal* 14 (7):1532-1541.
- Bylebyl GR, Belichenko I, Johnson ES (2003) The SUMO Isopeptidase Ulp2 Prevents Accumulation of SUMO Chains in Yeast. *Journal of Biological Chemistry* 278 (45):44113-44120.
- Capili AD, Lima CD (2007) Taking it Step by Step: Mechanistic insights from structural studies of Ubiquitin/Ubiquitin-like protein modification pathways. *Current opinion in structural biology* 17 (6):726-735.
- Chakrabarti SR, Sood R, Nandi S, Nucifora G (2000) Posttranslational modification of TEL and TEL/AML1 by SUMO-1 and cell-cycle-dependent assembly into nuclear bodies. *Proceedings of the National Academy of Sciences of the United States of America* 97 (24):13281-13285.
- Chang C-C, Naik Mandar T, Huang Y-S, Jeng J-C, Liao P-H, Kuo H-Y, Ho C-C, Hsieh Y-L, Lin C-H, Huang N-J, Naik Nandita M, Kung Camy CH, Lin S-Y, Chen R-H, Chang K-S, Huang T-H, Shih H-M (2011) Structural and Functional Roles of Daxx SIM Phosphorylation in SUMO Paralog-Selective Binding and Apoptosis Modulation. *Molecular Cell* 42 (1):62-74.
- Chen D, Dou QP (2010) The Ubiquitin-Proteasome System as a Prospective Molecular Target for Cancer Treatment and Prevention. *Current protein & peptide science* 11 (6):459-470.
- Cheng J, Kang X, Zhang S, Yeh ETH (2007) SUMO-specific Protease 1 is Essential for Stabilization of Hypoxia-inducible factor-1 α During Hypoxia. *Cell* 131 (3):584-595.
- Choudhury BK, Li SSL (1997) Identification and Characterization of the SMT3 cDNA and Gene from Nematode *Caenorhabditis elegans*. *Biochemical and Biophysical Research Communications* 234 (3):788-791.
- Chun-Jie Huang DW, Faheem Ahmed Khan, Li-Jun Huo (2015) DeSUMOylation: An Important Therapeutic Target and Protein Regulatory Event. *DNA AND CELL BIOLOGY* 34 (11):652-660.
- Daniel Gietz R, Woods RA (2002) Transformation of yeast by lithium acetate/single-stranded carrier DNA/polyethylene glycol method. In: Christine G, Gerald RF (eds) *Methods in Enzymology*, vol Volume 350. Academic Press, pp 87-96.
- de Albuquerque CP, Liang J, Gaut NJ, Zhou H (2016) Molecular circuitry of the SUMO pathway in controlling sumoylation homeostasis and suppressing genome rearrangements. *Journal of Biological Chemistry*.
- Denison C, Rudner AD, Gerber SA, Bakalarski CE, Moazed D, Gygi SP (2005) A Proteomic Strategy for Gaining Insights into Protein Sumoylation in Yeast. *Molecular & Cellular Proteomics* 4 (3):246-254.
- Dohmen RJ, Stappen R, McGrath JP, Forrov H, Kolarov J, Goffeau A, Varshavsky A (1995) An Essential Yeast Gene Encoding a Homolog of Ubiquitin-activating Enzyme. *Journal of Biological Chemistry* 270 (30):18099-18109.
- Dou H, Huang C, Singh M, Carpenter PB, Yeh ETH (2010) Regulation of DNA Repair through DeSUMOylation and SUMOylation of Replication Protein A Complex. *Molecular Cell* 39 (3):333-345.

- Drag M, Salvesen GS (2008) DeSUMOylating enzymes-SENPs. *IUBMB Life* 60 (11):734-742.
- Drenth J, Jansonius JN, Koekoek R, Swen HM, Wolthers BG (1968) Structure of Papain. *Nature* 218 (5145):929-932.
- Droescher M, Chaugule VK, Pichler A (2013) SUMO Rules: Regulatory Concepts and Their Implication in Neurologic Functions. *NeuroMolecular Medicine* 15 (4):639-660.
- Dye BT, Schulman BA (2007) Structural Mechanisms Underlying Posttranslational Modification by Ubiquitin-Like Proteins. *Annual Review of Biophysics and Biomolecular Structure* 36 (1):131-150.
- Dyson HJ, Wright PE (2005) Intrinsically unstructured proteins and their functions. *Nat Rev Mol Cell Biol* 6 (3):197-208.
- Elmore ZC, Donaher M, Matson BC, Murphy H, Westerbeck JW, Kerscher O (2011) Sumo-dependent substrate targeting of the SUMO protease Ulp1. *BMC Biology* 9:74-74.
- Emsley P, Lohkamp B, Scott WG, Cowtan K (2010) Features and development of Coot. *Acta Crystallographica Section D* 66 (4):486-501.
- Engh RA, Huber R (1991) Accurate bond and angle parameters for X-ray protein structure refinement. *Acta Crystallographica Section A* 47 (4):392-400.
- Flotho A, Melchior F (2013) Sumoylation: A Regulatory Protein Modification in Health and Disease. *Annual Review of Biochemistry* 82 (1):357-385.
- Fox JD, Waugh DS (2003) Maltose-Binding Protein as a Solubility Enhancer. In: Vaillancourt PE (ed) *E. coli Gene Expression Protocols*. Humana Press, Totowa, NJ, pp 99-117.
- Gan-Erdene T, Nagamalleswari K, Yin L, Wu K, Pan Z-Q, Wilkinson KD (2003) Identification and Characterization of DEN1, a Deneddylase of the ULP Family. *Journal of Biological Chemistry* 278 (31):28892-28900.
- Gareau JR, Lima CD (2010) The SUMO pathway: emerging mechanisms that shape specificity, conjugation and recognition. *Nat Rev Mol Cell Biol* 11 (12):861-871.
- Geiss-Friedlander R, Melchior F (2007) Concepts in sumoylation: a decade on. *Nat Rev Mol Cell Biol* 8 (12):947-956.
- Geng F, Wenzel S, Tansey WP (2012) Ubiquitin and Proteasomes in Transcription. *Annual review of biochemistry* 81:177-201.
- Geoffroy M-C, Hay RT (2009) An additional role for SUMO in ubiquitin-mediated proteolysis. *Nat Rev Mol Cell Biol* 10 (8):564-568.
- Goldberg AL (1995) Functions of the proteasome: the lysis at the end of the tunnel. *Science* 268 (5210):522-523.
- Goldknopf IL, Busch H (1977) Isopeptide linkage between nonhistone and histone 2A polypeptides of chromosomal conjugate-protein A24. *Proceedings of the National Academy of Sciences of the United States of America* 74 (3):864-868.
- Golebiowski F, Matic I, Tatham MH, Cole C, Yin Y, Nakamura A, Cox J, Barton GJ, Mann M, Hay RT (2009) System-Wide Changes to SUMO Modifications in Response to Heat Shock. *Science Signaling* 2 (72):ra24-ra24.
- Gong L, Millas S, Maul GG, Yeh ETH (2000) Differential Regulation of Sentrinized Proteins by a Novel Sentrin-specific Protease. *Journal of Biological Chemistry* 275 (5):3355-3359.
- Grabbe C, Dikic I (2009) Functional Roles of Ubiquitin-Like Domain (ULD) and Ubiquitin-Binding Domain (UBD) Containing Proteins. *Chemical Reviews* 109 (4):1481-1494.
- Groll M, Bajorek M, Kohler A, Moroder L, Rubin DM, Huber R, Glickman MH, Finley D (2000) A gated channel into the proteasome core particle. *Nat Struct Mol Biol* 7 (11):1062-1067.

- Guo D, Li M, Zhang Y, Yang P, Eckenrode S, Hopkins D, Zheng W, Purohit S, Podolsky RH, Muir A, Wang J, Dong Z, Brusko T, Atkinson M, Pozzilli P, Zeidler A, Raffel LJ, Jacob CO, Park Y, Serrano-Rios M, Larrad MTM, Zhang Z, Garchon H-J, Bach J-F, Rotter JI, She J-X, Wang C-Y (2004) A functional variant of SUMO4, a new I[κ]B[α] modifier, is associated with type 1 diabetes. *Nat Genet* 36 (8):837-841.
- Haas KF, Broadie K (2008) Roles of ubiquitination at the synapse. *Biochimica et biophysica acta* 1779 (8):495-506.
- Hannich JT, Lewis A, Kroetz MB, Li S-J, Heide H, Emili A, Hochstrasser M (2005) Defining the SUMO-modified Proteome by Multiple Approaches in *Saccharomyces cerevisiae*. *Journal of Biological Chemistry* 280 (6):4102-4110.
- Hattersley N, Shen L, Jaffray EG, Hay RT (2011) The SUMO protease SENP6 is a direct regulator of PML nuclear bodies. *Molecular Biology of the Cell* 22 (1):78-90.
- Hay RT (2007) SUMO-specific proteases: a twist in the tail. *Trends in Cell Biology* 17 (8):370-376.
- Hecker C-M, Rabiller M, Haglund K, Bayer P, Dikic I (2006) Specification of SUMO1- and SUMO2-interacting Motifs. *Journal of Biological Chemistry* 281 (23):16117-16127.
- Heideker J, Perry JJP, Boddy MN (2009) Genome Stability Roles of SUMO-targeted Ubiquitin Ligases. *DNA repair* 8 (4):517-524.
- Hendriks IA, D'Souza RCJ, Yang B, Verlaan-de Vries M, Mann M, Vertegaal ACO (2014) Uncovering global SUMOylation signaling networks in a site-specific manner. *Nat Struct Mol Biol* 21 (10):927-936.
- Hickey CM, Wilson NR, Hochstrasser M (2012) Function and regulation of SUMO proteases. *Nat Rev Mol Cell Biol* 13 (12):755-766.
- Hietakangas V, Anckar J, Blomster HA, Fujimoto M, Palvimo JJ, Nakai A, Sistonen L (2006) PDSM, a motif for phosphorylation-dependent SUMO modification. *Proceedings of the National Academy of Sciences of the United States of America* 103 (1):45-50.
- Hochstrasser M (1995) Ubiquitin, proteasomes, and the regulation of intracellular protein degradation. *Current Opinion in Cell Biology* 7 (2):215-223.
- Hu M, Li P, Li M, Li W, Yao T, Wu J-W, Gu W, Cohen RE, Shi Y (2002) Crystal Structure of a UBP-Family Deubiquitinating Enzyme in Isolation and in Complex with Ubiquitin Aldehyde. *Cell* 111 (7):1041-1054.
- Hu M, Li P, Song L, Jeffrey PD, Chenova TA, Wilkinson KD, Cohen RE, Shi Y (2005) Structure and mechanisms of the proteasome-associated deubiquitinating enzyme USP14. *The EMBO Journal* 24 (21):3747-3756.
- Hunter T, Sun H (2009) Crosstalk Between the SUMO and Ubiquitin Pathways. In: Jentsch S, Haendler B (eds) *The Ubiquitin System in Health and Disease*. Springer Berlin Heidelberg, Berlin, Heidelberg, pp 1-16.
- Ii T, Fung J, Mullen JR, Brill SJ (2007) The Yeast Slx5-Slx8 DNA Integrity Complex Displays Ubiquitin Ligase Activity. *Cell Cycle* 6 (22):2800-2809.
- Ishov AM, Sotnikov AG, Negorev D, Vladimirova OV, Neff N, Kamitani T, Yeh ETH, Strauss JF, Maul GG (1999) Pml Is Critical for Nd10 Formation and Recruits the Pml-Interacting Protein Daxx to This Nuclear Structure When Modified by Sumo-1. *The Journal of Cell Biology* 147 (2):221-234.
- Ivanov AV, Peng H, Yurchenko V, Yap KL, Negorev DG, Schultz DC, Psulkowski E, Fredericks WJ, White DE, Maul GG, Sadofsky MJ, Zhou M-M, Rauscher Iii FJ (2007) PHD Domain-Mediated E3 Ligase Activity Directs Intramolecular Sumoylation of an Adjacent Bromodomain Required for Gene Silencing. *Molecular Cell* 28 (5):823-837.

- Johnson E (2004) Protein Modification by SUMO. *Annual Review of Biochemistry* 73:355-382
- Johnson ES, Ma PCM, Ota IM, Varshavsky A (1995) A Proteolytic Pathway That Recognizes Ubiquitin as a Degradation Signal. *Journal of Biological Chemistry* 270 (29):17442-17456.
- Johnson ES, Schwienhorst I, Dohmen RJ, Blobel G (1997) The ubiquitin-like protein Smt3p is activated for conjugation to other proteins by an Aos1p/Uba2p heterodimer. *The EMBO Journal* 16 (18):5509-5519.
- Johnson ES, Blobel G (1999) Cell Cycle-Regulated Attachment of the Ubiquitin-Related Protein Sumo to the Yeast Septins. *The Journal of Cell Biology* 147 (5):981-994.
- Johnson ES, Gupta AA (2001) An E3-like Factor that Promotes SUMO Conjugation to the Yeast Septins. *Cell* 106 (6):735-744.
- Kabsch W (2010) XDS. *Acta Crystallographica Section D: Biological Crystallography* 66 (Pt 2):125-132.
- Kadaré G, Toutant M, Formstecher E, Corvol J-C, Carnaud M, Boutterin M-C, Girault J-A (2003) PIAS1-mediated Sumoylation of Focal Adhesion Kinase Activates Its Autophosphorylation. *Journal of Biological Chemistry* 278 (48):47434-47440.
- Kamitani T, Kito K, Nguyen HP, Yeh ETH (1997) Characterization of NEDD8, a Developmentally Down-regulated Ubiquitin-like Protein. *Journal of Biological Chemistry* 272 (45):28557-28562.
- Kamitani T, Kito K, Nguyen HP, Fukuda-Kamitani T, Yeh ETH (1998) Characterization of a Second Member of the Sentrin Family of Ubiquitin-like Proteins. *Journal of Biological Chemistry* 273 (18):11349-11353.
- Kerscher O, Felberbaum R, Hochstrasser M (2006) Modification of Proteins by Ubiquitin and Ubiquitin-Like Proteins. *Annual Review of Cell and Developmental Biology* 22 (1):159-180.
- Kerscher O (2007) SUMO junction—what's your function? *EMBO reports* 8 (6):550-555.
- Keusekotten K, Bade Veronika N, Meyer-Teschendorf K, Sriramachandran Annie M, Fischer-Schrader K, Krause A, Horst C, Schwarz G, Hofmann K, Dohmen R J, Praefcke Gerrit JK (2014) Multivalent interactions of the SUMO-interaction motifs in RING finger protein 4 determine the specificity for chains of the SUMO. *Biochemical Journal* 457 (Pt 1):207-214.
- Klug H, Xaver M, Chaugule VK, Koidl S, Mittler G, Klein F, Pichler A (2013) Ubc9 Sumoylation Controls SUMO Chain Formation and Meiotic Synapsis in *Saccharomyces cerevisiae*. *Mol Cell*.
- Köhler A, Bajorek M, Groll M, Moroder L, Rubin DM, Huber R, Glickman MH, Finley D (2001a) The substrate translocation channel of the proteasome. *Biochimie* 83 (3-4):325-332.
- Köhler A, Cascio P, Leggett DS, Woo KM, Goldberg AL, Finley D (2001b) The Axial Channel of the Proteasome Core Particle Is Gated by the Rpt2 ATPase and Controls Both Substrate Entry and Product Release. *Molecular Cell* 7 (6):1143-1152.
- Köhler JB, Tammsalu T, Jørgensen MM, Steen N, Hay RT, Thon G (2015) Targeting of SUMO substrates to a Cdc48-Ufd1-Npl4 segregase and STUbL pathway in fission yeast. *Nature Communications* 6:8827.
- Kolli N, Mikolajczyk J, Drag M, Mukhopadhyay D, Moffatt N, Dasso M, Salvesen G, Wilkinson KD (2010) Distribution and Paralog Specificity of Mammalian DeSUMOylating Enzymes. *The Biochemical journal* 430 (2):335-344.
- Komander D, Clague MJ, Urbe S (2009) Breaking the chains: structure and function of the deubiquitinases. *Nat Rev Mol Cell Biol* 10 (8):550-563.

- Komander D, Rape M (2012) The Ubiquitin Code. *Annual Review of Biochemistry* 81 (1):203-229.
- Kroetz MB, Su D, Hochstrasser M (2009) Essential Role of Nuclear Localization for Yeast Ulp2 SUMO Protease Function. *Molecular Biology of the Cell* 20 (8):2196-2206.
- Kuo M-L, den Besten W, Thomas MC, Sherr CJ (2008) Arf-induced turnover of the nucleolar nucleophosmin-associated SUMO-2/3 protease Senp3. *Cell Cycle* 7 (21):3378-3387.
- Kurepa J, Walker JM, Smalle J, Gosink MM, Davis SJ, Durham TL, Sung D-Y, Vierstra RD (2003) The Small Ubiquitin-like Modifier (SUMO) Protein Modification System in Arabidopsis : ACCUMULATION OF SUMO1 AND -2 CONJUGATES IS INCREASED BY STRESS. *Journal of Biological Chemistry* 278 (9):6862-6872.
- Lallemand-Breitenbach V, Jeanne M, Benhenda S, Nasr R, Lei M, Peres L, Zhou J, Zhu J, Raught B, de The H (2008) Arsenic degrades PML or PML-RAR[alpha] through a SUMO-triggered RNF4/ubiquitin-mediated pathway. *Nat Cell Biol* 10 (5):547-555.
- Lam YA, Xu W, DeMartino GN, Cohen RE (1997) Editing of ubiquitin conjugates by an isopeptidase in the 26S proteasome. *Nature* 385 (6618):737-740.
- Laney JD, Hochstrasser M (2001) Analysis of Protein Ubiquitination. In: *Current Protocols in Protein Science*. John Wiley & Sons, Inc.
- Lee MH, Mabb AM, Gill GB, Yeh ET, Miyamoto S (2011) NF- κ B Induction of the SUMO Protease SENP2: A Negative Feedback Loop to Attenuate Cell Survival Response to Genotoxic Stress. *Molecular cell* 43 (2):180-191.
- Lewis A, Felberbaum R, Hochstrasser M (2007) A nuclear envelope protein linking nuclear pore basket assembly, SUMO protease regulation, and mRNA surveillance. *The Journal of Cell Biology* 178 (5):813-827.
- Li S, Hochstrasser M (2000a) The yeast ULP2 (SMT4) gene encodes a novel protease specific for the ubiquitin-like Smt3 protein. *Mol Cell Biol* 20:2367 - 2377.
- Li S-J, Hochstrasser M (1999) A new protease required for cell-cycle progression in yeast. *Nature* 398 (6724):246-251.
- Li S-J, Hochstrasser M (2000b) The Yeast ULP2 (SMT4) Gene Encodes a Novel Protease Specific for the Ubiquitin-Like Smt3 Protein. *Molecular and Cellular Biology* 20 (7):2367-2377.
- Li S-J, Hochstrasser M (2003) The Ulp1 SUMO isopeptidase: distinct domains required for viability, nuclear envelope localization, and substrate specificity. *The Journal of Cell Biology* 160 (7):1069-1082.
- Li T, Evdokimov E, Shen R-F, Chao C-C, Tekle E, Wang T, Stadtman ER, Yang DCH, Chock PB (2004) Sumoylation of heterogeneous nuclear ribonucleoproteins, zinc finger proteins, and nuclear pore complex proteins: A proteomic analysis. *Proceedings of the National Academy of Sciences of the United States of America* 101 (23):8551-8556.
- Lima CD, Reverter D (2008) Structure of the Human SENP7 Catalytic Domain and Poly-SUMO Deconjugation Activities for SENP6 and SENP7. *Journal of Biological Chemistry* 283 (46):32045-32055.
- Lin D, Tatham MH, Yu B, Kim S, Hay RT, Chen Y (2002) Identification of a Substrate Recognition Site on Ubc9. *Journal of Biological Chemistry* 277 (24):21740-21748.
- Lin X, Liang Y-Y, Sun B, Liang M, Shi Y, Brunicardi FC, Shi Y, Feng X-H (2003) Smad6 Recruits Transcription Corepressor CtBP To Repress Bone Morphogenetic Protein-Induced Transcription. *Molecular and Cellular Biology* 23 (24):9081-9093.
- Liu X, Chen W, Wang Q, Li L, Wang C (2013) Negative Regulation of TLR Inflammatory Signaling by the SUMO-deconjugating Enzyme SENP6. *PLoS Pathogens* 9 (6):e1003480.

- Liu Y, Kieslich CA, Morikis D, Liao J (2014) Engineering pre-SUMO4 as efficient substrate of SENP2. *Protein Engineering, Design and Selection* 27 (4):117-126.
- Lowe J, Stock D, Jap B, Zwickl P, Baumeister W, Huber R (1995) Crystal structure of the 20S proteasome from the archaeon *T. acidophilum* at 3.4 Å resolution. *Science* 268 (5210):533-539.
- Mabb AM, Wuerzberger-Davis SM, Miyamoto S (2006) PIASy mediates NEMO sumoylation and NF- κ B activation in response to genotoxic stress. *Nat Cell Biol* 8 (9):986-993.
- Mahajan R, Delphin C, Guan T, Gerace L, Melchior F (1997) A Small Ubiquitin-Related Polypeptide Involved in Targeting RanGAP1 to Nuclear Pore Complex Protein RanBP2. *Cell* 88 (1):97-107.
- Mahajan R, Gerace L, Melchior F (1998) Molecular Characterization of the SUMO-1 Modification of RanGAP1 and Its Role in Nuclear Envelope Association. *The Journal of Cell Biology* 140 (2):259-270.
- Makhnevych T, Ptak C, Lusk CP, Aitchison JD, Wozniak RW (2007) The role of karyopherins in the regulated sumoylation of septins. *The Journal of Cell Biology* 177 (1):39-49.
- Matic I, van Hagen M, Schimmel J, Macek B, Ogg SC, Tatham MH, Hay RT, Lamond AI, Mann M, Vertegaal ACO (2008) In Vivo Identification of Human Small Ubiquitin-like Modifier Polymerization Sites by High Accuracy Mass Spectrometry and an in Vitro to in Vivo Strategy. *Molecular & Cellular Proteomics* 7 (1):132-144.
- Matic I, Schimmel J, Hendriks IA, van Santen MA, van de Rijke F, van Dam H, Gnad F, Mann M, Vertegaal ACO (2010) Site-Specific Identification of SUMO-2 Targets in Cells Reveals an Inverted SUMOylation Motif and a Hydrophobic Cluster SUMOylation Motif. *Molecular Cell* 39 (4):641-652.
- Matunis MJ, Coutavas E, Blobel G (1996) A novel ubiquitin-like modification modulates the partitioning of the Ran-GTPase-activating protein RanGAP1 between the cytosol and the nuclear pore complex. *The Journal of Cell Biology* 135 (6):1457-1470.
- Meluh PB, Koshland D (1995) Evidence that the MIF2 gene of *Saccharomyces cerevisiae* encodes a centromere protein with homology to the mammalian centromere protein CENP-C. *Molecular Biology of the Cell* 6 (7):793-807.
- Mendoza HM, Shen L-n, Botting C, Lewis A, Chen J, Ink B, Hay RT (2003) NEDP1, a Highly Conserved Cysteine Protease That deNEDDylates Cullins. *Journal of Biological Chemistry* 278 (28):25637-25643.
- Meulmeester E, Kunze M, Hsiao HH, Urlaub H, Melchior F (2008) Mechanism and Consequences for Paralog-Specific Sumoylation of Ubiquitin-Specific Protease 25. *Molecular Cell* 30 (5):610-619.
- Mikolajczyk J, Drag M, Békés M, Cao JT, Ronai Ze, Salvesen GS (2007) Small Ubiquitin-related Modifier (SUMO)-specific Proteases: PROFILING THE SPECIFICITIES AND ACTIVITIES OF HUMAN SENPs. *Journal of Biological Chemistry* 282 (36):26217-26224.
- Minty A, Dumont X, Kaghad M, Caput D (2000) Covalent Modification of p73 α by SUMO-1: TWO-HYBRID SCREENING WITH p73 IDENTIFIES NOVEL SUMO-1-INTERACTING PROTEINS AND A SUMO-1 INTERACTION MOTIF. *Journal of Biological Chemistry* 275 (46):36316-36323.
- Miteva M (2007) Proteolytic Mechanisms Controlling SUMO Protein Modification. University of Cologne, Cologne
- Mohideen F, Capili AD, Bilimoria PM, Yamada T, Bonni A, Lima CD (2009) A molecular basis for phosphorylation-dependent SUMO conjugation by the E2 UBC9. *Nat Struct Mol Biol* 16 (9):945-952.

- Mossessova E, Lima CD (2001) Ulp1-SUMO Crystal Structure and Genetic Analysis Reveal Conserved Interactions and a Regulatory Element Essential for Cell Growth in Yeast. *Molecular Cell* 5 (5):865-876.
- Mukhopadhyay D, Ayaydin F, Kolli N, Tan S-H, Anan T, Kametaka A, Azuma Y, Wilkinson KD, Dasso M (2006) SUSP1 antagonizes formation of highly SUMO2/3-conjugated species. *The Journal of Cell Biology* 174 (7):939-949.
- Mukhopadhyay D, Dasso M (2007) Modification in reverse: the SUMO proteases. *Trends in Biochemical Sciences* 32 (6):286-295.
- Mukhopadhyay D, Arnaoutov A, Dasso M (2010a) The SUMO protease SENP6 is essential for inner kinetochore assembly. *The Journal of Cell Biology* 188 (5):681-692.
- Mukhopadhyay D, Dasso M (2010b) The fate of metaphase kinetochores is weighed in the balance of SUMOylation during S phase. *Cell Cycle* 9 (16):3194-3201.
- Mullen JR, Chen C-F, Brill SJ (2010) Wss1 Is a SUMO-Dependent Isopeptidase That Interacts Genetically with the Slx5-Slx8 SUMO-Targeted Ubiquitin Ligase. *Molecular and Cellular Biology* 30 (15):3737-3748.
- Nacerddine K, Lehembre F, Bhaumik M, Artus J, Cohen-Tannoudji M, Babinet C, Pandolfi PP, Dejean A (2005) The SUMO Pathway Is Essential for Nuclear Integrity and Chromosome Segregation in Mice. *Developmental Cell* 9 (6):769-779.
- Nathan D, Ingvarsdottir K, Sterner DE, Bylebyl GR, Dokmanovic M, Dorsey JA, Whelan KA, Krsmanovic M, Lane WS, Meluh PB, Johnson ES, Berger SL (2006) Histone sumoylation is a negative regulator in *Saccharomyces cerevisiae* and shows dynamic interplay with positive-acting histone modifications. *Genes & Development* 20 (8):966-976.
- Nayak A, Muller S (2014) SUMO-specific proteases/isopeptidases: SENPs and beyond. *Genome Biology* 15 (7):422.
- Novatchkova M, Tomanov K, Hofmann K, Stuible H-P, Bachmair A (2012) Update on sumoylation: defining core components of the plant SUMO conjugation system by phylogenetic comparison. *New Phytologist* 195 (1):23-31.
- O'Neill BM, Hanway D, Winzeler EA, Romesberg FE (2004) Coordinated functions of WSS1, PSY2 and TOF1 in the DNA damage response. *Nucleic Acids Research* 32 (22):6519-6530.
- Olsen SK, Capili AD, Lu X, Tan DS, Lima CD (2010) Active site remodelling accompanies thioester bond formation in the SUMO E1. *Nature* 463 (7283):906-912.
- Palancade B, Liu X, Garcia-Rubio M, Aguilera A, Zhao X, Doye V (2007) Nucleoporins Prevent DNA Damage Accumulation by Modulating Ulp1-dependent Sumoylation Processes. *Molecular Biology of the Cell* 18 (8):2912-2923.
- Panse VG, Kuster B, Gerstberger T, Hurt E (2003) Unconventional tethering of Ulp1 to the transport channel of the nuclear pore complex by karyopherins. *Nat Cell Biol* 5 (1):21-27.
- Panse VG, Hardeland U, Werner T, Kuster B, Hurt E (2004) A Proteome-wide Approach Identifies Sumoylated Substrate Proteins in Yeast. *Journal of Biological Chemistry* 279 (40):41346-41351.
- Pedrioli PGA, Raught B, Zhang X-D, Rogers R, Aitchison J, Matunis M, Aebersold R (2006) Automated identification of SUMOylation sites using mass spectrometry and SUMMon pattern recognition software. *Nat Meth* 3 (7):533-539.
- Pelisch F, Sonnevile R, Pourkarimi E, Agostinho A, Blow JJ, Gartner A, Hay RT (2014) Dynamic SUMO modification regulates mitotic chromosome assembly and cell cycle progression in *Caenorhabditis elegans*. *Nature Communications* 5:5485.
- Pero R, Lembo F, Di Vizio D, Boccia A, Chieffi P, Fedele M, Pierantoni GM, Rossi P, Iuliano R, Santoro M, Viglietto G, Bruni CB, Fusco A, Chiariotti L (2001) RNF4 Is a

- Growth Inhibitor Expressed in Germ Cells but Not in Human Testicular Tumors. *The American Journal of Pathology* 159 (4):1225-1230.
- Perry JJP, Tainer JA, Boddy MN (2008) A SIM-ultaneous role for SUMO and ubiquitin. *Trends in Biochemical Sciences* 33 (5):201-208.
- Pettersen EF, Goddard TD, Huang CC, Couch GS, Greenblatt DM, Meng EC, Ferrin TE (2004) UCSF Chimera—A visualization system for exploratory research and analysis. *Journal of Computational Chemistry* 25 (13):1605-1612.
- Picard N, Caron V, Bilodeau S, Sanchez M, Mascle X, Aubry M, Tremblay A (2012) Identification of Estrogen Receptor β as a SUMO-1 Target Reveals a Novel Phosphorylated Sumoylation Motif and Regulation by Glycogen Synthase Kinase 3 β . *Molecular and Cellular Biology* 32 (14):2709-2721.
- Pichler A, Gast A, Seeler JS, Dejean A, Melchior F (2002) The Nucleoporin RanBP2 Has SUMO1 E3 Ligase Activity. *Cell* 108 (1):109-120.
- Pichler A, Knipscheer P, Oberhofer E, van Dijk WJ, Korner R, Olsen JV, Jentsch S, Melchior F, Sixma TK (2005) SUMO modification of the ubiquitin-conjugating enzyme E2-25K. *Nat Struct Mol Biol* 12 (3):264-269.
- Pinto MP, Carvalho AF, Grou CP, Rodríguez-Borges JE, Sá-Miranda C, Azevedo JE (2012) Heat shock induces a massive but differential inactivation of SUMO-specific proteases. *Biochimica et Biophysica Acta (BBA) - Molecular Cell Research* 1823 (10):1958-1966.
- Praefcke GJK, Hofmann K, Dohmen RJ (2012) SUMO playing tag with ubiquitin. *Trends in Biochemical Sciences* 37 (1):23-31.
- Prudden J, Pebernard S, Raffa G, Slavin DA, Perry JJP, Tainer JA, McGowan CH, Boddy MN (2007) SUMO - targeted ubiquitin ligases in genome stability. *The EMBO Journal* 26 (18):4089-4101.
- Read RJ, McCoy AJ (2011) Using SAD data in Phaser. *Acta Crystallographica Section D* 67 (4):338-344.
- Renatus M, Parrado SG, D'Arcy A, Eidhoff U, Gerhartz B, Hassiepen U, Pierrat B, Riedl R, Vinzenz D, Worpenberg S, Kroemer M (2006) Structural Basis of Ubiquitin Recognition by the Deubiquitinating Protease USP2. *Structure* 14 (8):1293-1302.
- Reverter D, Lima CD (2004) A Basis for SUMO Protease Specificity Provided by Analysis of Human Senp2 and a Senp2-SUMO Complex. *Structure* 12 (8):1519-1531.
- Reverter D, Lima CD (2005) Insights into E3 ligase activity revealed by a SUMO-RanGAP1-Ubc9-Nup358 complex. *Nature* 435 (7042):687-692.
- Reverter D, Lima CD (2006) Structural basis for SENP2 protease interactions with SUMO precursors and conjugated substrates. *Nat Struct Mol Biol* 13 (12):1060-1068.
- Rodríguez MS, Dargemont C, Hay RT (2001) SUMO-1 Conjugation in Vivo Requires Both a Consensus Modification Motif and Nuclear Targeting. *Journal of Biological Chemistry* 276 (16):12654-12659.
- Román González-Prieto SAC, Ramesh Kumar, Ivo A Hendriks, Alfred CO Vertegaal (2015) c-Myc is targeted to the proteasome for degradation in a SUMOylation-dependent manner, regulated by PIAS1, SENP7 and RNF4. *Cell Cycle* 14 (12):1859-1872.
- Ross PD, Scruggs RL (1964a) Electrophoresis of DNA. II. Specific interactions of univalent and divalent cations with DNA. *Biopolymers* 2 (1):79-89.
- Ross PD, Scruggs RL (1964b) Electrophoresis of DNA. III. The effect of several univalent electrolytes on the mobility of DNA. *Biopolymers* 2 (3):231-236.
- Ryu H, Gygi SP, Azuma Y, Arnautov A, Dasso M (2014) SUMOylation of Psmd1 controls Adrm1 Interaction with the Proteasome. *Cell reports* 7 (6):1842-1848.

- Saitoh H, Hinchev J (2000) Functional heterogeneity of small ubiquitin-related protein modifiers SUMO-1 versus SUMO-2/3. *J Biol Chem* 275 (9):6252-6258.
- Sampson DA, Wang M, Matunis MJ (2001) The Small Ubiquitin-like Modifier-1 (SUMO-1) Consensus Sequence Mediates Ubc9 Binding and Is Essential for SUMO-1 Modification. *Journal of Biological Chemistry* 276 (24):21664-21669.
- Sapetschnig A, Rischitor G, Braun H, Doll A, Schergaut M, Melchior F, Suske G (2002) Transcription factor Sp3 is silenced through SUMO modification by PIAS1. *The EMBO Journal* 21 (19):5206-5215.
- Sarge KD, Park-Sarge O-K (2009) Sumoylation and human disease pathogenesis. *Trends in Biochemical Sciences* 34 (4):200-205.
- Sauer RT, Baker TA (2011) AAA+ Proteases: ATP-Fueled Machines of Protein Destruction. *Annual Review of Biochemistry* 80 (1):587-612.
- Saurin AJ, Borden KLB, Boddy MN, Freemont PS (1996) Does this have a familiar RING? *Trends in Biochemical Sciences* 21 (6):208-214.
- Schou J, Kelstrup CD, Hayward DG, Olsen JV, Nilsson J (2014) Comprehensive Identification of SUMO2/3 Targets and Their Dynamics during Mitosis. *PLoS ONE* 9 (6):e100692.
- Schulman BA, Wade Harper J (2009) Ubiquitin-like protein activation by E1 enzymes: the apex for downstream signalling pathways. *Nat Rev Mol Cell Biol* 10 (5):319-331.
- Schulz S, Chachami G, Kozackiewicz L, Winter U, Stankovic-Valentin N, Haas P, Hofmann K, Urlaub H, Ovaa H, Wittbrodt J, Meulmeester E, Melchior F (2012) Ubiquitin-specific protease-like 1 (USPL1) is a SUMO isopeptidase with essential, non-catalytic functions. *EMBO Reports* 13 (10):930-938.
- Schwartz DC, Felberbaum R, Hochstrasser M (2007) The Ulp2 SUMO Protease Is Required for Cell Division following Termination of the DNA Damage Checkpoint. *Molecular Cell Biology* 27 (19):6948-6961.
- Schwienhorst I, Johnson, E.S., Dohmen, R.J. (2000) SUMO conjugation and deconjugation. *Molecular and General Genetics* 263:771-786.
- Seifert A, Schofield P, Barton GJ, Hay RT (2015) Proteotoxic stress reprograms the chromatin landscape of SUMO modification. *Sci Signal* 8 (384):rs7.
- Shen L, Tatham MH, Dong C, Zagórska A, Naismith JH, Hay RT (2006a) SUMO protease SENP1 induces isomerization of the scissile peptide bond. *Nature structural & molecular biology* 13 (12):1069-1077.
- Shen Lin N, Dong C, Liu H, Naismith James H, Hay Ronald T (2006b) The structure of SENP1-SUMO-2 complex suggests a structural basis for discrimination between SUMO paralogues during processing. *Biochemical Journal* 397 (Pt 2):279-288.
- Shen Z, Pardington-Purtymun PE, Comeaux JC, Moyzis RK, Chen DJ (1996) UBL1, a Human Ubiquitin-like Protein Associating with Human RAD51/RAD52 Proteins. *Genomics* 36 (2):271-279.
- Shin EJ, Shin HM, Nam E, Kim WS, Kim J-H, Oh B-H, Yun Y (2012) DeSUMOylating isopeptidase: a second class of SUMO protease. *EMBO Reports* 13 (4):339-346.
- Shin Y-C, Tang S-J, Chen J-H, Liao P-H, Chang S-C (2011) The Molecular Determinants of NEDD8 Specific Recognition by Human SENP8. *PLoS ONE* 6 (11):e27742.
- Song J, Durrin LK, Wilkinson TA, Krontiris TG, Chen Y (2004) Identification of a SUMO-binding motif that recognizes SUMO-modified proteins. *Proceedings of the National Academy of Sciences of the United States of America* 101 (40):14373-14378.
- Song J, Zhang Z, Hu W, Chen Y (2005) Small Ubiquitin-like Modifier (SUMO) Recognition of a SUMO Binding Motif: A REVERSAL OF THE BOUND ORIENTATION. *Journal of Biological Chemistry* 280 (48):40122-40129.

- Song J-G, Xie H-H, Li N, Wu K, Qiu J-g, Shen D-M, Huang C-J (2015) SUMO-specific protease 6 promotes gastric cancer cell growth via deSUMOylation of FoxM1. *Tumor Biology* 36 (12):9865-9871.
- Soustelle C, Vernis L, Fréon K, Reynaud-Angelin A, Chanet R, Fabre F, Heude M (2004) A New *Saccharomyces cerevisiae* Strain with a Mutant Smt3-Deconjugating Ulp1 Protein Is Affected in DNA Replication and Requires Srs2 and Homologous Recombination for Its Viability. *Molecular and Cellular Biology* 24 (12):5130-5143.
- Srikumar T, Lewicki MC, Raught B (2013) A global *S. cerevisiae* small ubiquitin-related modifier (SUMO) system interactome. *Molecular Systems Biology* 9:668-668.
- Sriramachandran AM, Dohmen RJ (2014) SUMO-targeted ubiquitin ligases. *Biochimica et Biophysica Acta (BBA) - Molecular Cell Research* 1843 (1):75-85.
- Stepanenko OV, Stepanenko OV, Kuznetsova IM, Verkhusha VV, Turoverov KK (2013) Beta-Barrel Scaffold of Fluorescent Proteins: Folding, Stability and Role in Chromophore Formation. *International review of cell and molecular biology* 302:221-278.
- Stingle J, Schwarz Michael S, Bloemeke N, Wolf Peter G, Jentsch S (2014) A DNA-Dependent Protease Involved in DNA-Protein Crosslink Repair. *Cell* 158 (2):327-338.
- Strunnikov AV, Aravind L, Koonin EV (2001) *Saccharomyces cerevisiae* SMT4 encodes an evolutionarily conserved protease with a role in chromosome condensation regulation. *Genetics* 158 (1):95-107.
- Su D, Hochstrasser M (2010) A WLM Protein with SUMO-Directed Protease Activity. *Molecular and Cellular Biology* 30 (15):3734-3736.
- Suh H-Y, Kim J-H, Woo J-S, Ku B, Shin EJ, Yun Y, Oh B-H (2012) Crystal structure of DeSI-1, a novel deSUMOylase belonging to a putative isopeptidase superfamily. *Proteins: Structure, Function, and Bioinformatics* 80 (8):2099-2104.
- Sun H, Levenson JD, Hunter T (2007) Conserved function of RNF4 family proteins in eukaryotes: targeting a ubiquitin ligase to SUMOylated proteins. *The EMBO Journal* 26 (18):4102-4112.
- Takahashi Y, Mizoi J, Toh-e A, Kikuchi Y (2000) Yeast Ulp1, an Smt3-Specific Protease, Associates with Nucleoporins. *Journal of Biochemistry* 128 (5):723-725.
- Takahashi Y, Toh-e A, Kikuchi Y (2003) Comparative Analysis of Yeast Pias-Type SUMO Ligases In Vivo and In Vitro. *Journal of Biochemistry* 133 (4):415-422.
- Takahashi Y, Iwase M, Strunnikov AV, Kikuchi Y (2008) Cytoplasmic sumoylation by Pias-type Siz1-SUMO ligase. *Cell Cycle* 7 (12):1738-1744.
- Tanaka K, Nishide J, Okazaki K, Kato H, Niwa O, Nakagawa T, Matsuda H, Kawamukai M, Murakami Y (1999) Characterization of a Fission Yeast SUMO-1 Homologue, Pmt3p, Required for Multiple Nuclear Events, Including the Control of Telomere Length and Chromosome Segregation. *Molecular and Cellular Biology* 19 (12):8660-8672.
- Tatham MH, Jaffray E, Vaughan OA, Desterro JMP, Botting CH, Naismith JH, Hay RT (2001) Polymeric Chains of SUMO-2 and SUMO-3 Are Conjugated to Protein Substrates by SAE1/SAE2 and Ubc9. *Journal of Biological Chemistry* 276 (38):35368-35374.
- Tatham MH, Geoffroy M-C, Shen L, Plechanovova A, Hattersley N, Jaffray EG, Palvimo JJ, Hay RT (2008) RNF4 is a poly-SUMO-specific E3 ubiquitin ligase required for arsenic-induced PML degradation. *Nat Cell Biol* 10 (5):538-546.
- Tsien RY (1998) THE GREEN FLUORESCENT PROTEIN. *Annual Review of Biochemistry* 67 (1):509-544.

- Ulrich HD (2005) Mutual interactions between the SUMO and ubiquitin systems: a plea of no contest. *Trends in Cell Biology* 15 (10):525-532.
- Ulrich HD (2008) The Fast-Growing Business of SUMO Chains. *Molecular Cell* 32 (3):301-305.
- Uzunova K, Götsche K, Miteva M, Weisshaar SR, Glanemann C, Schnellhardt M, Niessen M, Scheel H, Hofmann K, Johnson ES, Praefcke GJK, Dohmen RJ (2007) Ubiquitin-dependent Proteolytic Control of SUMO Conjugates. *Journal of Biological Chemistry* 282 (47):34167-34175.
- Varshavsky A (2011) The N-end rule pathway and regulation by proteolysis. *Protein Science : A Publication of the Protein Society* 20 (8):1298-1345.
- Verma R, Chen S, Feldman R, Schieltz D, Yates J, Dohmen J, Deshaies RJ (2000) Proteasomal Proteomics: Identification of Nucleotide-sensitive Proteasome-interacting Proteins by Mass Spectrometric Analysis of Affinity-purified Proteasomes. *Molecular Biology of the Cell* 11 (10):3425-3439.
- Vertegaal ACO, Andersen JS, Ogg SC, Hay RT, Mann M, Lamond AI (2006) Distinct and Overlapping Sets of SUMO-1 and SUMO-2 Target Proteins Revealed by Quantitative Proteomics. *Molecular & Cellular Proteomics* 5 (12):2298-2310.
- Vertegaal Alfred CO (2010) SUMO chains: polymeric signals. *Biochemical Society Transactions* 38 (1):46-49.
- Vijay-Kumar S, Bugg CE, Cook WJ (1987) Structure of ubiquitin refined at 1.8Å resolution. *Journal of Molecular Biology* 194 (3):531-544.
- Voges D, Zwickl P, Baumeister W (1999) The 26S Proteasome: A Molecular Machine Designed for Controlled Proteolysis. *Annual Review of Biochemistry* 68 (1):1015-1068.
- Waltersperger S, Olieric V, Pradervand C, Gletting W, Salathe M, Fuchs MR, Curtin A, Wang X, Ebner S, Panepucci E, Weinert T, Schulze-Briese C, Wang M (2015) PRIGo: a new multi-axis goniometer for macromolecular crystallography. *Journal of Synchrotron Radiation* 22 (Pt 4):895-900.
- Wang C-Y, She J-X (2008) SUMO4 and its role in type 1 diabetes pathogenesis. *Diabetes/Metabolism Research and Reviews* 24 (2):93-102.
- Wang Z, Jones GM, Prelich G (2006) Genetic Analysis Connects SLX5 and SLX8 to the SUMO Pathway in *Saccharomyces cerevisiae*. *Genetics* 172 (3):1499-1509.
- Weinert T, Olieric V, Waltersperger S, Panepucci E, Chen L, Zhang H, Zhou D, Rose J, Ebihara A, Kuramitsu S, Li D, Howe N, Schnapp G, Pautsch A, Bargsten K, Prota AE, Surana P, Kottur J, Nair DT, Basilico F, Cecatiello V, Pasqualato S, Boland A, Weichenrieder O, Wang B-C, Steinmetz MO, Caffrey M, Wang M (2015) Fast native-SAD phasing for routine macromolecular structure determination. *Nat Meth* 12 (2):131-133.
- Weisshaar SR, Keusekotten K, Krause A, Horst C, Springer HM, Götsche K, Dohmen RJ, Praefcke GJK (2008) Arsenic trioxide stimulates SUMO-2/3 modification leading to RNF4-dependent proteolytic targeting of PML. *FEBS Letters* 582 (21-22):3174-3468.
- Weisshaar Stefan R. KK, Krause Anke, Horst Christiane, Springer Helen M., Götsche Kerstin, Dohmen R. Jürgen and Praefcke Gerrit J.K. (2008) Arsenic trioxide stimulates SUMO-2/3 modification leading to RNF4-dependent proteolytic targeting of PML. *FEBS Letters* 582 (21-22):3174-2178.
- Welchman RL, Gordon C, Mayer RJ (2005) Ubiquitin and ubiquitin-like proteins as multifunctional signals. *Nat Rev Mol Cell Biol* 6 (8):599-609.
- Werner A, Flotho A, Melchior F (2012) The RanBP2/RanGAP1*SUMO1/Ubc9 Complex Is a Multisubunit SUMO E3 Ligase. *Molecular Cell* 46 (3):287-298.

- Westerbeck JW, Pasupala N, Guillotte M, Szymanski E, Matson BC, Esteban C, Kerscher O (2014) A SUMO-targeted ubiquitin ligase is involved in the degradation of the nuclear pool of the SUMO E3 ligase Siz1. *Molecular Biology of the Cell* 25 (1):1-16.
- Wimmer P, Schreiner S, Dobner T (2012) Human Pathogens and the Host Cell SUMOylation System. *Journal of Virology* 86 (2):642-654.
- Wohlschlegel JA, Johnson ES, Reed SI, Yates JR (2004) Global Analysis of Protein Sumoylation in *Saccharomyces cerevisiae*. *Journal of Biological Chemistry* 279 (44):45662-45668.
- Wohlschlegel JA, Johnson ES, Reed SI, Yates JR (2006) Improved Identification of SUMO Attachment Sites Using C-terminal SUMO Mutants and Tailored Protease Digestion Strategies. *Journal of proteome research* 5 (4):761-770.
- Wong KH, Todd RB, Oakley BR, Oakley CE, Hynes MJ, Davis MA (2008) Sumoylation in *Aspergillus nidulans*: sumO inactivation, overexpression and live-cell imaging. *Fungal Genetics and Biology* 45 (5):728-737.
- Wu K, Yamoah K, Dolios G, Gan-Erdene T, Tan P, Chen A, Lee C-g, Wei N, Wilkinson KD, Wang R, Pan Z-Q (2003) DEN1 Is a Dual Function Protease Capable of Processing the C Terminus of Nedd8 and Deconjugating Hyper-neddylated CUL1. *Journal of Biological Chemistry* 278 (31):28882-28891.
- Wykoff DD, O'Shea EK (2005) Identification of Sumoylated Proteins by Systematic Immunoprecipitation of the Budding Yeast Proteome. *Molecular & Cellular Proteomics* 4 (1):73-83.
- Xie Y, Kerscher O, Kroetz MB, McConchie HF, Sung P, Hochstrasser M (2007) The Yeast Hex3-Slx8 Heterodimer Is a Ubiquitin Ligase Stimulated by Substrate Sumoylation. *Journal of Biological Chemistry* 282 (47):34176-34184.
- Xu Y, Zuo Y, Zhang H, Kang X, Yue F, Yi Z, Liu M, Yeh ETH, Chen G, Cheng J (2010) Induction of SENP1 in Endothelial Cells Contributes to Hypoxia-driven VEGF Expression and Angiogenesis. *Journal of Biological Chemistry* 285 (47):36682-36688.
- Xu Z, Au Shannon W N (2005) Mapping residues of SUMO precursors essential in differential maturation by SUMO-specific protease, SENP1. *Biochemical Journal* 386 (Pt 2):325-330.
- Xu Z, Lam LSM, Lam LH, Chau SF, Ng TB, Au SWN (2008) Molecular basis of the redox regulation of SUMO proteases: a protective mechanism of intermolecular disulfide linkage against irreversible sulfhydryl oxidation. *The FASEB Journal* 22 (1):127-137.
- Xu Z, Chan HY, Lam WL, Lam KH, Lam LSM, Ng TB, Au SWN (2009) SUMO Proteases: Redox Regulation and Biological Consequences. *Antioxidants & Redox Signaling* 11 (6):1453-1484.
- Yan S, Sun X, Xiang B, Cang H, Kang X, Chen Y, Li H, Shi G, Yeh ETH, Wang B, Wang X, Yi J (2010) Redox regulation of the stability of the SUMO protease SENP3 via interactions with CHIP and Hsp90. *The EMBO Journal* 29 (22):3773-3786.
- Yang M, Hsu C-T, Ting C-Y, Liu LF, Hwang J (2006a) Assembly of a Polymeric Chain of SUMO1 on Human Topoisomerase I in Vitro. *Journal of Biological Chemistry* 281 (12):8264-8274.
- Yang SH, Galanis A, Witty J, Sharrocks AD (2006b) An extended consensus motif enhances the specificity of substrate modification by SUMO. *The EMBO Journal* 25 (21):5083-5093.
- Yang W, Paschen W (2015) SUMO proteomics to decipher the SUMO-modified proteome regulated by various diseases. *Proteomics* 15 (0):1181-1191.

- Zhao X, Wu C-Y, Blobel G (2004a) Mlp-dependent anchorage and stabilization of a desumoylating enzyme is required to prevent clonal lethality. *The Journal of Cell Biology* 167 (4):605-611.
- Zhao Y, Kwon SW, Anselmo A, Kaur K, White MA (2004b) Broad Spectrum Identification of Cellular Small Ubiquitin-related Modifier (SUMO) Substrate Proteins. *Journal of Biological Chemistry* 279 (20):20999-21002.
- Zhong J-L, Huang C-Z (2016) Ubiquitin proteasome system research in gastrointestinal cancer. *World Journal of Gastrointestinal Oncology* 8 (2):198-206.
- Zhou W, Ryan JJ, Zhou H (2004) Global Analyses of Sumoylated Proteins in *Saccharomyces cerevisiae*: INDUCTION OF PROTEIN SUMOYLATION BY CELLULAR STRESSES. *Journal of Biological Chemistry* 279 (31):32262-32268.
- Zhu J, Zhu S, Guzzo CM, Ellis NA, Sung KS, Choi CY, Matunis MJ (2008) Small Ubiquitin-related Modifier (SUMO) Binding Determines Substrate Recognition and Paralog-selective SUMO Modification. *The Journal of Biological Chemistry* 283 (43):29405-29415.
- Zhu S, Goeres J, Sixt KM, Békés M, Zhang X-D, Salvesen GS, Matunis MJ (2009) Protection from Isopeptidase-Mediated Deconjugation Regulates Paralog-Selective Sumoylation of RanGAP1. *Molecular cell* 33 (5):570-580.

List of Oligonucleotides

Tab. 9: Oligonucleotides used in this study

Name	Sequence (5'→3')	Description
JE4234	gatgaattcatggactacaaggacgacgatgacaaggagctccagattttcgcaagactttg a	EcoRI-FLAG-SacI-UBI_fw
JE4235	ggtggtaccacgctaatctgggacgctgatgggtattgtatagttcatccatgcca	GFP-HA-KpnI_rv
JE4236	gttccttctcttactatgcataccacctcttagccttagc	UBI-NsiI-Overlap_GFP_rv
JE4237	gctaagagggtgatgcatagtaaaggagaagaactttc	Overlap_UBI-NsiI-GFP_fw
JE4238	gatgaattcatggactacaag	FLAG-UBI_fw
JE4239	ggtggtaccacgctaatc	GFP-HA_rv
JE4240	ggtatgcatgtcaagcctgagactcac	NsiI-ΔN17SMT3_fw
JE4241	ttttctgcagaccaccaatctgttctctgt	ΔN17SMT3-PstI_rv
JE4242	aaaagagctctcggactcagaagtcaatca	SacI-SMT3_fw
JE4281	cgcgcatgcataccaccaatctgttctctgt	SMT3-NsiI_rv
JE4243	gcgctgcaggagaactgtactccagagcatgtctccagaaaacgcaagttaaatagtct c	PstI-TEVp.r.s.-ULP2_fw
JE4965	gcgcaagctttcactgtcatcgtcgtctttagtcggtaccagggtcttcatcttccaagag	ULP2-KpnI-FLAG- HindIII_rv
JE4245	gatggtgatgtaaatgggc	GFP sequencing (internal)
JE4246	gactacaaggacgacgatg	FLAG_fw
JE4247	tcggactcagaagtcaagaagc	SMT3_fw
JE4248	ctccttactatgcagacc	SMT3-GFP_rv (sequencing)
JE4353	ggggaattcatggactacaaggacgacgatgacaaggagctcggtagtaaggagaagaa ctttcactgg	EcoRI-FLAG-SacI-GFP_fw
JE4353	ggggaattcgactcggtagtcagatttctgcaagactttga	EcoRI-FLAG-UBI_fw
JE4250	ggatgtgctgcaaggcgc	pMALc2x_rv (sequencing)
JE4768	gctgaagtcttacgaggaag	pMALc2x_fw (sequencing)
JE4269	gaactgtacttccagagc	ULP2 sequencing (internal)
JE4270	cagccactgttgacgcc	ULP2 sequencing (internal)
JE4271	ctggggaatgggtcaccggaac	ULP2 sequencing (internal)
JE4272	ctgcaagctcgcctca	ULP2 sequencing (internal)
JE4273	ggactcgtattgccagc	ULP2 sequencing (internal)
JE4274	gggtaatgatagcattttgg	ULP2 sequencing (internal)
JE4275	cgatgccatcaactccg	ULP2 sequencing (internal)
JE4276	caattgttccaccggatttc	ULP2 sequencing (internal)
JE4277	gtggtgttcatgttattttg	ULP2 sequencing (internal)
JE4278	ccgtagtacgacagccc	ULP2 sequencing (internal)
JE4279	ctctatcgactgattctatgg	ULP2 sequencing (internal)
JE4280	gatgtggcatttagtagtc	ULP2 sequencing (internal)
JE4282	gtgctagcggttgagac	ULP2 sequencing (internal)
JE4283	ctggggaatgggtcaccggaac	ULP2 sequencing (internal)
JE4284	ctgcaagctcgcctca	ULP2 sequencing (internal)
JE4285	ggactcgtattgccagc	ULP2 sequencing (internal)
JE4286	gggtaatgatagcattttgg	ULP2 sequencing (internal)
JE4287	cgatgccatcaactccg	ULP2 sequencing (internal)
JE4288	gtggtgttcatgttattttg	ULP2 sequencing (internal)
JE4289	ccgtagtacgacagccc	ULP2 sequencing (internal)
JE4290	ctctatcgactgattctatgg	ULP2 sequencing (internal)
JE4530a	gcgcgatccgagaactgtactccagagcatgtcagttgaagtagataagcac	BamHI-TEVp.r.s.-ULP1_fw
JE4532a	gcgctgcagtcactgtcatcgtcgtccttagtcggctaccttttaaaagctcggttaaa atcaaatg	ULP1-KpnI-FLAG-STOP- PstI_rv
JE4361	gcttctcaaaaagcaattgtg	ULP1 sequencing (internal)
JE4362	gctaaatgacactatcattgag	ULP1 sequencing (internal)
JE4363	cacaattgctttttgagaagc	ULP1 sequencing (internal)

JE4364	ctcaatgatagtgtcatttagc	ULP1 sequencing (internal)
JE4406	gcgcgcgagctcgtcaagcctgagactcac	SacI-ΔN17SMT3_fw
JE4426	gcgcgagctcaccgggtcggactcagaagtcaatca	SacI-AgeI-SMT3-fw
JE4427	aaaagagctcaccgggtatgaaaatcgaagaaggtaaactgg	SacI-AgeI-MBP-fw
JE4505	aaaaaaatgcatagctcgcgctctttcagggcttc	MBP-NsiI_rv
JE4423	cgcgcggtaccatgcatagcaccatctgttctctgt	SMT3(G98A)-NsiI-KpnI_rv
JE4424	cgcgcgctgcagagcaccatctgttctctgtgagc	SMT3(G98A)-PstI_rv
JE4481**	aaaaaacgggtgagaactgtacttccagagctcggactcagaagtcaatca	AgeI-TEVp.r.s.-SMT3_fw
JE4482	gggggtaccgctctggaagtacaagtctcagcgaatctggacgtcg	HA-TEVp.r.s.-KpnI_rv
JE4581	gcgcgagctcagaaactgtacttccagagctcggactcagaagtcaatca	SacI-SUMO1_fw
JE4584	cgcgcatgcataccctccctgttctctg	SUMO1-NsiI_rv
JE4587	gcgcgcatgcatggtatgcagattttctgcaagactttga	NsiI-UBI_fw
JE4588	cgcgcgctgcagaccactcttagccttagcac	UBI-PstI_rv
JE4600*	gcgcggtaccgctctggaagtacaagtctcatgcataccaccaatctgttctctgt	SMT3-NsiI-TEVp.r.s.-KpnI_rv
JE4610	gcgcgagctcaccgggtgagaactgtacttccagagcgtcaagcctgagactcac	SacI-AgeI-TEVp.r.s.-ΔN17SMT3_fw
JE4616	gcgcgcgagctcgggtcgcgacgaaaagcccaagg	SacI-SUMO2_fw
JE4617	gcgcatgcataccctcccgtctgctgttgg	SUMO2-NsiI_rv
JE4624	gcgcgcatgcatgccgacgaaaagcccaagg	NsiI-SUMO2_fw
JE4625	cgcgcgctgcagacctcccgtctgctgttgg	SUMO2-PstI_rv
JE4966	gcgcatgcataccctcccgtctgctgttgggtgagcctcaataatcgttatcc	SMT3(EndM)-NsiI_rv
JE4967	aaactgaccacagaaccttccatcggacacctttaaattg	SMT3(M0)_rv (overlap)
JE4968	gatggtctgtggtgagatttaagatcaaaaagaccactcctttaaag	SMT3(M0)_fw (overlap)
JE4969	gattggttcccgtcaaatcggaaatctgatggagtcatttcttaccctgtc	SMT3(M1)_rv (overlap)
JE4970	atcagattccgatttgacgggcaaccaatcattcaagctgatcagaccctg	SMT3(M1)_fw (overlap)
JE4971	gaacacatcaattgtatcttcatctccatgtccaatcttc	SMT3(M2)_rv
JE4972	gcgcatgcataccaccaatctgttctctgaacacatcaattgtatcttc	SMT3(M2)-NsiI_rv
JE4658	aaaactgcaggagaactgtacttccag	PstI-TEVp.r.s_fw
JE4659	ttttaagcttccactgtcatcgtcg	FLAG-STOP-HindIII_rv
JE4660	gctaggtttaaacagttctggtgttcc	ULP2-PmeI_rv (internal)
JE4661	gtggaacaattgatgtatggaag	ULP2-MfeI_fw (internal)
JE4973	ccacttagtaactaatgaaagcgttcgctaaaagacagggttaag	SMT3(M4)_fw (overlap)
JE4974	gtttactaagtgggtatgcctttgatcttgaagaagatctctg	SMT3(M4)_rv (overlap)
JE4975	cagggtatgcaatgaggcagtttaagattctgtacgacgg	SMT3(M5)_fw (overlap)
JE4976	cattgacaatccctgtcgttcagcgaacgcttccatcagccttc	SMT3(M5)_rv (overlap)
JE4977	gcagggtgtctgtttcattaaattctaataaccgtctgacaag	SMT3(M6)_rv
JE4978	gcgcatgcataccaccaatctgttctctgtgagcctcaataatcgttatcttccattccaactgtgcaggtgtctg	SMT3(M6)-NsiI_rv
JE4675	cgtacaagaatcctaaggagtcatttcttccctgtcgttcacaatagcc	SUMO2(M1,M5)_rv
JE4676	ccttaagattctgtacgacggtattagaatcaatgaaacagacacacc	SUMO2(M1,M5)_fw
JE4677	gcgcatgcataccaccaatctgttctctgaacacatcaattgtatcttcatcc	SUMO2(EndM)_rv
JE4678	acaagaatcctaaggagtcatttcttaccaccggtcaaaagtcttgacgaaaatctgcat	UBI(M1,M5)_rv
JE4679	ccttaagattctgtacgacggtattagaggtggtgtaaaaccataacattggaag	UBI(M1,M5)_fw
JE4680	gcgcatgcataccaccaatctgttctctcacaagatgtaagggtgactcc	UBI(EndM)_rv
JE4733	aaaggaattgagtttgagaaagacttcaaaag	EcoRI-5'ΔULP1_fw
JE4734	gcccattgaaatttaaccgacgc	ΔULP1(I615N)_fw (overlap)
JE4735	gcgctcggttaattcaaatgggc	ΔULP1(I615N)_rv (overlap)
JE4736	tttggtacccacaatttacttactatctc	ULP1+495nt downstream-KpnI_rv
JE4737	gcgcaagcttctactgtcatcgtcgtcctttagtcggtacccttccagatagctgatgtaattgag	ULP2(693)-KpnI-FLAG-HindIII_rv
JE4739	ttttaccgggtaccacctttagccttagc	UBI-AgeI_rv
JE4743	gcgcaagcttctactgtcatcgtcgtcctttagtcggtaccattatcagttattttaccg	ULP2(774)-KpnI-FLAG-HindIII_rv
JE4746	gcgctgcaggagaactgtacttccagagctcaaatcagaatttgatgatgc	PstI-TEVp.r.s.-ULP2(411)_fw
JE4747	gcgctgcaggagaactgtacttccagagcatgagtagttgtgtctacagc	PstI-TEVp.r.s.-Ubc9_fw
JE4748	gcgcaagcttctatttagagtagctgttagctggaag	Ubc9-HindIII_fw

JE4755	ttttctgcagaccaccaatctgttctctg	SMT3(M2)-PstI_rv
JE4756	ttttctgcagacctcccgtctgctgttgg	SMT3(EndM)-PstI_rv
JE4774	gcgcaagctttcacttgcacgcgcctctgtagtcggtaccggctgtttttctcctcc	ULP2(710)-KpnI-FLAG-HindIII_rv
JE4798	gcgcctgcaggagaacttctacttccagagcgataagaagaactctttatggc	PstI-TEVp.r.s.-ULP2(201)_fw
JE4799	gcgcctgcaggagaacttctacttccagagcaattcacaagtaactctgctt	PstI-TEVp.r.s.-ULP2(209)_fw
JE4823	gatcctcaatggtgatgatggtggtgacctccgcgggtac	KpnI-3xGly-6xHis-HindIII_rv
JE4824	cggcggaggtcaccaccatcatcaccattgag	KpnI-3xGly-6xHis-HindIII_fw
JE4835	aaaaaggatccgactacaaggacgacgatgacaagggtgaatcgtcgtcgccgtcgc	BamHI-FLAG-TEVPROTEASE_fw
JE4836	ttttctgcagttaattcatgagttgagtcgcttcc	TEVPROTEASE-PstI_rv
JE4840	gcgcaagctttcaatggtgatgatggtggtgggtacctccaccgcgggtaccggctgtttttctcctcc	ULP2(710)-KpnI-3xGly-6xHis-HindIII_rv
JE4888	ggtatgcatactgagaacaacgatcatattaattg	NsiI-ΔN11SUMO2_fw
JE4889	gtctagcagcgaacgcttccatcagc	SMT3(K54A)_rv (overlap)
JE4890	ttcgtgctagacagggttaaggaaatg	SMT3(K54A)_fw (overlap)
JE4891	gtctttcagcgaacgcttccatcagc	SMT3(K54E)_rv (overlap)
JE4892	ttcgtgaaagacagggttaaggaaatg	SMT3(K54E)_fw (overlap)
JE4893	atttcagcaccctgtcttttagcgaacg	SMT3(K58A)_rv (overlap)
JE4894	gggtgctgaaatggactccttaagattc	SMT3(K58A)_fw (overlap)
JE4895	atttctcaccctgtcttttagcgaacg	SMT3(K58E)_rv (overlap)
JE4896	gggtgaagaaatggactccttaagattc	SMT3(K58E)_fw (overlap)
JE4897	gtccatagccttaccctgtcttttagcg	SMT3(E59A)_rv (overlap)
JE4898	ggtaaggctatggactccttaagattcttg	SMT3(E59A)_fw (overlap)
JE4899	gtccattcttaccctgtcttttagcg	SMT3(E59R)_rv (overlap)
JE4900	ggtaagagaatggactccttaagattcttg	SMT3(E59R)_fw (overlap)
JE4901	taaggaggccatttcttaccctgtc	SMT3(D61A)_rv (overlap)
JE4902	gaaatggcctccttaagattcttg	SMT3(D61A)_fw (overlap)
JE4903	taaggatctcatttcttaccctgtc	SMT3(D61R)_rv (overlap)
JE4904	gaaatgagatccttaagattcttg	SMT3(D61R)_fw (overlap)
JE4905	ccttaaggcgtccatttcttaccctg	SMT3(S62A)_rv (overlap)
JE4906	atggacgccttaagattcttctgacgac	SMT3(S62A)_fw (overlap)
JE4907	tattagaattcaagaagatcagaccctgaag	SMT3(A73E)_fw (overlap)
JE4908	ctgatcttctgaattctaataaccgtcgtac	SMT3(A73E)_rv (overlap)
JE4909	aattcaagctgctcagaccctgaag	SMT3(D74A)_fw (overlap)
JE4910	gtctgagcagcttgaattctaataaccg	SMT3(D74A)_rv (overlap)
JE4911	aattcaagctaaacagaccctgaagattg	SMT3(D74K)_fw (overlap)
JE4912	gtctgttagcttgaattctaataaccg	SMT3(D74K)_rv (overlap)
JE4913	aagctgatgacaccctgaagatttggac	SMT3(Q75D)_fw (overlap)
JE4914	aggggtgctcagcttgaattctaataaccg	SMT3(Q75D)_rv (overlap)
JE4915	aagctgatgacaccctgaagatttggac	SMT3(Q75A)_fw (overlap)
JE4916	aggggtgctcagcttgaattctaataaccg	SMT3(Q75A)_rv (overlap)
JE4917	cagaccctgcagatttggacatggaggataac	SMT3(E78A)_fw (overlap)
JE4918	atgtccaaatctcaggggtctgatcagcttg	SMT3(E78A)_rv (overlap)
JE4919	cagaccctcgagatttggacatggaggataac	SMT3(E78R)_fw (overlap)
JE4920	atgtccaaatctcaggggtctgatcagcttg	SMT3(E78R)_rv (overlap)
JE4921	cagaccctgaacgttggacatggaggataac	SMT3(D79A)_fw (overlap)
JE4922	catgtccaaacgttcaggggtctgatcagcttg	SMT3(D79A)_rv (overlap)
JE4923	cagaccctgaaaaattggacatggaggataac	SMT3(D79K)_fw (overlap)
JE4924	catgtccaaattttcaggggtctgatcagcttg	SMT3(D79K)_rv (overlap)
JE4925	cttcaggggtctgatcagcttggattggtgcccgctcaaatc	SUMO2(M6)_rv (overlap)
JE4926	ctgatcagaccctgaagatttggacatggaggatgaagatacaattg	SUMO2(M6)_fw (overlap)
MS1980	ggtatgcatactgagaacaacgatcatattaattg	GFP_rv (internal; sequencing)
T7-981079	taatacgactcactatag	pET11a sequencing
pET-RP	ctagttattgctcagcgg	pET11a sequencing

Appendix

Abbreviations

5-FOA	5-fluoroorotic acid
aa	amino acids
amp	ampicillin
AP	alkaline phosphatase
APS	Ammonium persulfate
ATB	activity test buffer
AVP	adenovirus processing protease
BSA	bovine serum albumin
CaCl ₂	calcium chloride
cam	chloramphenicol
Cdk1	cyclin-dependent kinase 1
CTD	carboxy-terminal non-catalytic domain
C-terminus	carboxyl terminus
CuSO ₄	copper sulfate
CV	column volume
Cys	cysteine
dATP	deoxyadenosine triphosphate
dCTP	deoxycytidine triphosphate
ddH ₂ O	double-distilled water
DeSI	deSUMOylation isopeptidase
DLS	dynamic light scattering
DMSO	dimethyl sulfoxide
dGTP	deoxyguanosine triphosphate
dNTP	deoxynucleoside triphosphate
DTT	dithiothreitol
dTTP	deoxythymidine triphosphate
DUB	deubiquitinating enzyme
E1	activating enzyme
E2	conjugating enzyme
E3	ligating enzyme
E.coli	Escherichia coli
EDTA	ethylenediaminetetraacetic acid
eGFP	enhanced green fluorescent protein
HEPES	4-(2-hydroxyethyl)-1-piperazineethanesulfonic acid
GFP	green fluorescent protein
Gly	glycine
h	hour
HCl	hydrochloric acid
His ₆	hexahistidine
HMW	high molecular weight
HRP	horseradish peroxidase
hygB	hygromycine

IPTG	isopropyl-beta-D-thio-galactoside
kan	kanamycine
kb	kilobasepairs
KCl	potassium chloride
kD/kDa	kilodalton
KH ₂ PO ₄	Potassium dihydrogen phosphate
KOH	Potassium hydroxide
LB	lysogeny broth
LB+Amp	LB medium containing 100 µg/ml ampicillin
LB+Cam	LB medium containing 25 µg/ml chloramphenicol
LiAc	lithium acetate
Lys	lysine
M	mol per litre
m	milli
MgCl ₂	Magnesium chloride
min	minute
Na ₂ HPO ₄	disodium hydrogen phosphate
NaH ₂ PO ₄	sodium dihydrogen phosphate
NaCl	sodium chloride
nat	nourseothricin
NEDD8	Neural-precursor-cell-expressed developmentally downregulated protein-8
NLS	nuclear localization signal
NPC	nuclear pore complex
NTD	amino-terminal non-catalytic domain
N-terminus	amino terminus
OD ₆₀₀	optical density at 600 nm
PAGE	polyacrylamide gel electrophoresis
PBS	phosphate-buffered saline
PBS-T	phosphate-buffered saline plus Tween-20
PCR	polymerase chain reaction
PML	promyelocytic leukemia
PMSF	phenylmethylsulfonyl fluoride
RING	really interesting new gene
r.m.s.d.	root mean square deviation
rpm	rounds per minute
SAE1	SUMO-activating enzyme subunit 1
SAE2	SUMO-activating enzyme subunit 1
<i>S. cerevisiae</i>	<i>Saccharomyces cerevisiae</i>
SDS	sodium dodecyl sulfate
SENP	sentrin-specific protease
SIM	SUMO-interacting motif
STUbL	SUMO-targeted ubiquitin ligase
SUMO	small ubiquitin-related modifier
TEMED	tetramethylethylenediamine
TEV	Tobacco Etch Virus
TEVp.r.s	TEV protease recognition site
Ubc9	ubiquitin-like modifier carrier 9
Uba2	ubiquitin-like modifier activating enzyme 2
Ubl	ubiquitin-like protein
Ubi	ubiquitin

UD	Ulp2 active domain
UFD	ubiquitin fusion degradation
Ulp	UBL-specific protease
ULS	ubiquitin ligases for sumoylated proteins
USPL1	ubiquitin-specific protease-like 1
Wss1	weak suppressor of smt3-33 1
SD	synthetic dextrose (medium)
TCEP	tris(2-carboxyethyl)phosphine
wt	wild type
w/v	weight per volume
YNB	yeast nitrogen base
YPD	yeast peptone medium containing 2 % glucose
µg	microgram

Acknowledgements

Disclaimer: I do not consider this section/page part of my intellectual work. So if anyone takes issue with a sassy tone, PLEASE TURN THE PAGE NOW!

This work would not have been possible without Jürgen Dohmen. Obviously, because it is his research group I was working in. But apart from this shallow fact, he gave me the opportunity to try out all the (sometimes ridiculous) ideas I had for my project. I can easily count the number of discussions we had during the ~3.5 years of my PhD work –they were scarce. But that was, because I usually followed my instincts and chose not to ask for advice or permission. It takes a lot of calmness, even coolness, for a senior scientist to let a “greenhorn” run that freely. And for that, Jürgen, for this liberty, I thank you from the bottom of my heart.

I always felt like I had a second, secrete, doctoral supervisor. Thank you, Uli Baumann, for being always encouraging and helpful, generously letting me use all the stuff in your laboratory for crystallization and sharing your wisdom, measuring my Ulp2 crystal at the SLS, and patiently answering every email with my stupid computer-related questions.

There are some scientists I met during my Bachelor and Master studies, I will never forget because they –in a regular, normal conversation– dropped a bomb of knowledge and wisdom on me that helped me to cope with any frustration, setback and attacks by my inner slave-driver during my PhD. Frank Landgraf, Siew-Ping Han, Jan Gambin, Viktor Stein. I guess you will never know what impact your words had on me... If we ever meet again: Beers on me!

A big hug goes out to Stefan Pabst, who set the gold standard for a lab mate. There is no one I would rather share a laboratory with. Thank you, R2, for stoically taking in my quirks, demonstrations of “hilarious songs/comedians, I recently found”, outbursts of weirdness, and all the pet names I gave you. Just thanks for being your wonderful self, Stefan (/R2/ Schnuckiputzi/ Schnuffelichen/ my little padawan/...).

Not to forget Vishal, Maria, Kerstin, Sigrid, Steffi, and other members of the Institute of Genetics for making laboratory work even more entertaining.

Also a “whoop whoop” to Christian Pichlo, with whom I joined forces to crystallize Ulp2. Couldn't have asked for a better crystal mate.

I have no idea what I would be without my school day friends Tschacki, Stääf, and Isi. After THAT much time and almost 10 years of considerable distance between us, each of you is still a very important part of my life. You guys are my best friends. You mean the world to me.

There are so many other people that make life wonderful for me...but here comes the catch: They have almost zero contact with my science life. All my other friends, family, sports partners, people I tackle the improv stages with, ... If anyone of you reads this (and, seriously, why would you do that?!): Do you even know what I am doing in my job? No! And I thank you for that, because you have saved me from becoming a complete and total nerd (Fachidiot). So if anyone feels left out: Don't! You kept my love and passion for science, for the laboratory work, for playing with chemicals (okay, that's an easy one,... for f***'s sake, what is greater than that?!?) alive by allowing me to step out of this fascinating world, letting me wear it like a T-Shirt, that I can take off every evening. Thank you for that!

Eidesstattliche Erklärung

Erklärung zur Dissertation

Ich versichere, dass ich die von mir vorgelegte Dissertation selbstständig angefertigt, die benutzten Quellen und Hilfsmittel vollständig angegeben und die Stellen der Arbeit – einschließlich Tabellen, Karten und Abbildungen –, die anderen Werken im Wortlaut oder dem Sinn nach entnommen sind, in jedem Einzelfall als Entlehnung kenntlich gemacht habe; dass diese Dissertation noch keiner anderen Fakultät oder Universität zur Prüfung vorgelegen hat; dass sie – abgesehen von unten angegebenen Teilpublikationen – noch nicht veröffentlicht worden ist sowie, dass ich eine solche Veröffentlichung vor Abschluss des Promotionsverfahrens nicht vornehmen werde.

Die Bestimmungen dieser Promotionsordnung sind mir bekannt. Die von mir vorgelegte Dissertation ist von Prof. Dr. R. Jürgen Dohmen betreut worden.

Nachfolgende Teilpublikation liegt vor:

Julia Eckhoff & R. Jürgen Dohmen (2015): In Vitro Studies Reveal a Sequential Mode of Chain Processing by the Yeast SUMO (Small Ubiquitin-related Modifier)-specific Protease Ulp2. *J. Biol. Chem.*; 290(19): 12268-12281

Promotionsbeginn: 01.12.2012
(Beginn der praktischen Arbeit)

Promotionsende: 07.2016
(Monat der mündlichen Prüfung)

Ich versichere, dass ich alle Angaben wahrheitsgemäß nach bestem Wissen und Gewissen gemacht habe und verpflichte mich, jedmögliche, die obigen Angaben betreffende Veränderungen, dem Dekanat unverzüglich mitzuteilen.

12.09.2016

Datum

Unterschrift